CAPITAL UNIVERSITY OF SCIENCE AND TECHNOLOGY, ISLAMABAD

Maxwell Nanofluid Flow with Thermophoretic Particle Deposition Using the Non-Fourier Double Diffusion Concept and Magnetic Field

by

Sana Javed

A thesis submitted in partial fulfillment for the degree of Master of Philosophy

in the

Faculty of Computing
Department of Mathematics

2024

This thesis is dedicated to my cherished parents, whose boundless love, unwavering support and belief in my abilities have been the driving force behind my academic journey. Their sacrifices, encouragement, and constant presence have inspired me to persevere and reach for excellence. I am forever grateful for the values and guidance they have instilled in me, which have shaped my character and ambitions. This work is a testament to their selfless dedication and the profound impact they have had on my life. I am privileged to have such remarkable parents who have always stood by me with unwavering love and care.

CERTIFICATE OF APPROVAL

Maxwell Nanofluid Flow with Thermophoretic Particle Deposition Using the Non-Fourier Double Diffusion Concept and Magnetic Field

by

Sana Javed

(MMT213004)

THESIS EXAMINING COMMITTEE

(a)	External Examiner	Dr. Ahmad Zeeshan	IIU, Islamabad
(b)	Internal Examiner	Dr. Muhammad Sabeel Khan	CUST, Islamabad
(c)	Supervisor	Dr. Muhammad Sagheer	CUST, Islamabad

Dr. Muhammad Sagheer
Thesis Supervisor
October, 2024

Dr. Muhammad Sagheer
Head
Dept. of Mathematics
October, 2024

Dr. M. Abdul Qadir
Dean
Faculty of Computing
October, 2024

Author's Declaration

I, **Sana Javed**, hereby state that my MPhil thesis titled "**Maxwell Nanofluid Flow with Thermophoretic Particle Deposition Using the Non-Fourier Double Diffusion Concept and Magnetic Field**" is my own work and has not been submitted previously by me for taking any degree from Capital University of Science and Technology, Islamabad or anywhere else in the country/abroad.

At any time if my statement is found to be incorrect even after my graduation, the University has the right to withdraw my MPhil Degree.

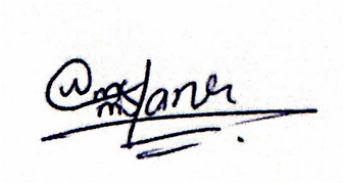

(Sana Javed)

Registration No: MMT213004

Plagiarism Undertaking

I solemnly declare that research work presented in this thesis titled "**Maxwell Nanofluid Flow with Thermophoretic Particle Deposition Using the Non-Fourier Double Diffusion Concept and Magnetic Field**" is solely my research work with no significant contribution from any other person. Small contribution/help wherever taken has been duly acknowledged and that complete thesis has been written by me.

I understand the zero tolerance policy of the HEC and Capital University of Science and Technology towards plagiarism. Therefore, I as an author of the above titled thesis declare that no portion of my thesis has been plagiarized and any material used as reference is properly referred/cited.

I undertake that if I am found guilty of any formal plagiarism in the above titled thesis even after award of MPhil Degree, the University reserves the right to withdraw/revoke my MPhil degree and that HEC and the University have the right to publish my name on the HEC/University website on which names of students are giarized work.

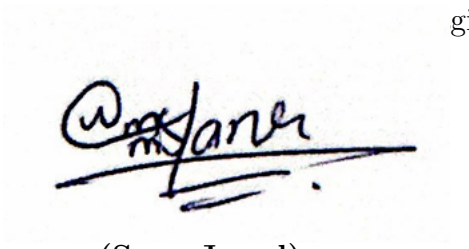

(Sana Javed)

Registration No: MMT213004

Acknowledgement

I would like to express my deepest gratitude and appreciation to all those who have contributed to the successful completion of this thesis.

First and foremost, I am immensely grateful to my supervisor, Dr. Muhammad Sagheer, for his unwavering guidance, encouragement, and support throughout this research journey. His expertise and valuable insights have been instrumental in shaping the direction and quality of this work.

I am also deeply grateful to my parents, **Javed Iqbal** and **Sajida Parveen**, for their unwavering support and encouragement throughout my academic journey. Their belief in my abilities and their constant reassurance have been invaluable in helping me reach this point. Their sacrifices, love, and guidance have provided me with the strength and motivation needed to complete this thesis. I am profoundly grateful for their patience, understanding, and for always being my greatest cheerleaders. This work is as much a reflection of their dedication and support as it is of my own efforts.

In conclusion, this thesis would not have been possible without the collective efforts of all those mentioned above.

(Sana Javed)

Registration No: MMT213004

Abstract

This research provides a comprehensive analysis of Maxwell nanofluid flow by examining various physical parameters in a two-dimensional, unsteady boundary layer flow over a stretching sheet. The study models and analyzes the governing equations while incorporating the Non-Fourier double diffusion effect, magnetic field influence, and porosity parameter. The coupled system of ordinary differential equations, derived through similarity transformations, is effectively solved using numerical technique, the shooting method. The research highlights the significant impact of Cattaneo-Christov heat flux and magnetic field on enhancing heat transfer efficiency, thereby improving thermal diffusion within the system. It also demonstrates how the inclusion of diffusion significantly affects velocity, temperature, and concentration profiles, as well as their rates of change. This transient behavior is crucial for understanding the dynamics of nanofluid flow and its practical implications in engineering applications.

Contents

List of Figures

List of Tables

Abbreviations

BCs	Boundary conditions
IVP	Initial value problem
MHD	Magnetohydrodynamics
ML	Maxwell liquid
NF	Nanofluid
ODEs	Ordinary differential equations
PDEs	Partial differential equations
RK-4	Range Kutta method of order 4
SS	Stretching surface
TPD	Thermophoretic particle deposition

Symbols

$\widetilde{u}, \widetilde{v}$	Velocity components
$\widetilde{U}_w$	Sheet velocity
$\tilde{\mu}$	Dynamic viscosity
$\widetilde{\nu}$	Kinematic viscosity
$\widetilde{\rho}$	Density
D	Diffusion coefficient
$\widetilde{T}$	Temperature of nanoparticles
$\widetilde{k}$	Thermal conductivity
$\widetilde{\rho}\widetilde{c_p}$	Heat capacity
$\widetilde{T}_w$	Wall constant temperature
$\widetilde{T}_\infty$	Ambient temperature of fluid
$\widetilde{C}$	Concentration
$\widetilde{C}_w$	Nanoparticles concentration at the stretching surface
$\widetilde{C}_\infty$	Ambient concentration
$\widetilde{q'''}$	Radiative heat flux
λ_0	Relaxiation time
$\widetilde{B}_o$	Magnatic field constant
$\widetilde{\sigma}^*$	Stefan Boltzmann constant
$\widetilde{k}^*$	Thermophoretic coefficient
γ	Unsteadiness parameter
β	Debora number
ζ	similarity variable
$f(\zeta)$	Dimensionless velocity
$\theta(\zeta)$	Dimensionless temperature

$\chi(\zeta)$	dimensionless concentration
$\widetilde{h}_f$	Cofficient of heat transfer
M	Magnetic field parameter
K_p	Porosity medium parameter
Pr	Prandtl number
Ec	Eckert number
τ	Thermophoretic parameter
a	constant
(A^*, B^*)	Space and temperature dependent heat source/sink parameter
Sc	Schmidt number
Sh	Sherwood number
Nu	Nusselt number
Cf	Skin fraction coefficient

Subscripts

f	fluid
nf	nanofluid

Chapter 1

Overview

1.1 Background

In recent years, there has been a growing focus on investigating heat and mass transfer processes. This focus has generated significant enthusiasm among researchers and engineers, due to the broad applications of these phenomena in manufacturing processes, engineering and various trades. For a more empathetic understanding of heat transfer, Classical Fourier's law [1] is still widely used to model heat transfer across different scenarios. Nonetheless, it has a notable limitations it produces a parabolic PDEs for the temperature distribution. This implies that the entire medium reacts instantaneously to initial disturbances, which contradicts the well-established principle of causality. By adding the idea of thermal relaxation time, Cattaneo [2] suggested a significant adjustment to Fourier's model in order to address this problem. This adjustment results in a hyperbolic energy equation, which facilitates heat transfer through the propagation of thermal waves with a finite speed. Moreover, this approach has practical implications in fields such as nanofluid flow and skin injury management.

In order to preserve the material-invariant formulation, Christov [3] substituted the Oldroyd upper-convected derivative for the time derivative in the Maxwell–Cattaneo model. We refer to this adaptation as the Cattaneo–Christov heat flow model.

Ciarletta and Straughan examined the uniqueness and physical stability of the solutions to the Cattaneo-Christov equations [4]. Han et al. [5] investigated slip flow and heat transfer in Maxwell fluids, taking into account the effects described by the Cattaneo–Christov model.

They employed HAM to solve the governing equations and validate their solutions by comparing them with numerical results obtained using the finite difference method. Hayat et al. [6] explored the impact of both heterogeneous and homogeneous reactions on Oldroyd-B fluids using the Cattaneo–Christov heat flux model. Their findings indicated that an increase in thermal relaxation time leads to a reduction in temperature distribution. Waqas et al. [7] examined the characteristics of the Cattaneo–Christov heat flux model applied to generalized Burgers fluid flow with varying thermal conductivity.

Khan et al. [8] studied the effects of the Cattaneo–Christov heat flux model on three-dimensional Burgers fluid flow over a bidirectional stretching surface. They found that changes in the thermal relaxation time have a significant impact on the temperature distribution. Recently, Khan et al. [9] performed a numerical study on generalized Fourier's and Fick's laws applied to Sisko fluid flow. They found that the concentration distribution is significantly influenced by the power-law index in both shear-thinning and shear-thickening scenarios. Subsequently, Khan et al. [10] explored the influence of Cattaneo–Christov double diffusion and chemical processes on three-dimensional Burgers fluid. Additional recent research related to the Cattaneo–Christov heat flux model can be found in [11–21].

Thermophoresis is a transport mechanism influenced by a temperature gradient. In the presence of such a gradient within a liquid medium, particles are subjected to a thermophoretic force that drives them from hotter areas to cooler ones. This phenomenon, where particles suspended in a liquid are deposited onto a solid surface due to thermophoresis, is referred to as thermophoretic deposition (TPD). TPD plays a critical role in various applications, such as aerosol research, nanoparticle

deposition, and surface coating. In the field of nanotechnology, thermophoresis is especially useful for depositing nanoparticles onto targeted surfaces, aiding in the development of functional coatings and controlled drug delivery systems. The importance of TPD in the context of nanofluid flows, such as those induced by a moving disk, has been thoroughly discussed by Gowda et al. [22]. Their research indicated that as the thermophoretic parameter increases, mass transport decreases. Shehzad et al. [23] investigated how thermophoretic deposition affects the flow of a Maxwell fluid over a rotating disk. Their study revealed that increasing the thermophoretic parameter results in a reduction in fluid concentration. Kumar et al. [24] explored the behavior of a Maxwell fluid flowing over a stretchable surface under the influence of thermophoretic deposition (TPD) and found that increasing the thermophoretic parameter led to a decrease in fluid concentration. Similarly, Bashir et al. [25] investigated fluid flow on a stretchable surface affected by TPD and noted a significant reduction in mass transport with higher values of the thermophoretic parameter. Additionally, Kumar et al. [26] analyzed the flow of a Casson fluid around a moving needle influenced by TPD and observed that lower values of the thermophoretic parameter improved concentration profiles.

Research on fluid flow involving graphene nanoparticle suspensions aims to understand how these particles interact with the fluid and respond to various flow conditions or external influences. This knowledge is essential for optimizing the performance of graphene-based nanofluids in diverse applications. Graphene nanoparticles can significantly impact the fluid's viscosity, thermal conductivity, and overall flow behavior. Their outstanding thermal conductivity can improve the heat transfer efficiency of the fluid, making these nanofluids valuable for applications in heat exchangers, cooling systems, and thermal management. The potential of graphene nanoparticle suspensions in fluid flow research opens up new avenues for advanced technological applications. By harnessing the exceptional properties of graphene, researchers and engineers are developing enhanced nanofluids with the potential to transform multiple industries. Ahmad et al. [27] studied the flow of Maxwell fluids with graphene nanoparticle suspensions over a stationary surface and found that increasing the volume fraction of graphene nanoparticles decreased the fluid flow.

In contrast, Chandrasekaran et al. [28] investigated the flow of Maxwell fluids with graphene nanoparticles over an expandable surface, revealing that graphene nanoparticles improved the fluid flow velocity. Bhattacharyya et al. [29] analyzed the flow of Maxwell fluid with graphene nanoparticle suspensions over a stretching surface, focusing on an electrically conducting hybrid nanofluid and its flow properties under velocity slip conditions.

Hussain et al. [30] examined the flow of graphene Maxwell nanofluid over a stretching surface, studying the effects of radiative Maxwell fluid containing graphene nanoparticles under thermal slip conditions. Algehyne et al. [31] explored the flow of Maxwell nanofluid over a stretchable surface with Joule heating, concluding that increasing the solid volume fraction of graphene nanoparticles raised the fluid's temperature.

Sodium alginate is a highly adaptable and useful substance known for its gelling, thickening, and biocompatible properties. This sodium salt of alginic acid is valued in many applications due to its remarkable qualities and is used in various commercial products and processes. Jamshed et al. [32] studied the flow characteristics of nanofluids based on sodium alginate over a flat surface, finding that increasing the solid volume fraction reduced the fluid's velocity profile.

Similarly, Tassaddiq et al. [33] investigated the heat transport in nanofluids with sodium alginate as the base fluid over a vertical surface, using the Atangana–Baleanu fractional derivative to analyze free convection in non-Newtonian fluids. Shaukat et al. [34] explored the flow of sodium-alginate-based nanofluid through a porous medium and showed that a higher volume fraction improves fluid flow velocity. Raza et al. [35] examined the flow of a hybrid nanofluid over an inclined plate, revealing that the solid volume fraction enhances the nanofluid's thermal profile. Dawar et al. [36] looked at sodium-alginate-based nanofluid flow over a curved surface and found that a higher solid volume fraction increases the Nusselt number. Turkyilmazoglu [37] assessed the effects of magnetic field slip flow

on an electrically conducting nonlinear liquid over a shrinking surface, concluding that the magnetic field notably affects both velocity and temperature profiles.

Building on these studies, this work aims to explore the unsteady Cattaneo-Christov heat and mass flux models applied to Maxwell nanofluid flow with thermophoretic particle deposition over a stretching surface. The study will present and discuss the effects of various emerging parameters through detailed graphical representations.

1.2 Thesis Structure

Chapter 2 serves as an introduction to the thesis and provides essential definitions and terminologies crucial for understanding the concepts discussed in subsequent chapters. Its purpose is to establish a foundational understanding of the key terms and concepts that will be utilized throughout the thesis.

Chapter 3 presents a comprehensive numerical study of the flow characteristics of Maxwell nanofluids with varying nanoparticle diameters, incorporating the effects of thermophoretic particle deposition. The proposed numerical model examines heat and mass transfer processes occurring across a stretched sheet. To derive the computational findings for the fundamental flow equations, the shooting technique is employed. This chapter examines the flow dynamics and heat transfer performance of Maxwell nanofluids under different operating conditions.

Building upon the model presented in Chapter 3, **Chapter 4** advances the analysis to encompass Maxwell nanofluid flow. In this chapter, we integrate the effect of the magnetic field and porosity parameter into the momentum equation, while also incorporating additional complexities such as the non-Fourier double diffusion concept into the energy and concentration equations of the proposed model.

Chapter 5 presents the concluding remarks and highlights the significant findings obtained from the research presented in this thesis Its aim is to provide a comprehensive summary of the main outcomes and contributions of the study.

Chapter 2

Preliminaries

In this chapter, we will elucidate fundamental definitions, essential laws, terminologies, and key concepts necessary for the analysis of nonlinear partial differential equations. These foundational elements are crucial for comprehending the subsequent chapters of this study and will offer a solid structure for the development of a comprehensive understanding.

2.1 Foundational Concepts

2.1.1 Fluid

"A substance in the liquid or gas phase is referred to as a fluid. Distinction between a solid and a fluid is made on the basis of the substances ability to resist an applied shear (or tangential) stress that to change its shape. A solid can resist an applied shear stress by deforming, whereas a fluid deforms continuously under the influence of shear stress no matter how small. In solids, stress is proportional to strain, but in uids, stress is proportional to strain rate." [38]

2.1.2 Fluid Mechanics

"Fluid mechanics is that branch of science which deals with the behavior of the fluids (liquids or gases) at rest as well as in motion." [39]

2.1.3 Fluid Dynamics

"Fluid dynamics is the study of the motion of liquids, gases and plasma from one place to another."[39]

2.1.4 Viscosity

" Viscosity is defined as the property of a fluid which offers resistance to the movement of one layers of fluid over another adjacent layer of the fluid. When two layers of a fluid, a distance 'dy' apart, move one over the other at different velocities, say u and $u+du$ as shown in the viscosity together with relative velocity causes a shear stress acting between the fluid layers." [39]

2.1.5 Kinematic Viscosity

"Kinematic viscosity is defined as the ratio between the dynamic viscosity and density of fluid. It is denoted by the Greek symbol ν, thus mathematically,

$$\nu = \frac{\text{Viscosity}}{\text{Density}} = \frac{\mu}{\rho}$$

where the unit of kinematic viscosity is m^2/sec ." [39]

2.1.10 Magnetohydrodynamics

"Magnetohydrodynamics (MHD) is concerned with the flow of electrically conducting fluids in the presence of magnetic fields, either externally applied or generated within the fluid by inductive action." [39]

2.2 Classification of Fluid

2.2.1 Ideal Fluid

"A fluid which is incompressible and is having no viscosity, is known as an ideal fluid. Ideal fluid is only an imaginary fluid as all the fluids, which exist, have some viscosity." [39]

2.2.2 Real Fluid

"A fluid, which possesses viscosity, is known as a real fluid. All the fluids, in actual practice, are real fluids." [39]

2.2.3 Newtonian Fluid

"A real fluid, in which shear stress is directly, proportional to the rate of shear strain (or velocity gradient), is known as a Newtonian fluid." [39]

2.2.4 Non-Newtonian Fluid

"A real fluid, in which the shear stress is not proportional to the rate of shear strain (or velocity gradient), is known as a Non-Newtonian fluid." [39]

2.2.4 Ideal Plastic Fluid

"A fluid, in which shear stress is more than the yield value and shear stress is proportional to the rate of shear strain (or velocity gradient), is known as ideal plastic fluid, e.g. water suspension of clay and fly ash." [39]

2.3 Modes of Heat Transfer

2.3.1 Conduction

"The mechanism of heat transfer due to a temperature gradient in a stationary medium is called conduction. The medium may be solid or a fluid. A very popular example of conduction heat transfer is that when one end of metallic spoon is dipped into a cup of hot tea, the other end becomes gradually hot. In solids, the conduction of heat is attributed to two effects:

(i) the flow of free electrons and

(ii) the lattice vibrational waves caused by the vibrational motions of the molecules at relatively fixed positions called a lattice." [40]

2.3.2 Convection

"The mode by which heat is transferred between a solid surface and the adjacent fluid in motion when there is a temperature difference between the two is known as convection heat transfer. The temperature of the fluid stream refers either to its bulk or free stream temperature."[40]

2.3.3 Forced Convection

"In forced convection, the fluid is forced to flow over a solid surface by external means such as fan, pump or atmospheric wind." [40]

2.3.4 Free Convection

"When the fluid motion is caused by the buoyancy forces that are induced by density differences due to the variation in temperature or species concentration (in case of multicomponent systems) in the fluid, the convection is called natural (or free) convection." [40]

2.3.5 Radiation

"Any substance at a finite temperature emits energy in the form of electromagnetic waves in all directions and at all wavelengths (from a very low one to a very high one). The energy emitted within a specific band of wavelength (0.1–100 μm) is termed thermal radiation. The exchange of such radiant energy between two bodies at different temperatures is defined as heat transfer between the bodies by radiation. We have seen earlier that the heat transfer by conduction or convection requires the presence of a medium. But the radiation heat transfer does not necessarily require a medium, rather it occurs most efficiently in a vacuum." [40]

2.4 Different Flow Classifications

2.4.1 Steady and Unsteady Flows

"Steady flow is defined as that type of flow in which the fluid characteristics like velocity, pressure, density, etc., at a point do not change with time. Thus for steady flow, mathematically, we have

$$\left(\frac{\partial u}{\partial t}\right)_{(x_0,y_0,z_0)} = 0, \quad \left(\frac{\partial p}{\partial t}\right)_{(x_0,y_0,z_0)} = 0, \quad \left(\frac{\partial \rho}{\partial t}\right)_{(x_0,y_0,z_0)} = 0$$

where (x_0, y_0, z_0) is fixed point in fluid field.

Unsteady flow is that type of flow, in which the velocity, pressure or density at a point changes with respect to time. thus, mathematically, for unsteady flow

$$\left(\frac{\partial u}{\partial t}\right)_{(x_0,y_0,z_0)} \neq 0, \quad \left(\frac{\partial p}{\partial t}\right)_{(x_0,y_0,z_0)} \neq 0 \text{ etc.}" \text{ [39]}$$

2.4.2 Uniform and Non-uniform Flow

"Uniform flow is defined as the type of flow in which the velocity at any given time does not change with respect to space (i.e., length of direction of the flow). Mathematically, for uniform flow

$$\left(\frac{\partial u}{\partial s}\right)_{r=\text{constant}} = 0$$

where ∂u= Change of velocity

∂s= Length of flow in the direction S.

Non-uniform flow is the type of flow in which the velocity at any given time changes with respect to space. Thus, mathematically, for non-uniform flow

$$\left(\frac{\partial u}{\partial s}\right)_{r=\text{constant}} \neq 0.\text{"} \text{ [39]}$$

2.4.3 Laminar and Turbulent Flows

"Laminar flow is defined as that type of flow in which the fluid particles move along well-defined paths or stream lines and all the stream-lines are straight and parallel. Thus the particles move in lamines or layers gliding smoothly over the adjacent layer. This type of flow is also called stream-line flow or viscus flow.

Turbulent flow is that type of flow in which the fluid particles move in a zig-zag way. due to the movement of fluid particles in a zig-zag way, the eddies formulation takes place which are responsible for high energy loss." [39]

2.4.4 Compressible and Incompressible Flows

"Compressible flow is that type of flow in which the density for the fluid changes from point to point or in other words the density (ρ) is not constant for the fluid. Thus, mathematically, for compressible flow

$$\rho \neq \text{constant}.$$

Incompressible flow is that type of flow in which the density is constant for the fluid flow. Liquids are generally incompressible while gases are compressible. Mathematically, for incompressible flow

$$\rho = \text{constant.}" \text{ [39]}$$

2.4.5 Rotational and Irrotational Flows

"Rotational flow is that type of flow in which the fluid particles while flowing along stream-lines, also rotate about their own axis. And if the fluid particles while flowing along stream-lines, do not rotate about their own axis then that type of flow is called irrotational flow." [39]

2.4.6 Inviscous Flow

"A flow in which viscosity of the fluid is equal to zero is known as inviscous (inviscid) flow."

2.5 Porous Material

2.5.1 Porous Material

"A solid containing holes or voids, either connected or non-connected, dispersed within it in either a regular or random manner known as porous material provided that holes occur relatively frequently within the solid.
Pores are either interconnected or non-interconnected. A fluid can flow through a porous material only if at least some of the pores are interconnected"[41]. Some natural porous materials are beach sand, limestone, sandstone, wood, loaf of bread and human lung etc.

2.5.2 Porosity

"The porosity of a porous material is the fraction of the bulk volume of the material occupied by voids. The symbol usually employed for this parameter is ϕ. Thus

$$\phi = \frac{V_P}{V_B} = \frac{\text{Volume of pores}}{\text{Bulk volume}}$$

Bulk volume , which is a dimensionless quantity. Since that portion of the bulk volume not occupied by pores is occupied by the solid grains or matrix of the material, it follows that

$$1 - \phi = \frac{V_S}{V_B} = \frac{\text{Volume of solids}}{\text{Bulk volume}}."[41]$$

2.5.3 Permeability

"Permeability is the property of a porous material which characterizes the ease with which a fluid may be made through the material by an applied pressure gradient. Permeability is the fluid conductivity of the porous material. If horizontal linear of an incompressible fluid is established through a sample of porous material of length L in the direction of flow, and cross sectional area A, then the permeability K of the material is defined as

$$K = \frac{q\mu}{A\left(\frac{\delta P}{L}\right)}.$$

Here q is the fluid flow rate in volume per unit time, μ is the viscosity of the fluid and δP is the applied pressure difference across the length of the specimen"[41].

2.6 Conservation Laws

2.6.1 Law of Conservation of Mass

"The principle of conservation of mass can be stated as the time rate of change of mass in a

fixed volume is equal to the net rate of ow of mass across the surface. The mathematical statement of the principle results in the following equation, known as the continuity (of mass) equation

$$\frac{\partial \rho}{\partial t} + \delta.(\rho V) = 0"[42]. \tag{2.1}$$

2.6.2 Equation of Momentum

"The principle of conservation of linear momentum (or Newton's Second Law of motion) states that the time rate of change of linear momentum of a given set of particles is equal to the vector sum of all the external forces acting on the particles of the set, provided Newton's Third Law of action and reaction governs the internal forces. Newton's Second Law can be written as

$$\frac{\partial}{\partial t}(\rho V) + \delta.(\rho V \otimes V) = \delta.\sigma + \rho f." [42]. \tag{2.2}$$

2.6.3 Law of Conservation of Energy

"The law of conservation of energy (or the First Law of Thermodynamics) states that the time rate of change of the total energy is equal to the sum of the rate of work done by applied forces and the change of heat content per unit time. In the general case, the First Law of Thermodynamics can be expressed in conservation form as

$$\frac{\partial \rho e^t}{\partial t} + \delta.\rho v e^t = -\delta.q + \delta.(\sigma.v) + Q + \rho f.v, \tag{2.3}$$

where $e^t = e + 1/2v.v$ is the total energy (J/m^3), e is the internal energy, q is he heat flux vector (W/m^2) and Q is the internal heat generation (W/m^3)" [42].

2.4.4 Newton's Law of Viscosity

"It states that the shear stress (τ) on a fluid element layer is proportional to the rate of shear strain. The constant of proportionally is called coefficient of viscosity. Mathematically, it is expressed as

$$\tau = \mu \frac{\partial u}{\partial y}."$$

2.7 Dimensionless Parameters

2.7.1 Nusselt Number (Nu)

"It is the relationship between the convective to the conductive heat transfer through the boundary of the surface. Mathematically, it is defined as

$$Nu = \frac{hL}{k},$$

where h stands for convective heat transfer, L stands for characteristic length and k stands for thermal conductivity." [43]

2.7.2 Prandtl Number (Pr)

"The ratio of kinematic diffusivity to heat the diffusivity is said to be Prandtl number. It is denoted by Pr. Mathematically, it can be written as

$$\begin{aligned} Pr &= \frac{\nu}{\alpha} \\ \Rightarrow \quad &= \frac{\mu c_p}{\rho k} \end{aligned}$$

where μ represent the dynamic viscosity, C_p denotes the specific heat and k stands for thermal conductivity." [43]

2.7.3 Skin Friction Coefficient (Cf_x)

"The skin friction coefficient is typically defined as

$$Cf = \frac{2\tau_w}{\rho U_w^2}$$

where τ_w is the local wall shear stress, ρ is the fluid density and U_w is the free stream velocity (usually taken outside the boundary layer or at the inlet)." [43]

2.7.4 Sherwood Number (Sh_x)

"It is a non-dimensional quantity which describes the ratio of the mass transport by convection to the transfer of mass by diffusion. Mathematically,

$$Sh = \frac{kL}{D},$$

where L is characteristics length, D is the mass diffusivity and k is the mass transfer coefficient." [43]

2.7.5 Thermophoresis Parameter

"In a temperature gradient, small particles are pushed towards the lower temperature because of the asymmetry of molecular impacts." [43]

2.7.6 Eckert Number

"It is a dimensionless number used in continuum mechanics. It describes the relation between flows and the boundary layer enthalpy difference and it is used for characterized heat dissipation. Mathematically,

$$Ec = \frac{u^2}{c_p \delta T}." [43]$$

2.8 Shooting Method

To elaborate the shooting method, take into account the subsequent nonlinear boundary value problem.

$$\left.\begin{aligned} h''(\zeta) - h(\zeta) + h^2(\zeta) = 0 \\ h'(0) = 0, \quad h(b) = 0. \end{aligned}\right\} \tag{2.4}$$

To reduce the order of the above BVP, introduce the following notations:

$$h(\zeta) = l_1, \quad h'(\zeta) = l_1' = l_2. \tag{2.5}$$

The system of first-order ordinary differential equations obtained from the conversion of (2.4) is given by:

$$l_1' = l_2, \qquad l_1(0) = 0. \tag{2.6}$$

$$l_2' = l_1^2 - l_1, \qquad l_2(0) = k, \tag{2.7}$$

where k is the initial condition which will be guessed. The $RK-4$ method will be used to numerically solve the above IVP. Choose missing condition k in such a way that

$$l_1(b,k) = 0. \tag{2.8}$$

The equation above can be solved using Newton's method with the iterative scheme provided:

$$k^{(m+1)} = k^{(m)} - \frac{l_1(b,k)^{(m)}}{\left(\frac{\partial\, l_1(b,k)}{\partial k}\right)^{(m)}} \tag{2.9}$$

To find $\left(\frac{\partial\, l_1(b,k)}{\partial k}\right)^{(m)}$, introduce the following notations:

$$\frac{\partial l_1}{\partial k} = l_3, \quad \frac{\partial l_2}{\partial k} = l_4. \tag{2.10}$$

With these new notations, Newton's iterative scheme will take the following form:

$$k^{(m+1)} = k^{(m)} - \frac{l_1(b,k)^{(m)}}{l_3(b,k)^{(m)}}. \tag{2.11}$$

Now, differentiating the system of two first order ODEs (2.6) and (2.7) regarding k, we obtain a different system of ODEs, as follows:

$$l_3' = l_4, \qquad l_3(0) = 0. \tag{2.12}$$

$$l_4' = 2l_1l_3 - l_3, \qquad l_4(0) = 1. \tag{2.13}$$

Writing all the four ODEs (2.6), (2.7), (2.12) and (2.13) together, following IVP is obtained:

$$\begin{aligned}
l_1' &= l_2, & l_1(0) &= 0.\\
l_2' &= l_1^2 - l_1, & l_2(0) &= k.\\
l_3' &= l_4, & l_3(0) &= 0.\\
l_4' &= 2l_1l_3 - l_3, & l_4(0) &= 1.
\end{aligned}$$

The above system together will be solved numericaly br $RK4$ method. The termination conditions for the Newton's technique is composed of:

$$|l_1(b,k)| < \epsilon,$$

where $\epsilon > 0$ is an arbitrary small positive number.

Chapter 3

Impact of Nanoparticle Diameter on Maxwell Nanofluid Flow with Thermophoretic Particle Deposition

3.1 Introduction

This chapter presents a thorough numerical study of a Maxwell nanofluid's flow characteristics, with graphene serving as the suspended nanoparticles and sodium alginate serving as the base fluid. In order to make this analysis easier, first use the relevant transformations to convert the controlling nonlinear partial differential equations into a set of dimensionless ordinary differential equations.

The shooting method implemented in MATLAB is then used to solve these dimensionless problems. In particular, the velocity profile $f'(\zeta)$, temperature profile $\theta(\zeta)$, and concentration profile $\chi(\zeta)$ are studied numerically for different parameters.

An extensive analysis of the work previously presented by Srilatha et al. [44] is provided in this chapter.

3.2 Physical Model

The behavior of a nanofluid flowing over a stretching sheet, specifically regarding two-dimensional, unsteady boundary layer flow, has been examined. In this setup, the coordinate axis along the stretched sheet is denoted as $\tilde{x}$, while that perpendicular to the sheet is $\tilde{y}$. Importantly, the wall is assumed to be incompressible, with the condition $\widetilde{u}_w(x) = \widetilde{u}$ as shown in Figure 3.1. The unsteady flow of nanofluid is governed by the following equations (3.1) - (3.4) along with the boundary conditions (3.5).

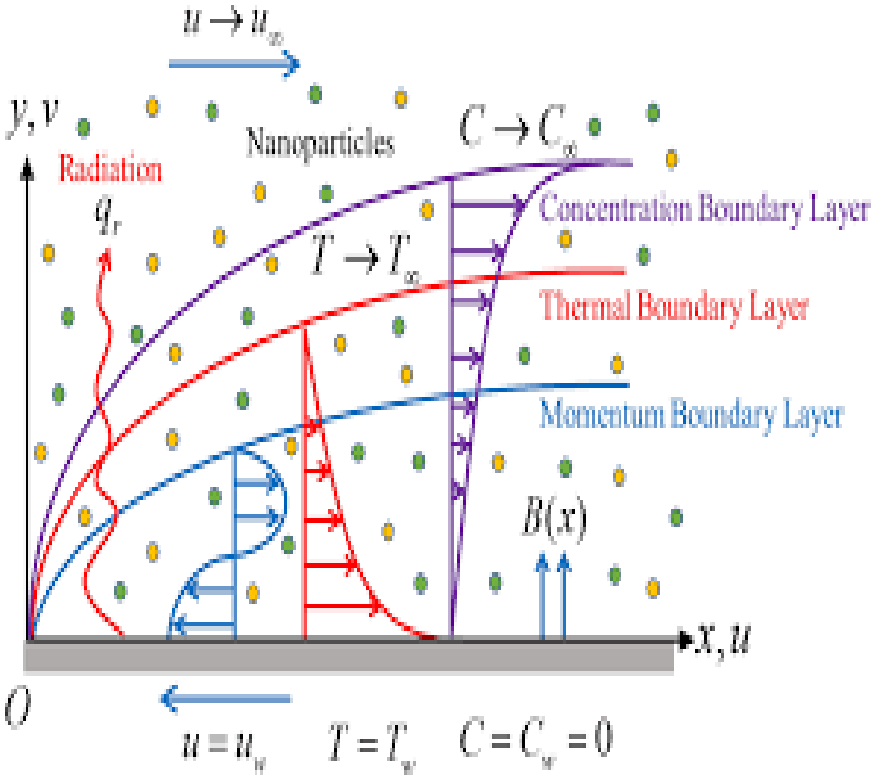

FIGURE 3.1: Problem schematic diagram[45]

Mass conservation equation:

$$\frac{\partial \widetilde{u}}{\partial \widetilde{x}} + \frac{\partial \widetilde{v}}{\partial \widetilde{y}} = 0. \tag{3.1}$$

Momentum equation:

$$\frac{\partial \widetilde{u}}{\partial \widetilde{t}}+\widetilde{u}\frac{\partial \widetilde{u}}{\partial \widetilde{x}}+\widetilde{v}\frac{\partial \widetilde{u}}{\partial \widetilde{y}}=\widetilde{\nu}_{nf}\frac{\partial^2 \widetilde{u}}{\partial \widetilde{y}^2}-\lambda_0\left(1-\alpha\widetilde{t}\right)\left(\widetilde{u}^2\frac{\partial^2 \widetilde{u}}{\partial \widetilde{x}^2}+\widetilde{v}^2\frac{\partial^2 \widetilde{u}}{\partial \widetilde{y}^2}+2\widetilde{u}\widetilde{v}\frac{\partial^2 \widetilde{u}}{\partial \widetilde{x}\partial \widetilde{y}}\right). \quad (3.2)$$

Energy equation:

$$\frac{\partial \widetilde{T}}{\partial \widetilde{t}}+\widetilde{u}\frac{\partial \widetilde{T}}{\partial \widetilde{x}}+\widetilde{v}\frac{\partial \widetilde{T}}{\partial \widetilde{y}}=\frac{\widetilde{k}_{nf}}{\left(\widetilde{\rho}\widetilde{C}_p\right)_{nf}}\frac{\partial}{\partial \widetilde{y}}\left(\frac{\partial \widetilde{T}}{\partial \widetilde{y}}\right)+\frac{1}{\left(\widetilde{\rho}\widetilde{C}_p\right)_{nf}}\widetilde{q}'''. \quad (3.3)$$

Concentration equation:

$$\frac{\partial \widetilde{C}}{\partial \widetilde{t}}+\widetilde{u}\frac{\partial \widetilde{C}}{\partial \widetilde{x}}+\widetilde{v}\frac{\partial \widetilde{C}}{\partial \widetilde{y}}=D\left(\frac{\partial^2 \widetilde{C}}{\partial \widetilde{x}^2}+\frac{\partial^2 \widetilde{C}}{\partial \widetilde{y}^2}\right)-\frac{\partial}{\partial \widetilde{y}}\left(\widetilde{V_T}\widetilde{C}\right). \quad (3.4)$$

Boundary conditions:

$$\left.\begin{aligned}
&\widetilde{u}=\widetilde{U}_w\left(\widetilde{x},\widetilde{t}\right)=\frac{\widetilde{a}\widetilde{x}}{\left(1-\alpha\widetilde{t}\right)},\ \ \widetilde{v}=\widetilde{V}_w=-\sqrt{\frac{\widetilde{\nu}_f\widetilde{U}_w}{\widetilde{x}}}\widetilde{f}_0,\\
&\widetilde{T}=\widetilde{T_w},\quad \widetilde{C}=\widetilde{C_w}=0,\ \ at\ \ \widetilde{y}=0,\\
&\widetilde{u}\longrightarrow 0,\quad \widetilde{T}\longrightarrow\widetilde{T}_\infty,\quad \widetilde{C}\longrightarrow\widetilde{C}_\infty,\quad as\ \ \widetilde{y}\longrightarrow\infty.
\end{aligned}\right\} \quad (3.5)$$

3.3 Non-dimensionalization

In this section, we outline the process of non-dimensionalizing the mathematical model for our Maxwell nanofluid flow. This procedure involves introducing dimensionless variables and parameters to simplify the original equations. By converting to dimensionless quantities, we gain deeper insights into the physical phenomena and enhance the manageability of the analysis. To accomplish this, the mathematical model will be transformed into a system of ordinary differential equations using the following similarity transformation:

$$\left.\begin{aligned}
&\zeta=\sqrt{\frac{\tilde{a}}{\widetilde{\nu}_f\left(1-\alpha\widetilde{t}\right)}}\widetilde{y},\ \ \tilde{u}=\frac{\tilde{a}\tilde{x}}{\left(1-\alpha\widetilde{t}\right)}f'(\zeta),\ \ \tilde{v}=-\sqrt{\frac{\tilde{a}\widetilde{\nu}_f}{\left(1-\alpha\widetilde{t}\right)}}f(\zeta),\\
&\theta(\zeta)=\frac{\widetilde{T}-\widetilde{T}_\infty}{\widetilde{T}_w-\widetilde{T}_\infty},\quad \chi(\zeta)=\frac{\widetilde{C}-\widetilde{C}_\infty}{\widetilde{C}_w-\widetilde{C}_\infty}.
\end{aligned}\right\} \quad (3.6)$$

To satisfy the mass conservation equation (3.1), the following derivatives are required:

$$\bullet \ \frac{\partial \tilde{u}}{\partial \tilde{x}} = \frac{\partial}{\partial \tilde{x}}\left[\frac{\tilde{a}\tilde{x}}{1-\alpha\tilde{t}} f'(\zeta)\right]$$
$$= \frac{\tilde{a}}{1-\alpha\tilde{t}} f'(\zeta). \tag{3.7}$$
$$\bullet \ \frac{\partial \tilde{v}}{\partial \tilde{y}} = \frac{\partial}{\partial \tilde{y}}\left[-\sqrt{\frac{\tilde{a}\tilde{\nu}_f}{1-\alpha\tilde{t}}} f(\zeta)\right]$$
$$= -\sqrt{\frac{\tilde{a}\tilde{\nu}_f}{1-\alpha\tilde{t}}} f'(\zeta).\frac{\partial \zeta}{\partial \tilde{y}}$$
$$= -\sqrt{\frac{\tilde{a}\tilde{\nu}_f}{1-\alpha\tilde{t}}} f'(\zeta).\sqrt{\frac{\tilde{a}}{\tilde{\nu}_f\left(1-\alpha\tilde{t}\right)}} \ \left(\text{using}(3.6)\right)$$
$$= -\frac{\tilde{a}}{1-\alpha\tilde{t}} f'(\zeta). \tag{3.8}$$

Finally, using equations (3.7) and (3.8) in (3.1), we obtain

$$\frac{\tilde{a}}{1-\alpha\tilde{t}} f'(\zeta) - \frac{\tilde{a}}{1-\alpha\tilde{t}} f'(\zeta) = 0.$$

Thus, equation (3.1) is identically satisfied.

The formulas for viscosity, density, heat capacity, thermal conductivity and electrical conductivity, along with the values for the fundamental thermo-physical properties of sodium alginate and graphene, have been summarized in Tables 3.1 and 3.2, [30, 44, 46].

TABLE 3.1: Formulas of Thermo-physical properties.

Properties	**Nanofluid**
Viscosity	$\tilde{\mu}_{nf} = \frac{\tilde{\mu}_f}{(1-\Phi)^{2.5}}$
Density	$\tilde{\rho}_{nf} = \tilde{\rho}_f(1-\Phi) + \Phi(\frac{\tilde{\rho}_s}{\tilde{\rho}_f})$
Heat Capacity	$(\tilde{\rho}\tilde{c}_p)_{nf} = (\tilde{\rho}\tilde{c}_p)_f(1-\Phi) + \Phi\frac{(\tilde{\rho}\tilde{c}_p)_s}{(\tilde{\rho}\tilde{c}_p)_f}$
Thermal Conductivity	$\frac{\tilde{K}_{nf}}{\tilde{K}_f} = \frac{\tilde{K}_s+(s_f-1)\tilde{K}_f-(s_f-1)\Phi(\tilde{K}_f-K_s)}{\tilde{K}_s+(s_f-1)\tilde{K}_f+\Phi(\tilde{K}_f-\tilde{K}_s)}$
Electrical Conductivity	$\frac{\tilde{\sigma}_{nf}}{\tilde{\sigma}_f} = \left(1+\frac{3\left(\frac{\sigma_s}{\sigma_f}-1\right)\phi}{\left(\frac{\sigma_s}{\sigma_f}+2\right)-\left(\frac{\sigma_s}{\sigma_f}-1\right)\phi}\right)$

TABLE 3.2: Thermo-physical characteristics of sodium alginate and graphene.

Physical Properties	*NaAlg*	*Graphene*
$\widetilde{\rho}\left(kg.m^{-3}\right)$	989	2250
$\widetilde{c_p}\left(J(kg.^ok)\right)$	4175	4179
$\widetilde{k}\left(W(m.^ok)\right)$	0.6376	2500
$\widetilde{\sigma}\left(\Omega.m\right)$	2.6×10^4	1×10^7

Some expressions involving the above thermo-physical properties, denoted by $\widetilde{P}_i$ $(i=1,2,3,4,5,6)$ have been defined below. These notations will simplify the dimensionless model to be achieved in the upcoming sections.

$$\widetilde{P}_1=\frac{\widetilde{\mu}_{nf}}{\widetilde{\mu}_f},\ \widetilde{P}_2=\frac{\widetilde{\rho}_{nf}}{\widetilde{\rho}_f},\ \widetilde{P}_3=\frac{\widetilde{P}_1}{\widetilde{P}_2},\ \widetilde{P}_4=\frac{(\widetilde{\rho c_p})_{nf}}{(\widetilde{\rho c_p})_f},\ \widetilde{P}_5=\frac{\widetilde{k}_{nf}}{\widetilde{k}_f},\ \widetilde{P}_6=\frac{\widetilde{\sigma}_{nf}}{\widetilde{\sigma}_f}.$$

3.3.1 Non-dimensionalization of Momentum Equation

For non-dimensionalization of the momentum equation (3.2), the following derivatives are needed:

- $$\begin{aligned}\frac{\partial\widetilde{u}}{\partial\widetilde{t}}&=\widetilde{a}\widetilde{x}\left(\frac{\alpha}{1-\alpha\widetilde{t}}f'(\zeta)+\frac{1}{1-\alpha\widetilde{t}}f''(\zeta)\frac{\widetilde{y}\sqrt{\widetilde{a}}}{\sqrt{\nu}_f}\left(-\frac{1}{2}\right)\left(1-\alpha\widetilde{t}\right)^{-\frac{3}{2}}(-\alpha)\right)\\&=\widetilde{a}\widetilde{x}\left(\frac{\alpha}{(1-\alpha\widetilde{t})^2}f'(\zeta)+\frac{\alpha}{2(1-\alpha\widetilde{t})^{\frac{5}{2}}}\frac{\widetilde{y}\sqrt{\widetilde{a}}}{\sqrt{\nu}_f}f''(\zeta)\right)\\&=\widetilde{a}\widetilde{x}\left(\frac{\alpha}{(1-\alpha\widetilde{t})^2}f'(\zeta)+\frac{\alpha}{2(1-\alpha\widetilde{t})^2}\sqrt{\frac{\tilde{a}}{\widetilde{\nu}_f\left(1-\alpha\widetilde{t}\right)}}\widetilde{y}f''(\zeta)\right)\\&=\frac{\widetilde{a}\widetilde{x}\alpha}{(1-\alpha\widetilde{t})^2}\left(f'(\zeta)+\frac{(\zeta)}{2}f''(\zeta)\right).\end{aligned}\tag{3.9}$$

- $\frac{\partial \widetilde{u}}{\partial \widetilde{x}} = \frac{\tilde{a}}{1-\alpha\widetilde{t}} f'(\zeta).$ (3.10)

- $\frac{\partial^2 \widetilde{u}}{\partial \widetilde{x}^2} = 0.$ (3.11)

- $$\begin{aligned}\frac{\partial \widetilde{u}}{\partial \widetilde{y}} &= \frac{\partial}{\partial \widetilde{y}}\left(\frac{\widetilde{a}}{1-\alpha\widetilde{t}}\widetilde{x} f'(\zeta)\right)\\ &= \frac{\widetilde{a}}{1-\alpha\widetilde{t}}\left(\widetilde{x} f''(\zeta)\frac{\partial}{\partial \widetilde{y}}(\zeta)\right)\\ &= \frac{\widetilde{a}}{1-\alpha\widetilde{t}}\left(\widetilde{x} f''(\zeta)\sqrt{\frac{\tilde{a}}{\widetilde{\nu}_f\left(1-\alpha\widetilde{t}\right)}}\right)\\ &= \frac{\widetilde{a}\sqrt{\widetilde{a}}}{(1-\alpha\widetilde{t})\sqrt{\widetilde{\nu}_f(1-\alpha\widetilde{t})}}\widetilde{x} f''(\zeta). \end{aligned}$$ (3.12)

(3.13)

- $$\begin{aligned}\frac{\partial^2 \widetilde{u}}{\partial \widetilde{y}^2} &= \frac{\partial}{\partial \widetilde{y}}\left(\frac{\partial \widetilde{u}}{\partial \widetilde{y}}\right)\\ &= \frac{\partial}{\partial \widetilde{y}}\left(\frac{\widetilde{a}\sqrt{\widetilde{a}}}{(1-\alpha\widetilde{t})\sqrt{\widetilde{\nu}_f(1-\alpha\widetilde{t})}}\widetilde{x} f''(\zeta)\right)\\ &= \frac{\widetilde{a}\sqrt{\widetilde{a}}}{(1-\alpha\widetilde{t})\sqrt{\widetilde{\nu}_f(1-\alpha\widetilde{t})}}\left(\widetilde{x} f''(\zeta)\sqrt{\frac{\tilde{a}}{\widetilde{\nu}_f\left(1-\alpha\widetilde{t}\right)}}\right)\\ &= \frac{\widetilde{a}^2}{\left(1-\alpha\widetilde{t}\right)^2\widetilde{\nu}_f}\left(\widetilde{x} f''(\zeta)\right). \end{aligned}$$ (3.14)

(3.15)

- $$\begin{aligned}\frac{\partial^2 \widetilde{u}}{\partial \widetilde{x}\partial \widetilde{y}} &= \frac{\partial}{\partial \widetilde{x}}\left(\frac{\partial \widetilde{u}}{\partial \widetilde{y}}\right)\\ &= \frac{\partial}{\partial \widetilde{x}}\left(\frac{\widetilde{a}\sqrt{\widetilde{a}}}{(1-\alpha\widetilde{t})\sqrt{\widetilde{\nu}_f(1-\alpha\widetilde{t})}}\widetilde{x} f''(\zeta)\right)\\ &= \frac{\widetilde{a}\sqrt{\widetilde{a}}}{(1-\alpha\widetilde{t})\sqrt{\widetilde{\nu}_f(1-\alpha\widetilde{t})}}\left(f''(\zeta) + x f''(\zeta)\frac{\partial}{\partial \widetilde{x}}(\zeta)\right)\\ &= \frac{\widetilde{a}\sqrt{\widetilde{a}}}{(1-\alpha\widetilde{t})\sqrt{\widetilde{\nu}_f(1-\alpha\widetilde{t})}} f''(\zeta). \end{aligned}$$ (3.16)

Now, we substitute all the partial derivatives (3.9) - (3.16), and velocity components (3.6), into equation (3.2), to get the following:

$$\frac{\widetilde{a}\widetilde{x}\alpha}{(1-\alpha\widetilde{t})^2}\left(f'+\frac{\zeta}{2}f''\right)+\left(\frac{\tilde{a}\tilde{x}}{1-\alpha\widetilde{t}}f'\right)\left(\frac{\tilde{a}}{1-\alpha\widetilde{t}}f'\right)-\left(\sqrt{\frac{\tilde{a}\widetilde{\nu}_f}{1-\alpha\widetilde{t}}}f\right)\left(\frac{\widetilde{a}\sqrt{\widetilde{a}}}{(1-\alpha\widetilde{t})\sqrt{\widetilde{\nu}_f(1-\alpha\widetilde{t})}}\widetilde{x}f''\right)=(\widetilde{\nu}_f)\left(\frac{\widetilde{a}^2}{\left(1-\alpha\widetilde{t}\right)^2\widetilde{\nu}_f}\widetilde{x}f''\right)$$

$$-\lambda_0\left(1-\alpha\widetilde{t}\right)\left[0+\left(\frac{\widetilde{a}\widetilde{\nu}_f}{1-\alpha\widetilde{t}}f^2\right)\left(\frac{\widetilde{a}^2}{\left(1-\alpha\widetilde{t}\right)^2\widetilde{\nu}_f}\widetilde{x}f''\right)-2\left(\frac{\tilde{a}\tilde{x}}{1-\alpha\widetilde{t}}f'\right)\left(\sqrt{\frac{\tilde{a}\widetilde{\nu}_f}{1-\alpha\widetilde{t}}}f\right)\left(\frac{\widetilde{a}\sqrt{\widetilde{a}}}{(1-\alpha\widetilde{t})\sqrt{\widetilde{\nu}_f(1-\alpha\widetilde{t})}}f''\right)\right].$$

$$\Rightarrow\quad\frac{\alpha}{\widetilde{a}}\left(f'+\frac{\zeta}{2}f''\right)+(f')^2-ff''=\frac{\widetilde{\nu}_n f}{\widetilde{\nu}_f}f'''-\lambda_0\widetilde{a}\left(f^2f'''-2ff'f''\right).$$

$$\Rightarrow\quad\gamma\left(f'+\frac{\zeta}{2}f''\right)+(f')^2-ff''=\frac{\widetilde{\nu}_n f}{\widetilde{\nu}_f}f'''-\beta\left(f^2f'''-2ff'f''\right).$$

$$\Rightarrow\quad\frac{\widetilde{\nu}_n f}{\widetilde{\nu}_f}f'''-\beta\left(f^2f'''-2ff'f''\right)-\gamma\left(f'+\frac{\zeta}{2}f''\right)-(f')^2+ff''=0.$$

$$\Rightarrow\quad\frac{\widetilde{P}_1}{\widetilde{P}_2}f'''-\beta\left(f^2f'''-2ff'f''\right)-\gamma\left(f'+\frac{\zeta}{2}f''\right)-(f')^2+ff''=0.$$

$$\Rightarrow\quad\widetilde{P}_3f'''-\beta\left(f^2f'''-2ff'f''\right)-\gamma\left(f'+\frac{\zeta}{2}f''\right)-(f')^2+ff''=0. \tag{3.17}$$

3.3.2 Non-dimensionalization of Energy Equation

For non-dimensionalization of the energy equation (3.3), the following derivatives are required:

$$\zeta=\sqrt{\frac{\tilde{a}}{\widetilde{\nu}_f\left(1-\alpha\widetilde{t}\right)}}\widetilde{y}$$
$$=\frac{\widetilde{y}\sqrt{\widetilde{a}}}{\sqrt{\widetilde{\nu}_f}}\left(1-\alpha\widetilde{t}\right)^{-\frac{1}{2}}.$$

- $\dfrac{\partial\zeta}{\partial\widetilde{t}} = \dfrac{\widetilde{y}\sqrt{\widetilde{a}}}{\sqrt{\widetilde{\nu}_f}}\left(-\dfrac{1}{2}\right)\left(1-\alpha\widetilde{t}\right)^{-\frac{3}{2}}(-\alpha)$

$$= \frac{\alpha\widetilde{y}\sqrt{\widetilde{a}}}{2\sqrt{\widetilde{\nu}_f}}\frac{1}{\sqrt{\left(1-\alpha\widetilde{t}\right)}}\frac{1}{1-\alpha\widetilde{t}}$$

$$= \frac{\alpha}{2\left(1-\alpha\widetilde{t}\right)}\sqrt{\frac{\tilde{a}}{\widetilde{\nu}_f\left(1-\alpha\widetilde{t}\right)}}\,\widetilde{y}$$

$$= \frac{\alpha\zeta}{2\left(1-\alpha\widetilde{t}\right)}.$$

$$\theta(\zeta) = \frac{\widetilde{T}-\widetilde{T}_\infty}{\widetilde{T}_w-\widetilde{T}_\infty}$$

$$\widetilde{T} = \widetilde{T}_\infty + (\widetilde{T}_w-\widetilde{T}_\infty)\theta(\zeta)$$

- $\dfrac{\partial\widetilde{T}}{\partial\widetilde{t}} = \dfrac{\partial}{\partial\widetilde{t}}(\theta(\widetilde{T}-\widetilde{T}_\infty))$

$$= (\widetilde{T}_w-\widetilde{T}_\infty)\theta'\frac{\partial\zeta}{\partial\widetilde{t}}$$

$$= (\widetilde{T}_w-\widetilde{T}_\infty)\theta'(\zeta)\frac{\alpha\zeta}{2\left(1-\alpha\widetilde{t}\right)}. \tag{3.18}$$

- $\dfrac{\partial\widetilde{T}}{\partial\widetilde{x}} = 0.$ (3.19)
- $\dfrac{\partial\widetilde{T}}{\partial\widetilde{y}} = \dfrac{\partial}{\partial\widetilde{y}}(\widetilde{T}_\infty + (\widetilde{T}_w-\widetilde{T}_\infty)\theta(\zeta))$

$$= \frac{\partial}{\partial\widetilde{y}}(\widetilde{T}_\infty) + \frac{\partial}{\partial\widetilde{y}}(\widetilde{T}_w-\widetilde{T}_\infty)\theta(\zeta)$$

$$= 0 + (\widetilde{T}_w-\widetilde{T}_\infty)\theta'(\zeta)\sqrt{\frac{\tilde{a}}{\widetilde{\nu}_f\left(1-\alpha\widetilde{t}\right)}}$$

$$= (\widetilde{T}_w-\widetilde{T}_\infty)\theta'\sqrt{\frac{\tilde{a}}{\widetilde{\nu}_f\left(1-\alpha\widetilde{t}\right)}}. \tag{3.20}$$

- $$\begin{aligned}\frac{\partial^2\widetilde{T}}{\partial\widetilde{y}^2} &= \frac{\partial}{\partial\widetilde{y}}\left(\frac{\partial\widetilde{T}}{\partial\widetilde{y}}\right)\\ &= \frac{\partial}{\partial\widetilde{y}}\left((\widetilde{T}_w-\widetilde{T}_\infty)\theta'\sqrt{\frac{\tilde{a}}{\widetilde{\nu}_f(1-\alpha\widetilde{t})}}\right)\\ &= (\widetilde{T}_w-\widetilde{T}_\infty)\sqrt{\frac{\tilde{a}}{\widetilde{\nu}_f(1-\alpha\widetilde{t})}}\left(\theta''(\zeta)\frac{\partial}{\partial\widetilde{y}}(\zeta)\right)\\ &= (\widetilde{T}_w-\widetilde{T}_\infty)\sqrt{\frac{\tilde{a}}{\widetilde{\nu}_f(1-\alpha\widetilde{t})}}\left(\theta''\sqrt{\frac{\tilde{a}}{\widetilde{\nu}_f(1-\alpha\widetilde{t})}}\right)\\ &= (\widetilde{T}_w-\widetilde{T}_\infty)\frac{\widetilde{a}}{\widetilde{\nu}_f\left(1-\alpha\widetilde{t}\right)}\theta''. \end{aligned} \tag{3.21}$$

Now we substitute all the partial derivatives (3.18) - (3.21), and velocity components from (3.6), into eqution (3.3), to get the following:

$$\begin{aligned}&(\widetilde{T}_w-\widetilde{T}_\infty)\theta'(\zeta)\frac{\alpha\zeta}{2\left(1-\alpha\widetilde{t}\right)}+0-\left(\sqrt{\frac{\tilde{a}\widetilde{\nu}_f}{1-\alpha\widetilde{t}}}f\right)\left((\widetilde{T}_w-\widetilde{T}_\infty)\theta'\sqrt{\frac{\tilde{a}}{\widetilde{\nu}_f(1-\alpha\widetilde{t})}}\right)\\ &\quad=\frac{\widetilde{k}_{nf}}{(\widetilde{\rho c}_p)_{nf}}(\widetilde{T}_w-\widetilde{T}_\infty)\frac{\widetilde{a}}{\widetilde{\nu}_f\left(1-\alpha\widetilde{t}\right)}\theta''\\ &\quad+\frac{1}{(\widetilde{\rho c}_p)_{nf}}\frac{\widetilde{k}_f\widetilde{U}_w\left(\widetilde{x},\widetilde{t}\right)}{\widetilde{x}\widetilde{\nu}_f}(\widetilde{T}_w-\widetilde{T}_\infty)\left[\widetilde{A}^*f'+\frac{\widetilde{T}-\widetilde{T}_\infty}{\widetilde{T}_w-\widetilde{T}_\infty}\widetilde{B}^*\right].\end{aligned}$$

$$\begin{aligned}\Rightarrow\quad &(\widetilde{T}_w-\widetilde{T}_\infty)\theta'(\zeta)\frac{\alpha\zeta}{2\left(1-\alpha\widetilde{t}\right)}-\frac{\widetilde{a}f\theta'}{1-\alpha\widetilde{t}}=\frac{\widetilde{k}_{nf}}{(\widetilde{\rho c}_p)_{nf}}(\widetilde{T}_w-\widetilde{T}_\infty)\frac{\widetilde{a}}{\widetilde{\nu}_f\left(1-\alpha\widetilde{t}\right)}\theta''\\ &+\frac{1}{(\widetilde{\rho c}_p)_{nf}}\widetilde{k}_f\frac{\frac{\widetilde{a}\widetilde{x}}{1-\alpha\widetilde{t}}}{\widetilde{x}\widetilde{\nu}_f}(\widetilde{T}_w-\widetilde{T}_\infty)(\widetilde{A}^*f'+\widetilde{B}^*\theta).\end{aligned}$$

$$\Rightarrow\quad \frac{\alpha}{\widetilde{a}}\frac{\theta'\zeta}{2}-f\theta'=\frac{\widetilde{k}_{nf}}{(\widetilde{\rho c}_p)_{nf}}\frac{\theta''}{\widetilde{\nu}_f}+\frac{\widetilde{k}_f}{(\widetilde{\rho c}_p)_{nf}\widetilde{\nu}_f}(\widetilde{A}^*f'+\widetilde{B}^*\theta).$$

$$\Rightarrow\quad \gamma\frac{\zeta}{2}\theta'-f\theta'=\frac{\widetilde{k}_{nf}}{(\widetilde{\rho c}_p)_{nf}}\frac{\theta''}{P_r\alpha_f}+\frac{\widetilde{k}_f}{(\widetilde{\rho c}_p)_{nf}P_r\alpha_f}(\widetilde{A}^*f'+\widetilde{B}^*\theta).$$

$$\Rightarrow\quad \gamma P_r(\frac{\zeta}{2}\theta')-P_r\left(f\theta'\right)=\frac{\widetilde{k}_{nf}}{(\widetilde{\rho c}_p)_{nf}}\frac{\theta''}{\alpha_f}+\frac{\widetilde{k}_f}{(\widetilde{\rho c}_p)_{nf}\alpha_f}(\widetilde{A}^*f'+\widetilde{B}^*\theta).$$

$$\Rightarrow\quad \gamma P_r(\frac{\zeta}{2}\theta')-P_r\left(f\theta'\right)=\frac{\widetilde{k}_{nf}}{(\widetilde{\rho c}_p)_{nf}}\frac{\theta''}{\frac{\widetilde{k}_f}{(\widetilde{\rho c}_p)}}+\frac{\widetilde{k}_f}{(\widetilde{\rho c}_p)_{nf}\frac{\widetilde{k}_f}{(\widetilde{\rho c}_p)}}(\widetilde{A}^*f'+\widetilde{B}^*\theta).$$

$$\Rightarrow\quad \gamma P_r(\frac{\zeta}{2}\theta')-P_r\left(f\theta'\right)=\frac{\widetilde{k}_{nf}}{(\widetilde{\rho c}_p)_{nf}}\frac{(\widetilde{\rho c}_p)_f\theta''}{\widetilde{k}_f}+\frac{\widetilde{k}_f(\widetilde{\rho c}_p)_f}{(\widetilde{\rho c}_p)_{nf}\widetilde{k}_f}(\widetilde{A}^*f'+\widetilde{B}^*\theta).$$

$$\Rightarrow \quad \gamma P_r(\frac{\zeta}{2}\theta') - P_r\,(f\theta') = \frac{(\widetilde{\rho c_p})_f}{(\widetilde{\rho c_p})_{nf}}\frac{\widetilde{k}_n f}{\widetilde{k}_f}\theta'' + \frac{(\widetilde{\rho c_p})_f}{(\widetilde{\rho c_p})_{nf}}(\widetilde{A}^* f' + \widetilde{B}^*\theta).$$

$$\Rightarrow \quad \frac{(\widetilde{\rho c_p})_f}{(\widetilde{\rho c_p})_{nf}}\frac{\widetilde{k}_n f}{\widetilde{k}_f}\theta'' - \gamma P_r\left(\frac{\zeta}{2}\theta'\right) - P_r\,(f\theta') + \frac{(\widetilde{\rho c_p})_f}{(\widetilde{\rho c_p})_{nf}}(\widetilde{A}^* f' + \widetilde{B}^*\theta) = 0. \tag{3.22}$$

3.3.3 Non-dimensionalization of Concentration Equation

For non-dimensionalization of the concentration equation (3.4), the following derivatives are required:

$$\begin{aligned}\zeta &= \sqrt{\frac{\tilde{a}}{\widetilde{\nu}_f\left(1-\alpha\widetilde{t}\right)}}\,\widetilde{y}\\ &= \frac{\widetilde{y}\sqrt{\widetilde{a}}}{\sqrt{\widetilde{\nu}_f}}\left(1-\alpha\widetilde{t}\right)^{-\frac{1}{2}}.\end{aligned}$$

- $$\begin{aligned}\frac{\partial\zeta}{\partial\widetilde{t}} &= \frac{\widetilde{y}\sqrt{\widetilde{a}}}{\sqrt{\widetilde{\nu}_f}}\left(-\frac{1}{2}\right)\left(1-\alpha\widetilde{t}\right)^{-\frac{3}{2}}(-\alpha)\\ &= \frac{\alpha\widetilde{y}\sqrt{\widetilde{a}}}{2\sqrt{\widetilde{\nu}_f}}\frac{1}{\sqrt{\left(1-\alpha\widetilde{t}\right)}}\frac{1}{1-\alpha\widetilde{t}}\\ &= \frac{\alpha}{2\left(1-\alpha\widetilde{t}\right)}\sqrt{\frac{\tilde{a}}{\widetilde{\nu}_f\left(1-\alpha\widetilde{t}\right)}}\,\widetilde{y}\\ &= \frac{\alpha\zeta}{2\left(1-\alpha\widetilde{t}\right)}\end{aligned}$$

- $$\begin{aligned}\chi(\zeta) &= \frac{\widetilde{C}-\widetilde{C}_\infty}{\widetilde{C}_w-\widetilde{T}_\infty}\\ \widetilde{C} &= \widetilde{C}_\infty + (\widetilde{C}_w-\widetilde{C}_\infty)\chi(\zeta).\end{aligned}$$

- $$\begin{aligned}\frac{\partial\widetilde{C}}{\partial\widetilde{t}} &= \frac{\partial}{\partial\widetilde{t}}(\chi(\widetilde{C}_w-\widetilde{C}_\infty))\\ &= (\widetilde{C}_w-\widetilde{C}_\infty)\chi'\frac{\partial\zeta}{\partial\widetilde{t}}\\ &= (\widetilde{C}_w-\widetilde{C}_\infty)\chi'(\zeta)\frac{\alpha\zeta}{2\left(1-\alpha\widetilde{t}\right)}.\end{aligned} \tag{3.23}$$

- $$\frac{\partial\widetilde{C}}{\partial\widetilde{x}} = 0. \tag{3.24}$$

- $$\frac{\partial^2\widetilde{C}}{\partial^2\widetilde{x}} = 0. \tag{3.25}$$

- $$\begin{aligned}\frac{\partial \widetilde{C}}{\partial \widetilde{y}} &= \frac{\partial}{\partial \widetilde{y}}(\widetilde{C}_\infty + (\widetilde{C}_w - \widetilde{C}_\infty)\chi(\zeta)) \\ &= \frac{\partial}{\partial \widetilde{y}}(\widetilde{C}_\infty) + \frac{\partial}{\partial \widetilde{y}}(\widetilde{C}_w - \widetilde{C}_\infty)\chi(\zeta) \\ &= 0 + (\widetilde{C}_w - \widetilde{C}_\infty)\chi'(\zeta)\sqrt{\frac{\tilde{a}}{\widetilde{\nu}_f(1-\alpha\widetilde{t})}} \\ &= (\widetilde{C}_w - \widetilde{C}_\infty)\chi'\sqrt{\frac{\tilde{a}}{\widetilde{\nu}_f(1-\alpha\widetilde{t})}}. \end{aligned} \tag{3.26}$$

- $$\begin{aligned}\frac{\partial^2 \widetilde{C}}{\partial \widetilde{y}^2} &= \frac{\partial}{\partial \widetilde{y}}\left(\frac{\partial \widetilde{C}}{\partial \widetilde{y}}\right) \\ &= \frac{\partial}{\partial \widetilde{y}}\left((\widetilde{C}_w - \widetilde{C}_\infty)\chi'\sqrt{\frac{\tilde{a}}{\widetilde{\nu}_f(1-\alpha\widetilde{t})}}\right) \\ &= (\widetilde{C}_w - \widetilde{C}_\infty)\sqrt{\frac{\tilde{a}}{\widetilde{\nu}_f(1-\alpha\widetilde{t})}}\left(\chi''(\zeta)\frac{\partial}{\partial \widetilde{y}}(\zeta)\right) \\ &= (\widetilde{C}_w - \widetilde{C}_\infty)\sqrt{\frac{\tilde{a}}{\widetilde{\nu}_f(1-\alpha\widetilde{t})}}\left(\chi''\sqrt{\frac{\tilde{a}}{\widetilde{\nu}_f(1-\alpha\widetilde{t})}}\right) \\ &= (\widetilde{C}_w - \widetilde{C}_\infty)\frac{\widetilde{a}}{\widetilde{\nu}_f\left(1-\alpha\widetilde{t}\right)}\chi''. \end{aligned} \tag{3.27}$$

- $$\begin{aligned}\frac{\partial}{\partial \widetilde{y}}(\widetilde{V_T}\widetilde{C}) &= \frac{\partial}{\partial \widetilde{y}}\left(-\widetilde{k}^*\frac{\widetilde{\nu}_f}{\widetilde{T}_r}\frac{\partial \widetilde{T}}{\partial \widetilde{y}}\widetilde{C}\right) \\ &= -\widetilde{k}^*\frac{\widetilde{\nu}_f}{\widetilde{T}_r}\frac{\partial}{\partial \widetilde{y}}\left(\frac{\partial \widetilde{T}}{\partial \widetilde{y}}\widetilde{C}\right) \\ &= -\widetilde{k}^*\frac{\widetilde{\nu}_f}{\widetilde{T}_r}\left(\frac{\partial^2 \widetilde{T}}{\partial \widetilde{y}^2}\widetilde{C} + \frac{\partial \widetilde{T}}{\partial \widetilde{y}}\frac{\partial \widetilde{C}}{\partial \widetilde{y}}\right) \\ &= -\widetilde{k}^*\frac{\widetilde{\nu}_f}{\widetilde{T}_r}\Bigg[(\widetilde{T}_w - \widetilde{T}_\infty)\frac{\widetilde{a}}{\widetilde{\nu}_f\left(1-\alpha\widetilde{t}\right)}\theta''(\widetilde{C}_\infty + (\widetilde{C}_w - \widetilde{C}_\infty)\chi(\zeta)) \\ &\quad + (\widetilde{T}_w - \widetilde{T}_\infty)\theta'\sqrt{\frac{\tilde{a}}{\widetilde{\nu}_f(1-\alpha\widetilde{t})}}(\widetilde{C}_w - \widetilde{C}_\infty)\chi'\sqrt{\frac{\tilde{a}}{\widetilde{\nu}_f(1-\alpha\widetilde{t})}}\Bigg] \\ &= -\widetilde{k}^*\frac{\widetilde{\nu}_f}{\widetilde{T}_r}(\widetilde{T}_w - \widetilde{T}_\infty)\left(\frac{\widetilde{a}}{\widetilde{\nu}_f\left(1-\alpha\widetilde{t}\right)}(\widetilde{C}_w - \widetilde{C}_\infty)\left(\theta''\chi + \theta'\chi'\right)\right) \\ &= \tau\frac{\widetilde{a}}{1-\alpha\widetilde{t}}(\widetilde{C}_w - \widetilde{C}_\infty)\left(\theta''\chi + \theta'\chi'\right). \end{aligned} \tag{3.28}$$

Now, we substitute all the partial derivatives (3.23) - (3.28), and velocity components from (3.6), into equation (3.4), to get the following:

$$
\begin{aligned}
&(\widetilde{C}_w - \widetilde{C}_\infty)\chi' \frac{\alpha\zeta}{2\left(1-\alpha\widetilde{t}\right)} - \left(\sqrt{\frac{\tilde{a}\widetilde{\nu}_f}{1-\alpha\widetilde{t}}} f\right)\left((\widetilde{C}_w - \widetilde{C}_\infty)\chi' \sqrt{\frac{\tilde{a}}{\widetilde{\nu}_f\left(1-\alpha\widetilde{t}\right)}}\right) \\
&= \frac{\widetilde{\nu}_f}{\widetilde{S}_c}(\widetilde{C}_w - \widetilde{C}_\infty)\frac{\widetilde{a}}{\widetilde{\nu}_f\left(1-\alpha\widetilde{t}\right)}\chi'' - \tau\frac{\widetilde{a}}{1-\alpha\widetilde{t}}(\widetilde{C}_w - \widetilde{C}_\infty)\left(\theta''\chi + \theta'\chi'\right)
\end{aligned}
$$

$$
\Rightarrow \quad \frac{\alpha}{\widetilde{a}}\frac{\zeta}{2}\chi' - f\chi' = \frac{1}{\widetilde{S}_c}\chi'' - \tau\left(\theta''\chi + \theta'\chi'\right).
$$

$$
\Rightarrow \quad \gamma\frac{\zeta}{2}\chi' - f\chi' = \frac{1}{\widetilde{S}_c}\chi'' - \tau\left(\theta''\chi + \theta'\chi'\right).
$$

$$
\Rightarrow \quad \frac{1}{\widetilde{S}_c}\chi'' - \gamma\frac{\zeta}{2}\chi' + f\chi' - \tau\left(\theta''\chi + \theta'\chi'\right) = 0. \tag{3.29}
$$

3.3.4 Non-dimensionalization of Boundary Conditions

The boundary conditions are reformulated in to their non-dimensional form according to the following procedure:

- $\widetilde{u} = \widetilde{U}_w\left(\widetilde{x}, \widetilde{t}\right)$ $\quad at \quad \tilde{y} = 0.$

  $\Rightarrow \quad \dfrac{\widetilde{a}\widetilde{x}}{\left(1-\alpha\widetilde{t}\right)} f'(\zeta) = \dfrac{\widetilde{a}\widetilde{x}}{\left(1-\alpha\widetilde{t}\right)}$ $\quad at \quad \zeta = 0.$

  $\Rightarrow \quad f'(\zeta) = 1$ $\quad at \quad \zeta = 0.$

  $\Rightarrow \quad f'(0) = 1$ $\quad at \quad \zeta = 0.$

- $\widetilde{v} = \widetilde{v}_w = -\sqrt{\dfrac{\widetilde{\nu}_f \widetilde{U}_w}{\widetilde{x}}}\widetilde{f}_0$ $\quad at \quad y = 0.$

  $\Rightarrow \quad -\sqrt{\dfrac{\tilde{a}\widetilde{\nu}_f}{\left(1-\alpha\widetilde{t}\right)}} f(\zeta) = -\sqrt{\dfrac{\widetilde{\nu}_f \frac{\widetilde{a}\widetilde{x}}{\left(1-\alpha\widetilde{t}\right)}}{\widetilde{x}}}\widetilde{f}_0$ $\quad at \quad \zeta = 0.$

  $\Rightarrow \quad f(\zeta) = \widetilde{f}_0$ $\quad at \quad \zeta = 0.$

  $\Rightarrow \quad f(0) = \widetilde{f}_0$ $\quad at \quad \zeta = 0.$

- $\widetilde{T} = \widetilde{T}_w$

  $\Rightarrow \quad \widetilde{T}_\infty + \left(\widetilde{T}_w - \widetilde{T}_\infty\right)\theta(\zeta) = \widetilde{T}_w \qquad at \quad \zeta = 0.$

  $\Rightarrow \quad \left(\widetilde{T}_w - \widetilde{T}_\infty\right)\theta(\zeta) = \widetilde{T}_w - \widetilde{T}_\infty \qquad at \quad \zeta = 0.$

  $\Rightarrow \quad \theta(\zeta) = 1 \qquad at \quad \zeta = 0.$

  $\Rightarrow \quad \theta(0) = 1 \qquad at \quad \zeta = 0.$

- $\widetilde{C} = \widetilde{C}_w$

  $\Rightarrow \quad \widetilde{C}_\infty + \left(\widetilde{C}_w - \widetilde{C}_\infty\right)\chi(\zeta) = \widetilde{C}_w \qquad at \quad \zeta = 0.$

  $\Rightarrow \quad \left(\widetilde{C}_w - \widetilde{C}_\infty\right)\chi(\zeta) = \widetilde{C}_w - \widetilde{C}_\infty \qquad at \quad \zeta = 0.$

  $\Rightarrow \quad \chi(\zeta) = 0 \qquad at \quad \zeta = 0.$

  $\Rightarrow \quad \chi(0) = 0 \qquad at \quad \zeta = 0.$

- $\widetilde{u} \longrightarrow 0 \qquad as \widetilde{y} \longrightarrow \infty.$

  $\Rightarrow \quad \dfrac{\widetilde{a}\widetilde{x}}{\left(1 - \alpha\widetilde{t}\right)} f'(\zeta) \longrightarrow 0 \qquad as \zeta \longrightarrow \infty.$

  $\Rightarrow \quad f'(\zeta) \longrightarrow 0 \qquad as \zeta \longrightarrow \infty.$

  $\Rightarrow \quad f'(\infty) \longrightarrow 0$

- $\widetilde{T} \longrightarrow \widetilde{T}_\infty \qquad as \widetilde{y} \longrightarrow \infty.$

  $\Rightarrow \quad \widetilde{T}_\infty + \left(\widetilde{T}_w - \widetilde{T}_\infty\right)\theta(\zeta) \longrightarrow \widetilde{T}_\infty \qquad as \zeta \longrightarrow \infty.$

  $\Rightarrow \quad \left(\widetilde{T}_w - \widetilde{T}_\infty\right)\theta(\zeta) \longrightarrow 0 \qquad as \zeta \longrightarrow \infty.$

  $\Rightarrow \quad \theta(\zeta) \longrightarrow 0 \qquad as \zeta \longrightarrow \infty.$

  $\Rightarrow \quad \theta(\infty) \longrightarrow 0$

- $\widetilde{C} \longrightarrow \widetilde{C}_\infty \qquad as \widetilde{y} \longrightarrow \infty.$

  $\Rightarrow \quad \widetilde{C}_\infty + \left(\widetilde{C}_w - \widetilde{C}_\infty\right)\chi(\zeta) \longrightarrow \widetilde{C}_\infty \qquad as \zeta \longrightarrow \infty.$

$$\Rightarrow \quad (\widetilde{C}_w - \widetilde{C}_\infty)\chi(\zeta) \longrightarrow 0 \qquad as\, \zeta \longrightarrow \infty.$$

$$\Rightarrow \quad \chi(\zeta) \longrightarrow 0 \qquad as\, \zeta \longrightarrow \infty.$$

$$\Rightarrow \quad \chi(\infty) \longrightarrow 0$$

3.3.5 Physical Quantities of interest

The physical quantities of interest are the skin friction coefficient C_f, the Nusselt number N_u, and the Sherwood number S_h. The formulas for these quantities are as follows:

Skin friction:

$$C_f = \frac{\widetilde{\tau}_w}{\widetilde{\rho}_{nf}\widetilde{U}_w^2\,(x,t)}.$$

Nusselt number:

$$N_u = \frac{\tilde{x}\widetilde{q}_w}{\widetilde{k}_{nf}\left(\widetilde{T}_w - \widetilde{T}_\infty\right)}.$$

Sherwood number:

$$S_h = \frac{\widetilde{x}\widetilde{q}_m}{D\left(\widetilde{C}_w - \widetilde{C}_\infty\right)}.$$

3.4 Solution Framework

To solve the ODE (3.16), the shooting method has been applied. The notations utilized in this work are as follows:

$$f(\zeta) = \widetilde{Y}_1, \qquad f'(\zeta) = \widetilde{Y}_1' = \widetilde{Y}_2, \qquad f''(\zeta) = \widetilde{Y}_2' = \widetilde{Y}_3.$$

The momentum equation is then, represented by the following system of first-order ODEs:

$$\widetilde{Y}_1' = \widetilde{Y}_2, \qquad \widetilde{Y}_1(0) = f_0,$$
$$\widetilde{Y}_2' = \widetilde{Y}_3, \qquad \widetilde{Y}_2(0) = 1,$$
$$\widetilde{Y}_3' = -\frac{2\beta\widetilde{Y}_1\widetilde{Y}_2\widetilde{Y}_3 - \gamma\left(\widetilde{Y}_2 + \frac{\zeta}{2}\widetilde{Y}_3\right) - \widetilde{Y}_2^2 + \widetilde{Y}_1\widetilde{Y}_3}{\widetilde{P}_3 - \beta\widetilde{Y}_1^2}, \qquad \widetilde{Y}_3(0) = l.$$

To apply the RK4 method for numerically IVP described above, it is essential to carefully select the missing condition l within the system of equations. This condition l should be chosen to ensure that:

$$\widetilde{Y}_2\big(\zeta_\infty, l\big) = 0.$$

Newton's method will be used to find l. This method has the following iterative scheme:

$$l^{(n+1)} = l^{(n)} - \frac{\widetilde{Y}_2\big(\zeta_\infty, l^{(n)}\big)}{\left(\frac{\partial}{\partial \widetilde{s}}\widetilde{Y}_2\big(\zeta_\infty, l\big)\right)^{(n)}}.$$

We further introduce the following notations:

$$\frac{\partial \widetilde{Y}_1}{\partial l} = \widetilde{Y}_4, \qquad \frac{\partial \widetilde{Y}_2}{\partial l} = \widetilde{Y}_5, \qquad \frac{\partial \widetilde{Y}_3}{\partial l} = \widetilde{Y}_6.$$

These additional notations give Newton's iterative scheme the following form:

$$l^{(n+1)} = l^{(n)} - \frac{\widetilde{Y}_2\big(\zeta_\infty, l^{(n)}\big)}{\widetilde{Y}_5\big(\zeta_\infty, l^{(n)}\big)}.$$

Now, differentiating the most recently presented system of three first order ODEs with respect to l, yields an additional system of ODEs, as detailed below:

$$\widetilde{Y}_4' = \widetilde{Y}_5, \qquad \widetilde{Y}_4(0) = 0,$$
$$\widetilde{Y}_5' = \widetilde{Y}_6, \qquad \widetilde{Y}_5(0) = 0,$$
$$\widetilde{Y}_6' = -\Bigg[\left(\frac{1}{\widetilde{P}_3 - \beta \widetilde{Y}_1^{\,2}} \right)^2 \left(\widetilde{P}_3 - \beta \widetilde{Y}_1^{\,2} \right) \left(2\beta \left(\widetilde{Y}_1 \widetilde{Y}_2 \widetilde{Y}_6 + \widetilde{Y}_1 \widetilde{Y}_5 \widetilde{Y}_3 + \widetilde{Y}_4 \widetilde{Y}_2 \widetilde{Y}_3 \right) \right)$$
$$- \gamma \left(\widetilde{Y}_5 + \frac{\zeta}{2} \widetilde{Y}_6 \right) - 2\widetilde{Y}_2 \widetilde{Y}_5 + \widetilde{Y}_1 \widetilde{Y}_6 + \widetilde{Y}_4 \widetilde{Y}_3 - 2\beta \widetilde{Y}_1 \widetilde{Y}_2 \widetilde{Y}_3 - \gamma \left(\widetilde{Y}_2 + \frac{\zeta}{2} \widetilde{Y}_3 \right)$$
$$- \widetilde{Y}_2^2 + \widetilde{Y}_1 \widetilde{Y}_3 \left(-2\beta \widetilde{Y}_1 \widetilde{Y}_4 \right) \Bigg], \qquad \widetilde{Y}_6(0) = 1.$$

The termination criteria for the Newton's techniques is set as:

$$\left| \widetilde{Y}_2(\zeta_\infty, l) \right| < \epsilon,$$

where $\epsilon > 0$ represents an arbitrarily small positive number. For the purposes of this analysis, ϵ has been set to 10^{-6}.

To numerically solve the energy equation using the shooting method, we will treat f and f'' as known functions. The following notations will be used to implement the shooting method:

$$\theta = \widetilde{Z}_1, \qquad \theta' = \widetilde{Z}_1' = \widetilde{Z}_2'.$$

The energy equation can be expressed as the following system of coupled first-order ODEs:

$$\widetilde{Z}_1' = \widetilde{Z}_2, \qquad \widetilde{Z}_1(0) = 1,$$
$$\widetilde{Z}_2' = \frac{\widetilde{p}_4}{\widetilde{P}_5} \left(\gamma P_r \left(\frac{\zeta}{2} \widetilde{Z}_2 \right) + P_r \left(\widetilde{d}_1 \widetilde{Z}_2 \right) + \frac{A^* \widetilde{d}_2 + B^* \widetilde{Z}_1}{\widetilde{P}_4} \right), \qquad \widetilde{Z}_2(0) = m.$$

To apply the RK4 method for the numerical solution of the initial value problem described above, it is crucial to carefully select the condition m within the system of equations. This condition m must be chosen to ensure that:

$$\widetilde{Z}_1(\zeta_\infty, m) = 0.$$

Newton's method will be employed to determine m using the following iterative scheme:

$$m^{(n+1)} = m^{(n)} - \frac{\widetilde{Z}_1\big(\zeta_\infty, m^{(n)}\big)}{\Big(\frac{\partial}{\partial \widetilde{m}}\widetilde{Z}_1\big(\zeta_\infty, m\big)\Big)^{(n)}}.$$

We further introduce the following notations:

$$\frac{\partial \widetilde{Z}_1}{\partial m} = \widetilde{Z}_3, \qquad \frac{\partial \widetilde{Z}_2}{\partial m} = \widetilde{Z}_4.$$

These additional notations give Newton's iterative scheme the following form:

$$m^{(n+1)} = m^{(n)} - \frac{\widetilde{Z}_1\big(\zeta_\infty, m^{(n)}\big)}{\widetilde{Z}_3\big(\zeta_\infty, m^{(n)}\big)}.$$

Now, differentiating the system of two first order ODEs with respect to m, we get another system of ODEs, as follows:

$$\widetilde{Z}_3' = \widetilde{Z}_4, \qquad \widetilde{Z}_3(0) = 1,$$
$$\widetilde{Z}_4' = \frac{\widetilde{p}_4}{\widetilde{P}_5}\left(\gamma P_r\left(\frac{\zeta}{2}\widetilde{Z}_4\right) + P_r\left(\widetilde{d}_1\widetilde{Z}_4\right) + \frac{B^*\widetilde{Z}_3}{\widetilde{P}_4}\right), \qquad \widetilde{Z}_4(0) = 0.$$

The stopping criteria for the Newton's technique is set as:

$$\left|\widetilde{Z}_1\big(\zeta_\infty, m\big)\right| < \epsilon.$$

To numerically solve the concentration equation using the shooting method, we will treat f as a known function. The following notations will be used for implementing the shooting method:

$$\chi = \widetilde{Q}_1, \qquad \chi' = \widetilde{Q}_1' = \widetilde{Q}_2'.$$

The energy equation can be formulated as the following system of first-order coupled ODEs:

$$\begin{aligned}
&\widetilde{Q}_1' = \widetilde{Q}_2, && \widetilde{Q}_1(0) = 0,\\
&\widetilde{Q}_2' = \widetilde{S}_c\Bigg[\gamma\frac{\zeta}{2}\widetilde{Q}_2 - \widetilde{d}_1\widetilde{Q}_2 + \tau\Bigg(\frac{\widetilde{p}_4}{\widetilde{P}_5}\Bigg(\gamma P_r\left(\frac{\zeta}{2}\widetilde{Z}_2\right) + P_r\left(\widetilde{d}_1\widetilde{Z}_2\right)\\
&\qquad + \frac{A^*\widetilde{d}_2 + B^*\widetilde{Z}_1}{\widetilde{P}_4}\Bigg)\widetilde{Q}_1 + \widetilde{Z}_2\widetilde{Q}_2\Bigg)\Bigg], && \widetilde{Q}_2(0) = r.
\end{aligned}$$

To apply the RK4 method for the numerical solution of the initial value problem outlined above, it is essential to carefully select the condition r within the system of equations. This condition r should be chosen to ensure that:

$$\widetilde{Q}_1\big(\zeta_\infty, r\big) = 0.$$

Newton's method will be used to find r with the following iterative scheme:

$$r^{(n+1)} = r^{(n)} - \frac{\widetilde{Q}_1\big(\zeta_\infty, r^{(n)}\big)}{\Big(\frac{\partial}{\partial \tilde{s}}\widetilde{Q}_1\big(\zeta_\infty, r\big)\Big)^{(n)}}.$$

We further introduce the following notations:

$$\frac{\partial\widetilde{Q}_1}{\partial r} = \widetilde{Q}_3, \qquad \frac{\partial\widetilde{Q}_2}{\partial r} = \widetilde{Q}_4.$$

These additional notations give Newton's iterative scheme the following form:

$$r^{(n+1)} = r^{(n)} - \frac{\widetilde{Q}_1\big(\zeta_\infty, r^{(n)}\big)}{\widetilde{Q}_3\big(\zeta_\infty, r^{(n)}\big)}.$$

Now, differentiating the system of two first order ODEs with respect to r, we get another system of ODEs, as follows:

$$\widetilde{Q}_3' = \widetilde{Q}_4, \qquad \widetilde{Q}_3(0) = 0,$$

$$\widetilde{Q}_4' = \widetilde{S}_c\Bigg[\gamma\frac{\zeta}{2}\widetilde{Q}_4 - \widetilde{d}_1\widetilde{Q}_4 + \tau\Bigg(\frac{\widetilde{p}_4}{\widetilde{P}_5}\Bigg(\gamma P_r\left(\frac{\zeta}{2}\widetilde{Z}_2\right) + P_r\left(\widetilde{d}_1\widetilde{Z}_2\right) + \frac{A^*\widetilde{d}_2 + B^*\widetilde{Z}_1}{\widetilde{P}_4}\Bigg)\widetilde{Q}_3 + \widetilde{Z}_2\widetilde{Q}_4\Bigg)\Bigg], \qquad \widetilde{Q}_4(0) = 1.$$

The termination conditions for the Newton's technique is composed of:

$$\left|\widetilde{Q}_1\big(\zeta_\infty, r\big)\right| < \epsilon.$$

3.5 Results Interpretation

This section focuses on analyzing the physical characteristics of velocity, energy and concentration profiles in relation to variations in several key physical parameters, including Deborah number (β), unsteadiness parameter (γ), space dependent heat source or sink (A^*), temperature dependent heat source or sink (B^*), Schmidt number (S_c), thermophoretic parameters (τ).

The analysis is performed using graphical representations of velocity, temperature and concentration profiles. Additionally, the effects of changing dimensionless parameters on physical quantities such as skin friction, Nusselt number and the sherwood number are investigated and summarized in the tabular form.

The graphical representations of velocity, temperature and concentration profiles offer valuable visual insights into the system's behavior as the physical parameters change. By examining these profiles, one can gain a clear understanding of the dynamics of various physical characteristics of the system. These visualizations facilitate the analysis of how variations in the parameters β, γ, A^*, B^*, S_c and τ leave an impact on the velocity, temperature and concentration profiles.

3.5.1 Analysis of Computational Results

Table 3.3 represents the results of skin fiction, for different inputs of β, γ, f_0 and ϕ. These results reveal that an increase in the value of β, γ and f_0 leads to augment the value of skin friction coefficient. In contrast, a higher value of ϕ results in a decrease in the skin friction coefficient.

Tables 3.4 and 3.5 show that an increases in the value of $A^*, B^* < 0$ and $A^*, B^* > 0$ decreases the value of Nusselt number, whereas Tables 3.6 and 3.7 reflect a decrement in the Sherwood number due to rise in the values of S_c ands τ.

TABLE 3.3: The skin friction coefficient

β	γ	f_0	ϕ	-$f''(0)$
0.1	0.1	0	0.01	1.052963
0.2				1.077357
0.3				1.101387
0.4				1.125052
0.5				1.148352
	0.2			1.085540
	0.3			1.117821
	0.4			1.149719
	0.5			1.181158
		-0.3		0.893694
		-0.2		0.942978
		-0.1		0.995965
		0.1		1.114317
		0.2		1.180406
		0.3		1.251654
			0	1.059527
			0.05	1.024993
			0.1	0.986405
			0.2	0.898546

TABLE 3.4: The Nusselt number for $A^*, B^* < 0$

β	γ	f_0	ϕ	A^*	B^*	N_u
0.1	0.1	0	0.01	-0.5	-0.5	2.924132
0.2						2.913703
0.3						2.903535
0.4						2.893618
0.5						2.885834
	0.2					2.835834
	0.3					2.746123
	0.4					2.665735
	0.5					2.593081
		-0.3				0.925723
		-0.2				1.447538
		-0.1				2.120091
		0.1				3.834959
		0.2				4.828873
		0.3				5.886044
			0			2.881918
			0.05			3.098460
			0.1			3.330697
			0.2			3.858513
				-0.4		2.881443
				-0.3		2.838754
				-0.2		2.796065
				-0.1		2.753375
					-0.4	2.908096
					-0.3	2.892004
					-0.2	2.875854
					-0.1	2.859647

TABLE 3.5: The Nusselt number for $A^*, B^* > 0$

β	γ	f_0	ϕ	A^*	B^*	N_u
0.1	0.1	0	0.01	0.1	0.1	2.556853
0.2						2.550144
0.3						2.543465
0.4						2.536822
0.5						2.530219
	0.2					2.452885
	0.3					2.340645
	0.4					2.185534
	0.5					2.178722
		-0.3				0.624655
		-0.2				1.116794
		-0.1				1.767405
		0.1				3.459463
		0.2				4.450486
		0.3				5.509134
			0			2.519002
			0.05			2.713142
			0.1			2.921296
			0.2			3.394291
				0.2		2.511818
				0.3		2.466784
				0.4		2.421749
				0.5		2.376714
					0.2	2.537941
					0.3	2.518912
					0.4	2.499765
					0.5	2.480496

TABLE 3.6: The Sherwood number for $A^*, B^* < 0$

β	γ	f_0	ϕ	A^*	B^*	$\widetilde{S}_c$	τ	S_h
0.1	0.1	0	0.01	-0.5	-0.5	1	0.1	-0.563530
0.2								-0.553747
0.3								-0.544378
0.4								-0.535388
0.5								-0.526768
	0.2							-0.510093
	0.3							-0.446969
	0.4							-0.371070
	0.5							-0.284326
		-0.3						-0.394718
		-0.2						-0.447476
		-0.1						-0.503810
		0.1						-0.626279
		0.2						-0.691869
		0.3						-0.760016
			0					-0.562567
			0.05					- 0.567866
			0.1					-0.574597
			0.2					-0.591728
				-0.4				-0.558467
				-0.3				-0.553493
				-0.2				-0.548579
				-0.1				-0.543725
					-0.4			-0.563316
					-0.3			-0.563131
					-0.2			-0.562946
					-0.1			-0.562763
						1.2		-0.644076
						1.4		-0.721404
						1.6		-0.795459
						1.8		-0.866470
							0.3	-0.628805
							0.5	-0.699627
							0.7	-0.776436
							0.9	-0.859797

TABLE 3.7: The Sherwood number for $A^*, B^* > 0$

β	γ	f_0	ϕ	A^*	B^*	$\widetilde{S}_c$	τ	S_h
0.1	0.1	0	0.01	0.1	0.1	1	0.1	-0.531178
0.2								-0.523207
0.3								-0.515473
0.4								-0.507985
0.5								-0.500742
	0.2							-0.478497
	0.3							-0.417226
	0.4							-0.346437
	0.5							-0.268987
		-0.3						-0.362713
		-0.2						-0.415294
		-0.1						-0.471508
		0.1						-0.594094
		0.2						-0.660020
		0.3						-0.728713
			0					-0.529613
			0.05					-0.537824
			0.1					-0.546987
			0.2					-0.526207
				0.2				-0.521299
				0.3				-0.516454
				0.4				-0.511669
				0.5				-0.530657
					0.2			-0.530129
					0.3			-0.529596
					0.4			-0.529056
					0.5			-0.602559
						1.2		-0.796545
						1.4		-0.527936
						1.6		-0.795459
						1.8		-0.866470
							0.3	-0.527936
							0.5	-0.524683
							0.7	-0.521415
							0.9	-0.518128

3.5.2 Velocity Profile

Insights into the velocity profile, denoted as $f'(\zeta)$, with respect to various physical parameters have deen presented. Specifically, Figures 3.2 - 3.5 illustrate the impact of β, γ, f_0 and ϕ on the dimensionless velocity $f'(\zeta)$. Figure 3.2 displays the effect of Deborah number on the velocity profile. It reflects a significant reduction in velocity profile as the value of β increases. The Deborah number indicates a measure of fluid's viscoelasticity. When working with viscoelastic liquids, which are elastic and viscous, this value is crucial. Higher Deborah number values inhibit fluid's mobility and reduce the velocity profile. The effect of γ on the velocity profile is displayed in Figure 3.3. There is a noticeable decline in the velocity profile as γ values rise, which suggests that the momentum boundary layer close to the wall is getting smaller. The influence of f_0 on velocity distribution is shown in 3.4. In the boundary layer, suction $f_0 > 0$ results in a decreased fluid velocity. The velocity significantly drops as the suction parameter increases. The fluid's velocity increases as a result of injection $f_0 < 0$. As the injection parameter is increased, the velocity profile exhibits a rising trend. Suction reduces the boundary layer velocity, while injection enhances it.

Figure 3.5 illustrates the effects of ϕ on the dimensionless velocity $f'(\zeta)$. It is observed that there is a significant gain in the flow velocity as the values of this parameter increase. When nanoparticles are added to the base fluid, the average heat absorption capacity is reduced overall. As a result, this change in the heat absorption properties causes the fluid's velocity profile to rise.

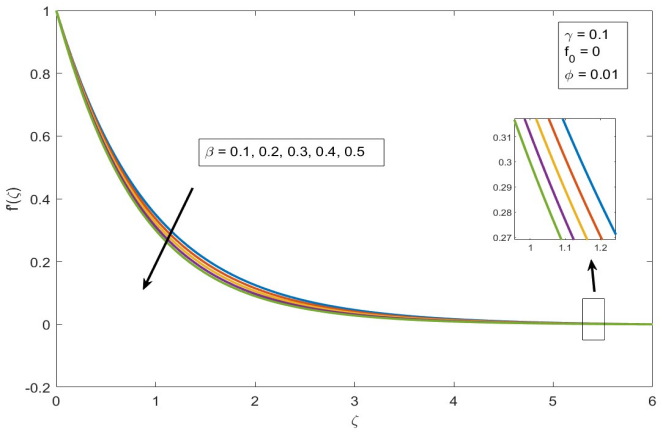

FIGURE 3.2: Impact of β on velocity profile $f'(\zeta)$

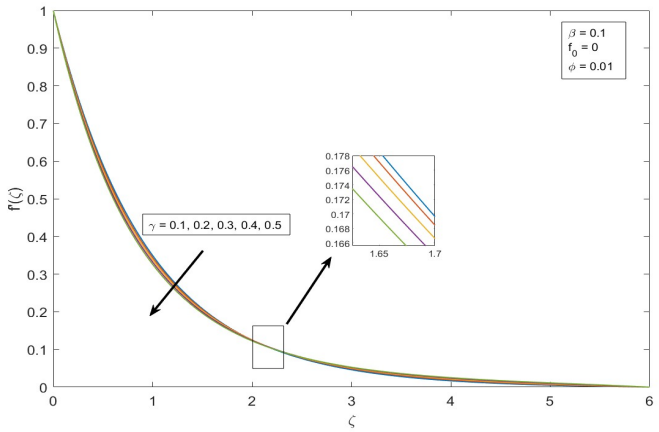

FIGURE 3.3: Impact of γ on velocity profile $f'(\zeta)$

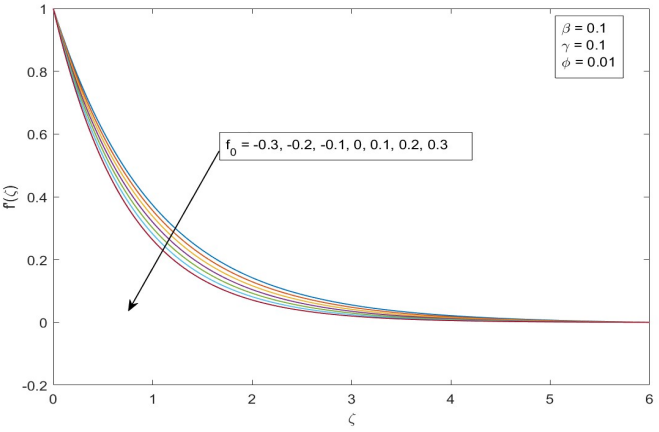

FIGURE 3.4: Impact of f_0 on velocity profile $f'(\zeta)$

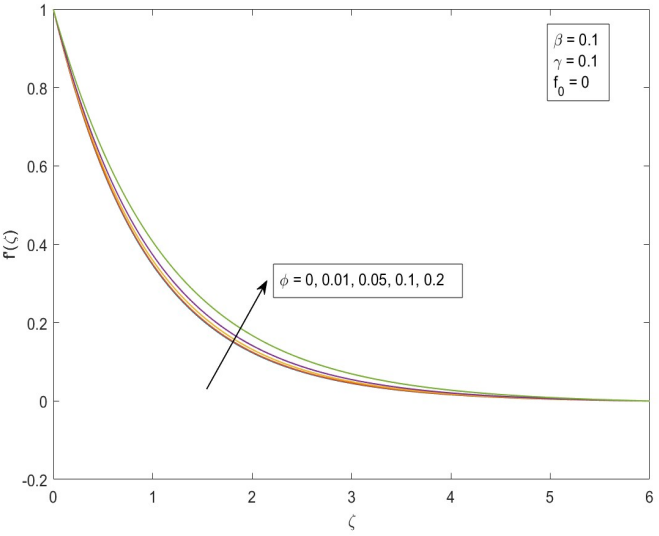

FIGURE 3.5: Impact of ϕ on velocity profile $f'(\zeta)$

3.5.3 Temperature Profile

Figures 3.6 - 3.7 illustrate the impact of heat source and heat sink on the temperature profile. By adding more heat to the system, a heat source scenario ($A^*, B^* > 0$) improves the thermal conductivity and raises the temperature profile. The temperature of the nanofluid rises when a heat source is present. Removing heat from the system, namely the heat sink ($A^*, B^* < 0$) lowers the temperature profile. When the heat sink parameter is increased, the temperature profile becomes less pronounced. A heat sink lowers the temperature by taking heat out of the system, whereas a heat source raises the temperature profile by adding more heat to the system. There is a direct correlation between the change in temperature profile and the magnitude of the heat source/sink parameter.

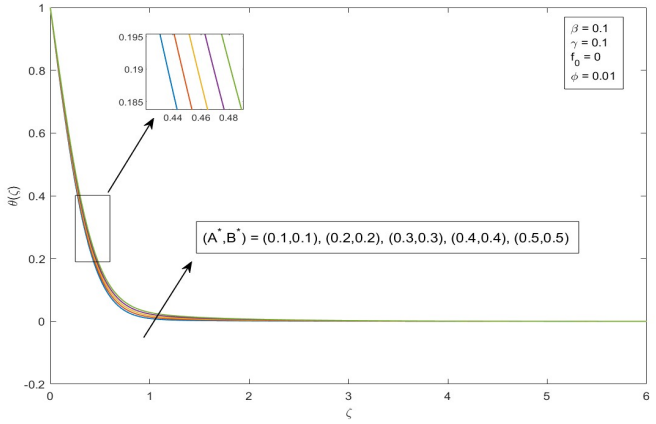

FIGURE 3.6: Impact of $A^*, B^* > 0$ on temperature profile $f'(\zeta)$

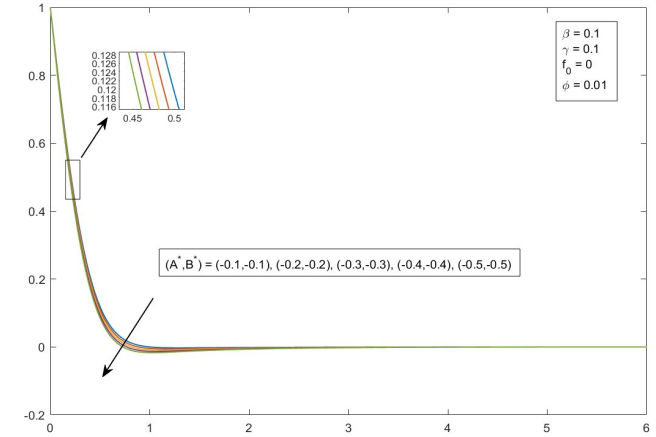

FIGURE 3.7: Impact of $A^*, B^* < 0$ on temperature profile $\theta(\zeta)$

3.5.4 Concentration Profile

Figures 3.8 - 3.9 illustrate the impact of the Schmidt number on the concentration profile with respect to heat source and heat sink. It is observed that as the Schmidt number increases, the concentration gradient also intensifies. Greater molecular mobility and stronger viscous diffusion are correlated with higher Schmidt numbers. In a liquid flow, the dimensionless Schmidt number formally characterizes the relationship between mass and momentum diffusivities. It's interesting to note that the largest concentration of nanoparticles coincides with the lowest Schmidt number. The figures also display the thickness of the boundary layer for the hydrodynamic flow and the species of nanoparticles, indicating a concentration gradient that is steepening.

Additionally, Figures 3.10 - 3.11 demonstrate the effect of the thermophoretic parameter with respect to heat source and heat sink on the concentration profile. A decrease in the thermophoretic parameter results in a higher concentration profile. This is because of the thermophoretic effect, which causes the particles to behave in a suction-like manner, cooling the surface and reducing mass transfer as a result.

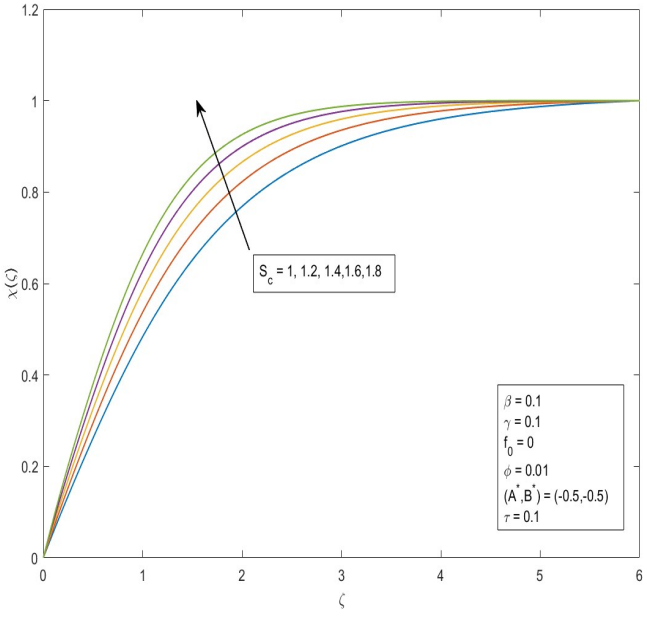

FIGURE 3.8: Impact of S_c on concentration profile $\chi(\zeta)$

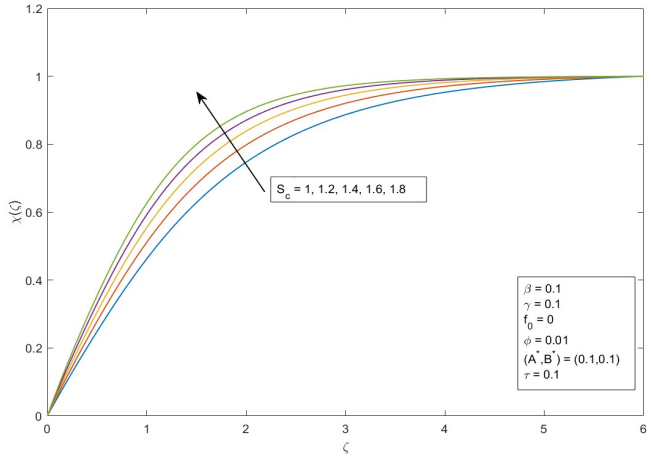

FIGURE 3.9: Impact of S_c on concentration profile $\chi(\zeta)$

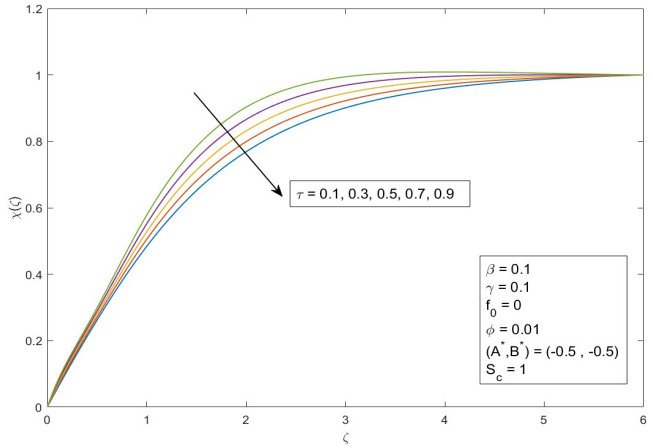

FIGURE 3.10: Impact of τ on concentration profile $\chi(\zeta)$

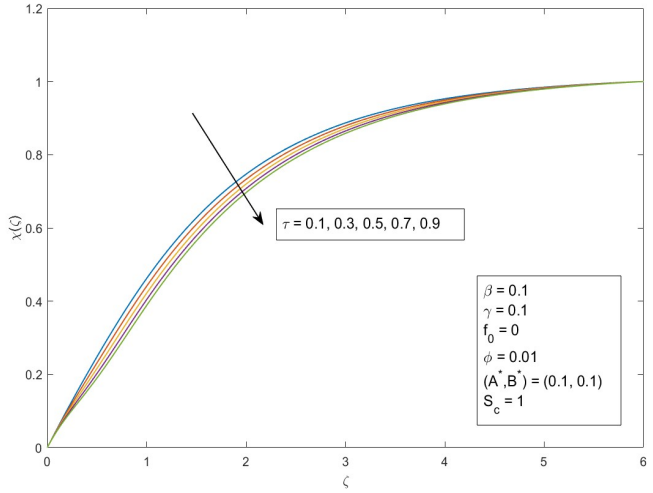

FIGURE 3.11: Impact of τ on concentration profile $\chi(\zeta)$

Chapter 4

Maxwell Nanofluid Flow with Thermophoretic Particle Deposition Using the Non-Fourier Double Diffusion Concept and Magnetic Field

4.1 Introduction

This chapter aims to advance the research conducted by Srilatha et al. [44] discussed in the preceding chapter. Specifically, the extension involves incorporating the Cattaneo-Christov non-Fourier double diffusion model with activation energy into the analysis. An appropriate similarity transformation is used to transform the governing PDEs into ODEs. The shooting method is then employed to derive numerical solutions. MATLAB is employed for numerical computation. The

chapter also includes graphical representations to elucidate the impact of varying parameters. Additionally, tables are also utilized to present and examine the numerical results obtained.

4.2 Mathematical Modeling

The equations governing the flow are as follows:

Mass conservation:

$$\frac{\partial \widetilde{u}}{\partial \widetilde{x}} + \frac{\partial \widetilde{v}}{\partial \widetilde{y}} = 0. \tag{4.1}$$

Momentum Equation:

$$\begin{aligned} &\frac{\partial \widetilde{u}}{\partial \widetilde{t}} + \widetilde{u}\frac{\partial \widetilde{u}}{\partial \widetilde{x}} + \widetilde{v}\frac{\partial \widetilde{u}}{\partial \widetilde{y}} + \frac{\widetilde{\sigma}_{nf}}{\widetilde{\rho}_{nf}} B_o^2 \widetilde{u} + \frac{\widetilde{\mu}_{nf}}{\widetilde{\rho}_{nf}} \frac{\widetilde{u}}{k^*} \\ &\quad = \widetilde{\nu}_{nf} \frac{\partial^2 \widetilde{u}}{\partial \widetilde{y}^2} - \lambda_0 \left(1 - \alpha \widetilde{t}\right) \left(\widetilde{u}^2 \frac{\partial^2 \widetilde{u}}{\partial \widetilde{x}^2} + \widetilde{v}^2 \frac{\partial^2 \widetilde{u}}{\partial \widetilde{y}^2} + 2\widetilde{u}\widetilde{v} \frac{\partial^2 \widetilde{u}}{\partial \widetilde{x} \partial \widetilde{y}} \right). \end{aligned} \tag{4.2}$$

Energy Equation:

$$\begin{aligned} &\frac{\partial \widetilde{T}}{\partial \widetilde{t}} + \widetilde{u}\frac{\partial \widetilde{T}}{\partial \widetilde{x}} + \widetilde{v}\frac{\partial \widetilde{T}}{\partial \widetilde{y}} + \lambda_E \Bigg(\frac{\partial^2 \widetilde{T}}{\partial \widetilde{t}^2} + \widetilde{u}\frac{\partial \widetilde{u}}{\partial \widetilde{x}} \frac{\partial \widetilde{T}}{\partial \widetilde{x}} + \widetilde{v}\frac{\partial \widetilde{v}}{\partial \widetilde{y}} \frac{\partial \widetilde{T}}{\partial \widetilde{y}} + \widetilde{u}\frac{\partial \widetilde{v}}{\partial \widetilde{x}} \frac{\partial \widetilde{T}}{\partial \widetilde{y}} + \widetilde{v}\frac{\partial \widetilde{u}}{\partial \widetilde{x}} \frac{\partial \widetilde{T}}{\partial \widetilde{x}} \\ &\quad + 2\widetilde{u}\widetilde{v} \frac{\partial^2 \widetilde{T}}{\partial \widetilde{x} \partial \widetilde{y}} + \widetilde{u}^2 \frac{\partial^2 \widetilde{T}}{\partial \widetilde{x}^2} + \widetilde{v}^2 \frac{\partial^2 \widetilde{T}}{\partial \widetilde{y}^2} + \frac{\partial \widetilde{u}}{\partial \widetilde{t}} \frac{\partial \widetilde{T}}{\partial \widetilde{x}} + 2\widetilde{u} \frac{\partial^2 \widetilde{T}}{\partial \widetilde{x} \partial \widetilde{t}} + \frac{\partial \widetilde{v}}{\partial \widetilde{t}} \frac{\partial \widetilde{T}}{\partial \widetilde{y}} + 2\widetilde{v} \frac{\partial^2 \widetilde{T}}{\partial \widetilde{y} \partial \widetilde{t}} \Bigg) \\ &\quad = \frac{\widetilde{k}_{nf}}{(\widetilde{\rho}\widetilde{C}_p)_{nf}} \frac{\partial}{\partial \widetilde{y}} \left(\frac{\partial \widetilde{T}}{\partial \widetilde{y}} \right) + \frac{1}{(\widetilde{\rho}\widetilde{C}_p)_{nf}} \widetilde{q}''' + \frac{\widetilde{\sigma}_{nf} B_o^2}{(\widetilde{\rho}\widetilde{C}_p)_{nf}} \widetilde{u}^2. \end{aligned} \tag{4.3}$$

Concentration Equation:

$$\begin{aligned} &\frac{\partial \widetilde{C}}{\partial \widetilde{t}} + \widetilde{u}\frac{\partial \widetilde{C}}{\partial \widetilde{x}} + \widetilde{v}\frac{\partial \widetilde{C}}{\partial \widetilde{y}} + \lambda_C \Bigg(\frac{\partial^2 \widetilde{C}}{\partial \widetilde{t}^2} + \widetilde{u}\frac{\partial \widetilde{u}}{\partial \widetilde{x}} \frac{\partial \widetilde{C}}{\partial \widetilde{x}} + \widetilde{v}\frac{\partial \widetilde{v}}{\partial \widetilde{y}} \frac{\partial \widetilde{C}}{\partial \widetilde{y}} + \widetilde{u}\frac{\partial \widetilde{v}}{\partial \widetilde{x}} \frac{\partial \widetilde{C}}{\partial \widetilde{y}} + \widetilde{v}\frac{\partial \widetilde{u}}{\partial \widetilde{x}} \frac{\partial \widetilde{C}}{\partial \widetilde{x}} \\ &\quad + 2\widetilde{u}\widetilde{v} \frac{\partial^2 \widetilde{C}}{\partial \widetilde{x} \partial \widetilde{y}} + \widetilde{u}^2 \frac{\partial^2 \widetilde{C}}{\partial \widetilde{x}^2} + \widetilde{v}^2 \frac{\partial^2 \widetilde{C}}{\partial \widetilde{y}^2} + \frac{\partial \widetilde{u}}{\partial \widetilde{t}} \frac{\partial \widetilde{C}}{\partial \widetilde{x}} + 2\widetilde{u} \frac{\partial^2 \widetilde{C}}{\partial \widetilde{x} \partial \widetilde{t}} + \frac{\partial \widetilde{v}}{\partial \widetilde{t}} \frac{\partial \widetilde{C}}{\partial \widetilde{y}} + 2\widetilde{v} \frac{\partial^2 \widetilde{C}}{\partial \widetilde{y} \partial \widetilde{t}} \Bigg) \\ &\quad = D \left(\frac{\partial^2 \widetilde{C}}{\partial \widetilde{x}^2} + \frac{\partial^2 \widetilde{C}}{\partial \widetilde{y}^2} \right) - \frac{\partial}{\partial \widetilde{y}} (\widetilde{V_T} \widetilde{C}). \end{aligned} \tag{4.4}$$

Boundary Conditions:

The corresponding boundary conditions have been specified as follows.

$$\left.\begin{aligned} &\widetilde{u} = \widetilde{U}_w\left(\widetilde{x},\widetilde{t}\right) = \frac{\widetilde{a}\widetilde{x}}{\left(1-\alpha\widetilde{t}\right)}, \quad \widetilde{v} = \widetilde{v}_w = -\sqrt{\frac{\widetilde{\nu}_f\widetilde{U}_w}{\widetilde{x}}}\widetilde{f}_0, \\ &\widetilde{T} = \widetilde{T_w}, \quad \widetilde{C} = \widetilde{C_w} = 0, \quad at \quad \widetilde{y} = 0, \\ &\widetilde{u} \longrightarrow 0, \quad \widetilde{T} \longrightarrow \widetilde{T}_\infty, \quad \widetilde{C} \longrightarrow \widetilde{C}_\infty, \quad as \ \widetilde{y} \longrightarrow \infty. \end{aligned}\right\} \tag{4.5}$$

4.3 Non-dimensionalization

The following similarity transformation has been applied to convert equations (4.1) - (4.4) into a system of ODEs:

$$\left.\begin{aligned} &\zeta = \sqrt{\frac{\tilde{a}}{\widetilde{\nu}_f\left(1-\alpha\widetilde{t}\right)}}\widetilde{y}, \quad \widetilde{u} = \frac{\tilde{a}\tilde{x}}{1-\alpha\widetilde{t}}f'(\zeta), \quad \tilde{v} = -\sqrt{\frac{\tilde{a}\widetilde{\nu}_f}{1-\alpha\widetilde{t}}}f(\zeta), \\ &\theta(\zeta) = \frac{\widetilde{T}-\widetilde{T}_\infty}{\widetilde{T}_w-\widetilde{T}_\infty}, \ \chi(\zeta) = \frac{\widetilde{C}-\widetilde{C}_\infty}{\widetilde{C}_w-\widetilde{C}_\infty}. \end{aligned}\right\} \tag{4.6}$$

$\tilde{u}$ and $\tilde{v}$ represent the velocity components in the x and y directions, respectively, while $\theta(\zeta)$ and $\chi(\zeta)$ indicate the dimensionless temperature and concentration profiles. TABLE 4.1 lists the parameters used in the future ODEs along with their BCs.

TABLE 4.1: Multiple dimensionless parameters used in the governing ODEs

Symbols	**Name**	**Appearance**
M	Magnetic field	$M = \frac{\tilde{\sigma}_f\tilde{B}_o^2}{\tilde{\rho}_f\tilde{a}}$
Kp	Porosity medium	$Kp = \frac{\widetilde{\nu}_f\left(1-\alpha\widetilde{t}\right)}{\tilde{a}k^*}$
Pr	Prandtl number	$Pr = \frac{\widetilde{\nu}_f\left(\widetilde{\rho c_p}\right)_f}{\tilde{K}_f}$
Ec	Eckert number	$Ec = \frac{\tilde{a}^2\widetilde{x}^2}{\left(\widetilde{c_p}\right)_f\left(\widetilde{T}_w-\widetilde{T}_\infty\right)}$
$\beta_{e,c}$	Time Relaxation	$\beta_{e,c} = \frac{\widetilde{a}}{\left(1-\alpha\widetilde{t}\right)}\lambda_{E,C}$
γ	Chemical reaction	$\gamma = \frac{\alpha}{\widetilde{a}}$

4.3.1 Non-dimensionalization of Momentum Equation

The governing momentum equation (4.2), is transformed into the non-dimensional form in this subsection. In order to do this, we enter each partial derivative in the range of (3.6) to (3.16) into equation (4.2). The outcome of this process is as follows:

$$\begin{aligned}
&\frac{\widetilde{a}\widetilde{x}\alpha}{(1-\alpha\widetilde{t})^2}\left(f'+\frac{(\zeta)}{2}f''\right)+\left(\frac{\tilde{a}\tilde{x}}{1-\alpha\widetilde{t}}f'\right)\left(\frac{\tilde{a}}{1-\alpha\widetilde{t}}f'\right)-\left(\sqrt{\frac{\tilde{a}\widetilde{\nu}_f}{1-\alpha\widetilde{t}}}f\right)\\
&\frac{\widetilde{a}\sqrt{\widetilde{a}}}{(1-\alpha\widetilde{t})\sqrt{\widetilde{\nu}_f(1-\alpha\widetilde{t})}}\widetilde{x}f''+\frac{\widetilde{\sigma}_{nf}}{\widetilde{\rho}_{nf}}B_o^2\left(\frac{\tilde{a}\tilde{x}}{1-\alpha\widetilde{t}}f'\right)+\frac{\widetilde{\mu}_{nf}}{\widetilde{\rho}_{nf}}\frac{\frac{\tilde{a}\tilde{x}}{1-\alpha\widetilde{t}}f'}{k^*}\\
&=\widetilde{\nu}_f\left(\frac{\widetilde{a}^2}{(1-\alpha\widetilde{t})^2\widetilde{\nu}_f}\widetilde{x}f''\right)-\lambda_0\left(1-\alpha\widetilde{t}\right)\left(0+\left(\frac{\widetilde{a}\widetilde{\nu}_f}{1-\alpha\widetilde{t}}f^2\right)\right.\\
&\left(\frac{\widetilde{a}^2}{(1-\alpha\widetilde{t})^2\widetilde{\nu}_f}\widetilde{x}f''\right)\\
&\left.-2\left(\frac{\tilde{a}\tilde{x}}{1-\alpha\widetilde{t}}f'\right)\left(\sqrt{\frac{\tilde{a}\widetilde{\nu}_f}{1-\alpha\widetilde{t}}}f\right)\left(\frac{\widetilde{a}\sqrt{\widetilde{a}}}{(1-\alpha\widetilde{t})\sqrt{\widetilde{\nu}_f(1-\alpha\widetilde{t})}}f''\right)\right).
\end{aligned}$$

$$\begin{aligned}
\Rightarrow\ &\frac{\widetilde{a}\widetilde{x}\alpha}{(1-\alpha\widetilde{t})^2}\left(f'+\frac{\zeta}{2}f''\right)+\frac{\widetilde{a}^2\widetilde{x}}{(1-\alpha\widetilde{t})^2}(f')^2-\frac{\widetilde{a}^2\widetilde{x}}{(1-\alpha\widetilde{t})^2}ff''\\
&+\frac{\frac{\widetilde{\sigma}_{nf}}{\widetilde{\sigma}_f}}{\frac{\widetilde{\rho}_{nf}}{\widetilde{\rho}_f}}\left(\frac{\widetilde{\sigma}_f}{\widetilde{\rho}_f}\widetilde{B}_0^2\right)\left(\frac{\tilde{a}\tilde{x}}{1-\alpha\widetilde{t}}f'\right)+\frac{\widetilde{\mu}_{nf}}{\widetilde{\rho}_{nf}}\frac{\widetilde{\nu}_f}{\widetilde{\nu}_f}\left(\frac{\tilde{a}\tilde{x}}{(1-\alpha\widetilde{t})\widetilde{k^*}}f'\right)\\
&=\frac{\widetilde{\nu}_{nf}}{\widetilde{\nu}_f}\frac{\widetilde{a}^2\widetilde{x}}{(1-\alpha\widetilde{t})^2}f'''-\lambda_0\left(1-\alpha\widetilde{t}\right)\left(\frac{\widetilde{a}^3}{(1-\alpha\widetilde{t})^3}\widetilde{x}f^2f'''\right.\\
&\left.-2\frac{\widetilde{a}^3}{(1-\alpha\widetilde{t})^3}\widetilde{x}ff'f''\right).
\end{aligned}$$

$$\begin{aligned}
\Rightarrow\ &\frac{\alpha}{\widetilde{a}}\left(f'+\frac{\zeta}{2}f''\right)+(f')^2-ff''+\frac{\frac{\widetilde{\sigma}_{nf}}{\widetilde{\sigma}_f}}{\frac{\widetilde{\rho}_{nf}}{\widetilde{\rho}_f}}Mf'+\frac{\frac{\widetilde{\mu}_{nf}}{\widetilde{\mu}_f}}{\frac{\widetilde{\rho}_{nf}}{\widetilde{\rho}_f}}K_pf'=\frac{\widetilde{\nu}_{nf}}{\widetilde{\nu}_f}f'''-\beta\left(f^2f'''-2ff'f''\right).\\
\Rightarrow\ &\frac{\widetilde{\nu}_{nf}}{\widetilde{\nu}_f}f'''-\gamma\left(f'+\frac{\zeta}{2}f''\right)-f'^2+ff''-\frac{\frac{\widetilde{\sigma}_{nf}}{\widetilde{\sigma}_f}}{\frac{\widetilde{\rho}_{nf}}{\widetilde{\rho}_f}}Mf'-\frac{\frac{\widetilde{\mu}_{nf}}{\widetilde{\mu}_f}}{\frac{\widetilde{\rho}_{nf}}{\widetilde{\rho}_f}}K_pf'-\beta\left(f^2f'''-2ff'f''\right)=0.\\
\Rightarrow\ &\widetilde{P}_3f'''-\gamma\left(f'+\frac{\zeta}{2}f''\right)-f'^2+ff''-\frac{\widetilde{P}_6}{\widetilde{P}_1}Mf'-\widetilde{P}_3K_pf'-\beta\left(f^2f'''-2ff'f''\right)=0. \quad (4.7)
\end{aligned}$$

4.3.2 Non-dimensionalization of Energy Equation

Here are the following derivatives which are going to be use in equation (4.3):

- $$\frac{\partial \widetilde{T}}{\partial \widetilde{t}} = (\widetilde{T}_w - \widetilde{T}_\infty)\theta'(\zeta)\frac{\alpha\zeta}{2\left(1-\alpha\widetilde{t}\right)}$$
$$= (\widetilde{T}_w - \widetilde{T}_\infty)\frac{\alpha}{2}\sqrt{\frac{\widetilde{a}}{\widetilde{\nu}_f}}\frac{\widetilde{y}}{\left(1-\alpha\widetilde{t}\right)^{\frac{3}{2}}}\theta'.$$
- $$\frac{\partial^2 \widetilde{T}}{\partial \widetilde{t}^2} = (\widetilde{T}_w - \widetilde{T}_\infty)\frac{\alpha}{2}\sqrt{\frac{\widetilde{a}}{\widetilde{\nu}_f}}\widetilde{y}\frac{\partial}{\partial \widetilde{t}}\left(\left(1-\alpha\widetilde{t}\right)^{-\frac{3}{2}}\theta'\right)$$
$$= (\widetilde{T}_w - \widetilde{T}_\infty)\frac{\alpha}{2}\sqrt{\frac{\widetilde{a}}{\widetilde{\nu}_f}}\widetilde{y}\left(-\frac{3}{2}\left(1-\alpha\widetilde{t}\right)^{-\frac{5}{2}}(-\alpha)\theta' + \left(1-\alpha\widetilde{t}\right)^{-\frac{3}{2}}\theta''\frac{\partial\zeta}{\partial\widetilde{t}}\right)$$
$$= (\widetilde{T}_w - \widetilde{T}_\infty)\frac{\alpha}{2}\sqrt{\frac{\widetilde{a}}{\widetilde{\nu}_f}}\widetilde{y}\left(\frac{3\alpha}{2\left(1-\alpha\widetilde{t}\right)^{\frac{5}{2}}} + \frac{\alpha\zeta}{2\left(1-\alpha\widetilde{t}\right)^{\frac{5}{2}}}\theta''\right)$$
$$= (\widetilde{T}_w - \widetilde{T}_\infty)\frac{\alpha^2}{4\left(1-\alpha\widetilde{t}\right)^{\frac{5}{2}}}\sqrt{\frac{\widetilde{a}}{\nu_f}}\widetilde{y}(3\theta' + \zeta\theta'')$$

$$= (\widetilde{T}_w - \widetilde{T}_\infty)\frac{\alpha^2\zeta}{4\left(1-\alpha\widetilde{t}\right)^2}(3\theta' + \zeta\theta''). \tag{4.8}$$

- $$\widetilde{v}\frac{\partial\widetilde{v}}{\partial\widetilde{y}}\frac{\partial\widetilde{T}}{\partial\widetilde{y}} = \left(-\sqrt{\frac{\widetilde{a}\nu_f}{1-\alpha\widetilde{t}}}f\right)\left(\frac{-\widetilde{a}}{1-\alpha\widetilde{t}}f'\right)\left((\widetilde{T}_w - \widetilde{T}_\infty)\theta'\sqrt{\frac{\widetilde{a}}{\widetilde{\nu}_f\left(1-\alpha\widetilde{t}\right)}}\right)$$
$$= \frac{\widetilde{a}^2}{\left(1-\alpha\widetilde{t}\right)^2}ff'\theta'(\widetilde{T}_w - \widetilde{T}_\infty). \tag{4.9}$$

- $$\widetilde{u}\frac{\partial\widetilde{u}}{\partial\widetilde{x}}\frac{\partial\widetilde{T}}{\partial\widetilde{x}} = 0. \tag{4.10}$$
- $$\widetilde{u}\frac{\partial\widetilde{v}}{\partial\widetilde{x}}\frac{\partial\widetilde{T}}{\partial\widetilde{y}} = 0. \tag{4.11}$$
- $$\widetilde{v}\frac{\partial\widetilde{u}}{\partial\widetilde{x}}\frac{\partial\widetilde{T}}{\partial\widetilde{x}} = 0. \tag{4.12}$$
- $$2\widetilde{u}\widetilde{v}\frac{\partial^2\widetilde{T}}{\partial\widetilde{x}\partial\widetilde{y}} = 0. \tag{4.13}$$
- $$\widetilde{u}^2\frac{\partial^2\widetilde{T}}{\partial\widetilde{x}^2} = 0. \tag{4.14}$$

- $\widetilde{v}^2\dfrac{\partial^2\widetilde{T}}{\partial\widetilde{y}^2}=\left(\dfrac{\widetilde{a}\widetilde{\nu}_f}{1-\alpha\widetilde{t}}f^2\right)\left(\left(\widetilde{T}_w-\widetilde{T}_\infty\right)\dfrac{\widetilde{a}}{\widetilde{\nu}_f\left(1-\alpha\widetilde{t}\right)}\right)$

$$=\left(\frac{\widetilde{a}^2}{\left(1-\alpha\widetilde{t}\right)^2}\right)\left(\widetilde{T}_w-\widetilde{T}_\infty\right)f^2\theta''. \tag{4.15}$$

- $$\frac{\partial\widetilde{u}}{\partial\widetilde{t}}\frac{\partial\widetilde{T}}{\partial\widetilde{x}}=0. \tag{4.16}$$

- $$2\widetilde{u}\frac{\partial^2\widetilde{T}}{\partial\widetilde{x}\partial\widetilde{t}}=0. \tag{4.17}$$

- $$\begin{aligned}\frac{\partial\widetilde{v}}{\partial\widetilde{t}}&=-\sqrt{\widetilde{a}\widetilde{\nu}_f}\frac{\partial}{\partial\widetilde{t}}\left(\left(1-\alpha\widetilde{t}\right)^{-\frac{1}{2}}f(\zeta)\right)\\&=-\sqrt{\widetilde{a}\widetilde{\nu}_f}\left(-\frac{1}{2}\left(1-\alpha\widetilde{t}\right)^{-\frac{3}{2}}(-\alpha)f+\left(1-\alpha\widetilde{t}\right)^{-\frac{1}{2}}f'\frac{\partial\zeta}{\partial\widetilde{t}}\right)\\&=-\sqrt{\widetilde{a}\widetilde{\nu}_f}\left(\frac{\alpha f}{2\left(1-\alpha\widetilde{t}\right)^{\frac{3}{2}}}+\left(1-\alpha\widetilde{t}\right)^{-\frac{1}{2}}f'\frac{\alpha\zeta}{2\left(1-\alpha\widetilde{t}\right)}\right)\\&=-\sqrt{\widetilde{a}\widetilde{\nu}_f}\left(\frac{\alpha f}{2\left(1-\alpha\widetilde{t}\right)^{\frac{3}{2}}}+\frac{\alpha\zeta f'}{2\left(1-\alpha\widetilde{t}\right)\left(1-\alpha\widetilde{t}\right)^{\frac{1}{2}}}\right)\\&=-\sqrt{\widetilde{a}\widetilde{\nu}_f}\left(\frac{\alpha f}{2\left(1-\alpha\widetilde{t}\right)^{\frac{3}{2}}}+\frac{\alpha\zeta f'}{2\left(1-\alpha\widetilde{t}\right)^{\frac{3}{2}}}\right)\\&=-\sqrt{\widetilde{a}\widetilde{\nu}_f}\frac{\alpha}{2\left(1-\alpha\widetilde{t}\right)^{\frac{3}{2}}}\left(f+\zeta f'\right).\end{aligned}$$

- $\dfrac{\partial\widetilde{v}}{\partial\widetilde{t}}\dfrac{\partial\widetilde{T}}{\partial\widetilde{y}}=\left(-\sqrt{\widetilde{a}\widetilde{\nu}_f}\dfrac{\alpha}{2\left(1-\alpha\widetilde{t}\right)^{\frac{3}{2}}}\left(f+\zeta\right)f'\right)\left((\widetilde{T}_w-\widetilde{T}_\infty)\theta'\sqrt{\dfrac{\widetilde{a}}{\widetilde{\nu}_f\left(1-\alpha\widetilde{t}\right)}}\right)$

$$=-\frac{\widetilde{a}\alpha\left(\widetilde{T}_w-\widetilde{T}_\infty\right)}{2(1-\alpha\widetilde{t})^2}\left(f\theta'+\zeta f'\theta'\right). \tag{4.18}$$

- $\dfrac{\partial\widetilde{T}}{\partial\widetilde{y}}=(\widetilde{T}_w-\widetilde{T}_\infty)\theta'\sqrt{\dfrac{\widetilde{a}}{\widetilde{\nu}_f\left(1-\alpha\widetilde{t}\right)}}.$

- $$\begin{aligned}\frac{\partial^2\widetilde{T}}{\partial\widetilde{y}\partial\widetilde{t}}&=\sqrt{\frac{\widetilde{a}}{\widetilde{\nu}_f}}(\widetilde{T}_w-\widetilde{T}_\infty)\frac{\partial}{\partial\widetilde{t}}\left(\frac{\theta'}{\left(1-\alpha\widetilde{t}\right)^{\frac{1}{2}}}\right)\\&=\sqrt{\frac{\widetilde{a}}{\widetilde{\nu}_f}}(\widetilde{T}_w-\widetilde{T}_\infty)\left(\frac{\left(1-\alpha\widetilde{t}\right)^{\frac{1}{2}}\theta''\frac{\partial\zeta}{\partial\widetilde{t}}-\frac{1}{2}\left(1-\alpha\widetilde{t}\right)^{-\frac{1}{2}}(-\alpha)\theta'}{\left(\left(1-\alpha\widetilde{t}\right)^{\frac{1}{2}}\right)^2}\right)\end{aligned}$$

$$= \sqrt{\frac{\widetilde{a}}{\widetilde{\nu}_f}}(\widetilde{T}_w - \widetilde{T}_\infty)\left(\frac{\left(1-\alpha\widetilde{t}\right)^{\frac{1}{2}}\theta''\frac{\alpha\zeta}{2\left(1-\alpha\widetilde{t}\right)} + \frac{\alpha}{2}\left(1-\alpha\widetilde{t}\right)^{-\frac{1}{2}}\theta'}{\left(1-\alpha\widetilde{t}\right)}\right)$$

$$= \sqrt{\frac{\widetilde{a}}{\widetilde{\nu}_f}}(\widetilde{T}_w - \widetilde{T}_\infty)\left(\frac{\theta''\frac{\alpha\zeta}{2} + \frac{\alpha}{2}\theta'}{\left(1-\alpha\widetilde{t}\right)^{\frac{3}{2}}}\right)$$

$$= \sqrt{\frac{\widetilde{a}}{\widetilde{\nu}_f\left(1-\alpha\widetilde{t}\right)}}\frac{(\widetilde{T}_w - \widetilde{T}_\infty)}{2\left(1-\alpha\widetilde{t}\right)}\frac{\alpha}{2}\left(\zeta\theta'' + \theta'\right).$$

$$\bullet\ 2\widetilde{v}\frac{\partial^2\widetilde{T}}{\partial\widetilde{y}\partial\widetilde{t}} = 2\left(-\sqrt{\frac{\widetilde{a}\widetilde{\nu}_f}{1-\alpha\widetilde{t}}}f\right)\sqrt{\frac{\widetilde{a}}{\widetilde{\nu}_f\left(1-\alpha\widetilde{t}\right)}}\frac{(\widetilde{T}_w - \widetilde{T}_\infty)}{2\left(1-\alpha\widetilde{t}\right)}\frac{\alpha}{2}\left(\zeta\theta'' + \theta'\right)$$

$$= -\frac{\widetilde{a}\alpha}{\left(1-\alpha\widetilde{t}\right)^2}(\widetilde{T}_w - \widetilde{T}_\infty)\left(\zeta f\theta'' + f\theta'\right). \tag{4.19}$$

By substituting all the partial derivatives mentioned (3.18) - (3.21), (4.6) - (4.19), and velocity component (3.6), into equation (4.3), we get the following:

$$(\widetilde{T}_w - \widetilde{T}_\infty)\theta'(\zeta)\frac{\alpha\zeta}{2\left(1-\alpha\widetilde{t}\right)} - \left(\sqrt{\frac{\tilde{a}\widetilde{\nu}_f}{1-\alpha\widetilde{t}}}f\right)\left((\widetilde{T}_w - \widetilde{T}_\infty)\theta'\sqrt{\frac{\tilde{a}}{\widetilde{\nu}_f(1-\alpha\widetilde{t})}}\right)$$
$$+\lambda_E\left((\widetilde{T}_w - \widetilde{T}_\infty)\frac{\alpha^2\zeta}{4\left(1-\alpha\widetilde{t}\right)^2}\left(3\theta' + \zeta\theta''\right) + \frac{\widetilde{a}^2}{\left(1-\alpha\widetilde{t}\right)^2}ff'\theta'\left(\widetilde{T}_w - \widetilde{T}_\infty\right)\right.$$
$$+\left(\frac{\widetilde{a}^2}{\left(1-\alpha\widetilde{t}\right)^2}\right)(\widetilde{T}_w - \widetilde{T}_\infty)f^2\theta'' - \frac{\widetilde{a}\alpha\left(\widetilde{T}_w - \widetilde{T}_\infty\right)}{2\left(1-\alpha\widetilde{t}\right)^2}\left(f\theta' + \zeta f'\theta'\right)$$
$$\left.-\frac{\widetilde{a}\alpha}{\left(1-\alpha\widetilde{t}\right)^2}(\widetilde{T}_w - \widetilde{T}_\infty)\left(\zeta f\theta'' + f\theta'\right)\right) = \frac{\widetilde{k}_{nf}}{\left(\widetilde{\rho}\widetilde{C}_p\right)_{nf}}\left(\widetilde{T}_w - \widetilde{T}_\infty\right)\frac{\widetilde{a}}{\widetilde{\nu}_f\left(1-\alpha\widetilde{t}\right)}\theta''$$
$$+\frac{1}{\left(\widetilde{\rho}\widetilde{C}_p\right)_{nf}}\frac{\widetilde{k}_f\frac{\widetilde{a}\widetilde{x}}{\left(1-\alpha\widetilde{t}\right)}}{\widetilde{x}\widetilde{\nu}_f}(\widetilde{T}_w - \widetilde{T}_\infty)\left(\widetilde{A}^*f' + \widetilde{B}^*\theta\right) + \frac{\sigma_{nf}}{\left(\widetilde{\rho}\widetilde{C}_p\right)_{nf}}\widetilde{B}_0^2\frac{\widetilde{a}^2\widetilde{x}^2}{\left(1-\alpha\widetilde{t}\right)^2}f'^2.$$

$$\Rightarrow \frac{\alpha}{\widetilde{a}}\frac{\zeta}{2}\theta' - f\theta' + \lambda_E\left(\frac{\alpha^2}{4\widetilde{a}\left(1-\alpha\widetilde{t}\right)}\left(3\zeta\theta' + \zeta^2\theta''\right) + \frac{\widetilde{a}}{\left(1-\alpha\widetilde{t}\right)}ff'\theta' + \frac{\widetilde{a}}{\left(1-\alpha\widetilde{t}\right)}f^2\theta''\right.$$
$$\left.-\frac{\alpha}{2\left(1-\alpha\widetilde{t}\right)}\left(f\theta' + \zeta f'\theta'\right) - \frac{\alpha}{\left(1-\alpha\widetilde{t}\right)}\left(\zeta f\theta'' + f\theta'\right)\right) = \frac{\widetilde{k}_{nf}}{\left(\widetilde{\rho}\widetilde{C}_p\right)_{nf}}\frac{\theta''}{\widetilde{\nu}_f}$$
$$+\frac{\widetilde{k}_f}{\left(\widetilde{\rho}\widetilde{C}_p\right)_{nf}}(\widetilde{A}^*f' + \widetilde{B}^*\theta) + \frac{\widetilde{\sigma}_{nf}}{\left(\widetilde{\rho}\widetilde{C}_p\right)_{nf}}\frac{\widetilde{B}_0^2\left(1-\alpha\widetilde{t}\right)}{\widetilde{a}\left(\widetilde{T}_w - \widetilde{T}_\infty\right)}\left(\frac{\widetilde{a}^2\widetilde{x}^2}{\left(1-\alpha\widetilde{t}\right)^2}\right)f'^2.$$

$$\Rightarrow \frac{\alpha}{\widetilde{a}}\frac{\zeta}{2}\theta' - f\theta' + \lambda_E\Bigg(\frac{\alpha^2\widetilde{a}}{4\widetilde{a}^2\left(1-\alpha\widetilde{t}\right)}\left(3\zeta\theta' + \zeta^2\theta''\right) + \frac{\widetilde{a}}{\left(1-\alpha\widetilde{t}\right)}ff'\theta' + \frac{\widetilde{a}}{\left(1-\alpha\widetilde{t}\right)}f^2\theta''$$

$$- \frac{\widetilde{a}\alpha}{2\widetilde{a}\left(1-\alpha\widetilde{t}\right)}\left(f\theta' + \zeta f'\theta'\right) - \frac{\widetilde{a}\alpha}{\widetilde{a}\left(1-\alpha\widetilde{t}\right)}\left(\zeta f\theta'' + f\theta'\right)\Bigg)$$

$$= \frac{\widetilde{k}_{nf}}{\left(\widetilde{\rho}\widetilde{C}_p\right)_{nf}}\frac{\theta''}{\widetilde{\nu}_f} + \frac{\widetilde{k}_f}{\left(\widetilde{\rho}\widetilde{C}_p\right)_{nf}\widetilde{\nu}_f}(\widetilde{A}^* f' + \widetilde{B}^*\theta)$$

$$+ \frac{\widetilde{\sigma}_{nf}}{\left(\widetilde{\rho}\widetilde{C}_p\right)_{nf}}\frac{\widetilde{\sigma}_f}{\widetilde{\sigma}_f}\frac{\left(\widetilde{\rho}\widetilde{C}_p\right)_f}{\left(\widetilde{\rho}\widetilde{C}_p\right)_f}\frac{\widetilde{B}_0^2\left(1-\alpha\widetilde{t}\right)}{\widetilde{a}\left(\widetilde{T}_w - \widetilde{T}_\infty\right)}\left(\frac{\widetilde{a}^2\widetilde{x}^2}{\left(1-\alpha\widetilde{t}\right)^2}\right)f'^2.$$

$$\Rightarrow \frac{\alpha}{\widetilde{a}}\frac{\zeta}{2}\theta' - f\theta' + \frac{\widetilde{a}}{\left(1-\alpha\widetilde{t}\right)}\lambda_E\Bigg(\frac{\alpha^2}{4\widetilde{a}^2}\left(3\zeta\theta' + \zeta^2\theta''\right) + ff'\theta' + f^2\theta'' - \frac{\alpha}{2\widetilde{a}}\left(f\theta' + \zeta f'\theta'\right)$$

$$- \frac{\alpha}{\widetilde{a}}\left(\zeta f\theta'' + f\theta'\right)\Bigg) = \frac{\widetilde{k}_{nf}}{\left(\widetilde{\rho}\widetilde{C}_p\right)_{nf}}\frac{\theta''}{P_r\alpha_f} + \frac{\widetilde{k}_f}{\left(\widetilde{\rho}\widetilde{C}_p\right)_{nf}P_r\alpha_f}$$

$$\left(\widetilde{A}^* f' + \widetilde{B}^*\theta\right)\frac{\frac{\widetilde{\sigma}_{nf}}{\widetilde{\sigma}_f}}{\frac{\left(\widetilde{\rho}\widetilde{C}_p\right)_{nf}}{\left(\widetilde{\rho}\widetilde{C}_p\right)_f}}\frac{\widetilde{\sigma}_f\widetilde{B}_0^2\left(1-\alpha\widetilde{t}\right)}{\widetilde{\rho}_f\widetilde{a}}\frac{\widetilde{a}^2\widetilde{x}^2}{\left(\widetilde{C}_p\right)_f\left(\widetilde{T}_w - \widetilde{T}_\infty\right)\left(1-\alpha\widetilde{t}\right)^2}.$$

$$\Rightarrow P_r\gamma\frac{\zeta}{2}\theta' - P_r f\theta' + \beta_e P_r\Bigg(\frac{\gamma^2}{4}\left(3\zeta\theta' + \zeta^2\theta''\right) + ff'\theta' + f^2\theta''$$

$$- \frac{\gamma}{2}\left(f\theta' + \zeta f'\theta'\right) - \gamma\left(\zeta f\theta'' + f\theta'\right)\Bigg) = \frac{\widetilde{k}_{nf}}{\left(\widetilde{\rho}\widetilde{C}_p\right)_{nf}}\frac{\theta''}{\alpha_f}$$

$$+ \frac{\widetilde{k}_f}{\left(\widetilde{\rho}\widetilde{C}_p\right)_{nf}\alpha_f}\left(\widetilde{A}^* f' + \widetilde{B}^*\theta\right) + P_r\frac{\frac{\widetilde{\sigma}_{nf}}{\widetilde{\sigma}_f}}{\frac{\left(\widetilde{\rho}\widetilde{C}_p\right)_{nf}}{\left(\widetilde{\rho}\widetilde{C}_p\right)_f}}ME_c f'^2.$$

$$\Rightarrow P_r\gamma\frac{\zeta}{2}\theta' - P_r f\theta' + \beta_e P_r\Bigg(\frac{\gamma^2}{4}\left(3\zeta\theta' + \zeta^2\theta''\right) + \left(ff'\theta' + f^2\theta'' - \gamma\zeta f\theta''\right)$$

$$- \frac{\gamma}{2}\left(\zeta f'\theta' + 3f\theta'\right)\Bigg) = \frac{\widetilde{k}_{nf}}{\left(\widetilde{\rho}\widetilde{C}_p\right)_{nf}}\frac{\theta''}{\frac{\widetilde{k}_f}{\left(\widetilde{\rho}\widetilde{C}_p\right)_f}}$$

$$+ \frac{\widetilde{k}_f}{\left(\widetilde{\rho}\widetilde{C}_p\right)_{nf}\frac{\widetilde{k}_f}{\left(\widetilde{\rho}\widetilde{C}_p\right)_f}}\left(\widetilde{A}^* f' + \widetilde{B}^*\theta\right) + P_r\frac{\frac{\widetilde{\sigma}_{nf}}{\widetilde{\sigma}_f}}{\frac{\left(\widetilde{\rho}\widetilde{c}_p\right)_{nf}}{\left(\widetilde{\rho}\widetilde{c}_p\right)_f}}ME_c f'^2.$$

$$\Rightarrow P_r\gamma\frac{\zeta}{2}\theta' - P_r f\theta' + \beta_e P_r\Bigg(\frac{\gamma^2}{4}\left(3\zeta\theta' + \zeta^2\theta''\right) + \left(ff'\theta' + f^2\theta'' - \gamma\zeta f\theta''\right) - \frac{\gamma}{2}\left(\zeta f'\theta' + 3f\theta'\right)\Bigg) = \left(\frac{\widetilde{k}_{nf}}{\left(\widetilde{\rho}\widetilde{C}_p\right)_{nf}}\frac{\left(\widetilde{\rho}\widetilde{C}_p\right)_f}{\widetilde{k}_f}\right)\theta'' + \frac{\widetilde{k}_f}{\left(\widetilde{\rho}\widetilde{C}_p\right)_{nf}}\frac{\left(\widetilde{\rho}\widetilde{C}_p\right)_f}{\widetilde{k}_f}\left(A^*f' + B^*\theta\right) + P_r\frac{\frac{\widetilde{\sigma}_{nf}}{\widetilde{\sigma}_f}}{\frac{\left(\widetilde{\rho}\widetilde{C}_p\right)_{nf}}{\left(\widetilde{\rho}\widetilde{C}_p\right)_f}}ME_c f'^2.$$

$$\Rightarrow P_r\gamma\frac{\zeta}{2}\theta' - P_r f\theta' + \beta_e P_r\Bigg(\frac{\gamma^2}{4}\left(3\zeta\theta' + \zeta^2\theta''\right) + \left(ff'\theta' + f^2\theta'' - \gamma\zeta f\theta''\right) - \frac{\gamma}{2}\left(\zeta f'\theta' + 3f\theta'\right)\Bigg) = \left(\frac{\left(\widetilde{\rho}\widetilde{C}_p\right)_f}{\left(\widetilde{\rho}\widetilde{C}_p\right)_{nf}}\frac{\widetilde{k}_{nf}}{\widetilde{k}_f}\right)\theta'' + \frac{\left(\widetilde{\rho}\widetilde{C}_p\right)_f}{\left(\widetilde{\rho}\widetilde{C}_p\right)_{nf}}\left(A^*f' + B^*\theta\right) + P_r\frac{\frac{\widetilde{\sigma}_{nf}}{\widetilde{\sigma}_f}}{\frac{\left(\widetilde{\rho}\widetilde{C}_p\right)_{nf}}{\left(\widetilde{\rho}\widetilde{C}_p\right)_f}}ME_c f'^2.$$

$$\Rightarrow\Bigg[\left(\frac{\left(\widetilde{\rho}\widetilde{C}_p\right)_f}{\left(\widetilde{\rho}\widetilde{C}_p\right)_{nf}}\frac{\widetilde{k}_{nf}}{\widetilde{k}_f}\right) - \beta_e P_r\left(\frac{\gamma^2}{4}\zeta^2 + f^2 - \gamma\zeta f\right)\Bigg]\theta'' = P_r\gamma\frac{\zeta}{2}\theta' - P_r f\theta' + \beta_e P_r\Bigg(\frac{\gamma^2}{4}3\zeta\theta' + ff'\theta' - \frac{\zeta}{2}\left(\zeta f'\theta' + 3f\theta'\right)\Bigg) - \frac{\left(\widetilde{\rho}\widetilde{C}_p\right)_f}{\left(\widetilde{\rho}\widetilde{C}_p\right)_{nf}}\left(A^*f' + B^*\theta\right) - P_r\frac{\frac{\widetilde{\sigma}_{nf}}{\widetilde{\sigma}_f}}{\frac{\left(\widetilde{\rho}\widetilde{C}_p\right)_{nf}}{\left(\widetilde{\rho}\widetilde{C}_p\right)_f}}ME_c f'^2.$$

$$\Rightarrow\Bigg[\left(\frac{\widetilde{P}_5}{\widetilde{P}_4}\right) - \beta_e P_r\left(\frac{\gamma^2}{4}\zeta^2 + f^2 - \gamma\zeta f\right)\Bigg]\theta'' = P_r\gamma\frac{\zeta}{2}\theta' - P_r f\theta' + \beta_e P_r\Bigg(\frac{\gamma^2}{4}3\zeta\theta' + ff'\theta' - \frac{\zeta}{2}\left(\zeta f'\theta' + 3f\theta'\right)\Bigg) - \frac{\left(A^*f' + B^*\theta\right)}{\widetilde{P}_4} - P_r\frac{\widetilde{P}_6}{\widetilde{P}_4}ME_c f'^2. \quad (4.20)$$

4.3.3 Non-dimensionalization of Concentration Equation

Here are the following derivatives that will be use in equation (4.4):

- $\dfrac{\partial \widetilde{C}}{\partial \widetilde{t}} = (\widetilde{C}_w - \widetilde{C}_\infty)\chi'(\zeta)\dfrac{\alpha\zeta}{2\left(1-\alpha\widetilde{t}\right)}$

$$= (\widetilde{C}_w - \widetilde{C}_\infty)\frac{\alpha}{2}\sqrt{\frac{\widetilde{a}}{\widetilde{\nu}_f}}\frac{\widetilde{y}}{\left(1-\alpha\widetilde{t}\right)^{\frac{3}{2}}}\chi'.$$

- $\dfrac{\partial^2 \widetilde{C}}{\partial \widetilde{t}^2} = (\widetilde{C}_w - \widetilde{C}_\infty)\dfrac{\alpha}{2}\sqrt{\dfrac{\widetilde{a}}{\widetilde{\nu}_f}}\widetilde{y}\dfrac{\partial}{\partial \widetilde{t}}\Big(\left(1-\alpha\widetilde{t}\right)^{-\frac{3}{2}}\chi'\Big)$

$$= (\widetilde{C}_w - \widetilde{C}_\infty)\frac{\alpha}{2}\sqrt{\frac{\widetilde{a}}{\widetilde{\nu}_f}}\widetilde{y}\Big(-\frac{3}{2}\left(1-\alpha\widetilde{t}\right)^{-\frac{5}{2}}(-\alpha)\chi' + \left(1-\alpha\widetilde{t}\right)^{-\frac{3}{2}}\chi''\frac{\partial\zeta}{\partial\widetilde{t}}\Big)$$

$$= (\widetilde{C}_w - \widetilde{C}_\infty)\frac{\alpha}{2}\sqrt{\frac{\widetilde{a}}{\widetilde{\nu}_f}}\widetilde{y}\Big(\frac{3\alpha}{2\left(1-\alpha\widetilde{t}\right)^{\frac{5}{2}}} + \frac{\alpha\zeta}{2\left(1-\alpha\widetilde{t}\right)^{\frac{5}{2}}}\chi''\Big)$$

$$= (\widetilde{C}_w - \widetilde{C}_\infty)\frac{\alpha^2}{4\left(1-\alpha\widetilde{t}\right)^{\frac{5}{2}}}\sqrt{\frac{\widetilde{a}}{\nu_f}}\widetilde{y}\left(3\theta' + \zeta\chi''\right)$$

$$= (\widetilde{C}_w - \widetilde{C}_\infty)\frac{\alpha^2\zeta}{4\left(1-\alpha\widetilde{t}\right)^{2}}\left(3\chi' + \zeta\chi''\right). \tag{4.21}$$

- $\widetilde{v}\dfrac{\partial \widetilde{v}}{\partial \widetilde{y}}\dfrac{\partial \widetilde{C}}{\partial \widetilde{y}} = \left(-\sqrt{\dfrac{\widetilde{a}\nu_f}{1-\alpha\widetilde{t}}}f\right)\left(\dfrac{-\widetilde{a}}{1-\alpha\widetilde{t}}f'\right)\left((\widetilde{C}_w - \widetilde{C}_\infty)\chi'\sqrt{\dfrac{\widetilde{a}}{\widetilde{\nu}_f\left(1-\alpha\widetilde{t}\right)}}\right)$

$$= \frac{\widetilde{a}^2}{\left(1-\alpha\widetilde{t}\right)^2}ff'\chi'(\widetilde{T}_w - \widetilde{T}_\infty). \tag{4.22}$$

- $\widetilde{u}\dfrac{\partial \widetilde{u}}{\partial \widetilde{x}}\dfrac{\partial \widetilde{C}}{\partial \widetilde{x}} = 0.$ (4.23)

- $\widetilde{u}\dfrac{\partial \widetilde{v}}{\partial \widetilde{x}}\dfrac{\partial \widetilde{C}}{\partial \widetilde{y}} = 0.$ (4.24)

- $\widetilde{v}\dfrac{\partial \widetilde{u}}{\partial \widetilde{x}}\dfrac{\partial \widetilde{C}}{\partial \widetilde{x}} = 0.$ (4.25)

- $2\widetilde{u}\widetilde{v}\dfrac{\partial^2 \widetilde{C}}{\partial \widetilde{x}\partial \widetilde{y}} = 0.$ (4.26)

- $\widetilde{u}^2\dfrac{\partial^2 \widetilde{C}}{\partial \widetilde{x}^2} = 0.$ (4.27)

- $\widetilde{v}^2\dfrac{\partial^2 \widetilde{C}}{\partial \widetilde{y}^2} = \left(\dfrac{\widetilde{a}\widetilde{\nu}_f}{1-\alpha\widetilde{t}}f^2\right)\left((\widetilde{C}_w - \widetilde{C}_\infty)\dfrac{\widetilde{a}}{\widetilde{\nu}_f\left(1-\alpha\widetilde{t}\right)}\right)$

$$= \left(\frac{\widetilde{a}^2}{\left(1-\alpha\widetilde{t}\right)^2}\right)(\widetilde{C}_w - \widetilde{C}_\infty)f^2\chi''. \tag{4.28}$$

- $\dfrac{\partial \widetilde{u}}{\partial \widetilde{t}}\dfrac{\partial \widetilde{C}}{\partial \widetilde{x}} = 0.$ (4.29)

- $2\widetilde{u}\dfrac{\partial^2 \widetilde{C}}{\partial \widetilde{x}\partial \widetilde{t}} = 0.$ (4.30)

  - $$\begin{aligned}\frac{\partial \widetilde{v}}{\partial \widetilde{t}} &= -\sqrt{\widetilde{a}\widetilde{\nu}_f}\frac{\partial}{\partial \widetilde{t}}\left(\left(1-\alpha\widetilde{t}\right)^{-\frac{1}{2}} f(\zeta)\right)\\ &= -\sqrt{\widetilde{a}\widetilde{\nu}_f}\left(-\frac{1}{2}\left(1-\alpha\widetilde{t}\right)^{-\frac{3}{2}}(-\alpha) f + \left(1-\alpha\widetilde{t}\right)^{-\frac{1}{2}} f'\frac{\partial \zeta}{\partial \widetilde{t}}\right)\\ &= -\sqrt{\widetilde{a}\widetilde{\nu}_f}\left(\frac{\alpha f}{2\left(1-\alpha\widetilde{t}\right)^{\frac{3}{2}}} + \left(1-\alpha\widetilde{t}\right)^{-\frac{1}{2}} f'\frac{\alpha\zeta}{2\left(1-\alpha\widetilde{t}\right)}\right)\\ &= -\sqrt{\widetilde{a}\widetilde{\nu}_f}\left(\frac{\alpha f}{2\left(1-\alpha\widetilde{t}\right)^{\frac{3}{2}}} + \frac{\alpha\zeta f'}{2\left(1-\alpha\widetilde{t}\right)\left(1-\alpha\widetilde{t}\right)^{\frac{1}{2}}}\right)\\ &= -\sqrt{\widetilde{a}\widetilde{\nu}_f}\left(\frac{\alpha f}{2\left(1-\alpha\widetilde{t}\right)^{\frac{3}{2}}} + \frac{\alpha\zeta f'}{2\left(1-\alpha\widetilde{t}\right)^{\frac{3}{2}}}\right)\\ &= -\sqrt{\widetilde{a}\widetilde{\nu}_f}\frac{\alpha}{2\left(1-\alpha\widetilde{t}\right)^{\frac{3}{2}}}\left(f+\zeta f'\right).\end{aligned}$$

  - $$\begin{aligned}\frac{\partial \widetilde{v}}{\partial \widetilde{t}}\frac{\partial \widetilde{C}}{\partial \widetilde{y}} &= \left(-\sqrt{\widetilde{a}\widetilde{\nu}_f}\frac{\alpha}{2\left(1-\alpha\widetilde{t}\right)^{\frac{3}{2}}}\left(f+\zeta\right)f'\right)\left((\widetilde{C}_w-\widetilde{C}_\infty)\chi'\sqrt{\frac{\widetilde{a}}{\widetilde{\nu}_f\left(1-\alpha\widetilde{t}\right)}}\right)\\ &= -\frac{\widetilde{a}\alpha(\widetilde{C}_w-\widetilde{C}_\infty)}{2\left(1-\alpha\widetilde{t}\right)^2}\left(f\chi'+\zeta f'\chi'\right).\end{aligned}$$ (4.31)

  - $\dfrac{\partial \widetilde{C}}{\partial \widetilde{y}} = (\widetilde{C}_w-\widetilde{C}_\infty)\chi'\sqrt{\dfrac{\widetilde{a}}{\widetilde{\nu}_f\left(1-\alpha\widetilde{t}\right)}}.$

  - $$\begin{aligned}\frac{\partial^2 \widetilde{C}}{\partial \widetilde{y}\partial \widetilde{t}} &= \sqrt{\frac{\widetilde{a}}{\widetilde{\nu}_f}}(\widetilde{C}_w-\widetilde{C}_\infty)\frac{\partial}{\partial \widetilde{t}}\left(\frac{\chi'}{\left(1-\alpha\widetilde{t}\right)^{\frac{1}{2}}}\right)\\ &= \sqrt{\frac{\widetilde{a}}{\widetilde{\nu}_f}}(\widetilde{C}_w-\widetilde{C}_\infty)\left(\frac{\left(1-\alpha\widetilde{t}\right)^{\frac{1}{2}}\chi''\frac{\partial\zeta}{\partial\widetilde{t}} - \frac{1}{2}\left(1-\alpha\widetilde{t}\right)^{-\frac{1}{2}}(-\alpha)\theta'}{\left(\left(1-\alpha\widetilde{t}\right)^{\frac{1}{2}}\right)^2}\right)\\ &= \sqrt{\frac{\widetilde{a}}{\widetilde{\nu}_f}}(\widetilde{C}_w-\widetilde{C}_\infty)\left(\frac{\left(1-\alpha\widetilde{t}\right)^{\frac{1}{2}}\chi''\frac{\alpha\zeta}{2\left(1-\alpha\widetilde{t}\right)} + \frac{\alpha}{2}\left(1-\alpha\widetilde{t}\right)^{\frac{-1}{2}}\chi'}{\left(1-\alpha\widetilde{t}\right)}\right)\\ &= \sqrt{\frac{\widetilde{a}}{\widetilde{\nu}_f}}(\widetilde{C}_w-\widetilde{C}_\infty)\left(\frac{\chi''\frac{\alpha\zeta}{2}+\frac{\alpha}{2}\chi'}{\left(1-\alpha\widetilde{t}\right)^{\frac{3}{2}}}\right)\\ &= \sqrt{\frac{\widetilde{a}}{\widetilde{\nu}_f\left(1-\alpha\widetilde{t}\right)}}\frac{(\widetilde{C}_w-\widetilde{C}_\infty)}{2\left(1-\alpha\widetilde{t}\right)}\frac{\alpha}{2}\left(\zeta\chi''+\chi'\right)\end{aligned}$$

  - $2\widetilde{v}\dfrac{\partial^2 \widetilde{C}}{\partial \widetilde{y}\partial \widetilde{t}} = 2\left(-\sqrt{\dfrac{\widetilde{a}\widetilde{\nu}_f}{\left(1-\alpha\widetilde{t}\right)}}f\right)\sqrt{\dfrac{\widetilde{a}}{\widetilde{\nu}_f\left(1-\alpha\widetilde{t}\right)}}\dfrac{(\widetilde{C}_w-\widetilde{C}_\infty)}{2\left(1-\alpha\widetilde{t}\right)}\dfrac{\alpha}{2}\left(\zeta\chi''+\chi'\right)$

$$= -\frac{\widetilde{a}\alpha}{\left(1-\alpha\widetilde{t}\right)^2}(\widetilde{C}_w - \widetilde{C}_\infty)\left(\zeta f\chi'' + f\chi'\right). \tag{4.32}$$

By substituting (3.23) - (3.28), (4.21) - (4.32), and velocity component (3.6), into (4.4), we get the following:

$$\begin{aligned}
&(\widetilde{C}_w - \widetilde{C}_\infty)\chi'\frac{\alpha\zeta}{2\left(1-\alpha\widetilde{t}\right)} - \left(\sqrt{\frac{\widetilde{a}\widetilde{\nu}_f}{1-\alpha\widetilde{t}}}f\right)\left((\widetilde{C}_w - \widetilde{C}_\infty)\chi'\sqrt{\frac{\widetilde{a}}{\widetilde{\nu}_f\left(1-\alpha\widetilde{t}\right)}}\right)\\
&\quad + \lambda_C\Bigg((\widetilde{C}_w - \widetilde{C}_\infty)\frac{\alpha^2\zeta}{4\left(1-\alpha\widetilde{t}\right)^2}\left(3\chi' + \zeta\chi''\right)\\
&\quad + \frac{\widetilde{a}^2}{\left(1-\alpha\widetilde{t}\right)^2}ff'\chi'(\widetilde{C}_w - \widetilde{C}_\infty) + \left(\frac{\widetilde{a}^2}{\left(1-\alpha\widetilde{t}\right)^2}\right)(\widetilde{C}_w - \widetilde{C}_\infty)f^2\chi''\\
&\quad - \frac{\widetilde{a}\alpha(\widetilde{C}_w - \widetilde{C}_\infty)}{2\left(1-\alpha\widetilde{t}\right)^2}\left(f\chi' + \zeta f'\chi'\right) - \frac{\widetilde{a}\alpha}{\left(1-\alpha\widetilde{t}\right)^2}(\widetilde{C}_w - \widetilde{C}_\infty)\left(\zeta f\chi'' + f\chi'\right)\Bigg)\\
&\quad = \frac{\widetilde{\nu}_f}{\widetilde{S}_c}(\widetilde{C}_w - \widetilde{C}_\infty)\frac{\widetilde{a}}{\widetilde{\nu}_f\left(1-\alpha\widetilde{t}\right)}\chi'' - \tau\frac{\widetilde{a}}{1-\alpha\widetilde{t}}\left(\widetilde{C}_w - \widetilde{C}_\infty\right)\left(\theta''\chi + \theta'\chi'\right)
\end{aligned}$$

$$\begin{aligned}
\Rightarrow\ &\frac{\alpha}{\widetilde{a}}\frac{\zeta}{2}\chi' - f\chi' + \lambda_C\Bigg(\frac{\alpha^2}{4\widetilde{a}\left(1-\alpha\widetilde{t}\right)}\left(3\zeta\chi' + \zeta^2\chi''\right) + \frac{\widetilde{a}}{1-\alpha\widetilde{t}}ff'\chi' + \frac{\widetilde{a}}{1-\alpha\widetilde{t}}f^2\chi''\\
&\quad - \frac{\alpha}{2\left(1-\alpha\widetilde{t}\right)}\left(f\chi' + \zeta f'\chi'\right) - \frac{\alpha}{1-\alpha\widetilde{t}}\left(\zeta f\chi'' + f\chi'\right)\Bigg) = \frac{1}{\widetilde{S}_c}\chi''\\
&\quad - \tau\left(\theta''\chi + \theta'\chi'\right).
\end{aligned}$$

$$\begin{aligned}
\Rightarrow\ &\frac{\alpha}{\widetilde{a}}\frac{\zeta}{2}\chi' - f\chi' + \lambda_C\Bigg(\frac{\alpha^2}{4\widetilde{a}\left(1-\alpha\widetilde{t}\right)}\left(3\zeta\chi' + \zeta^2\chi''\right) + \frac{\widetilde{a}}{1-\alpha\widetilde{t}}ff'\chi' + \frac{\widetilde{a}}{1-\alpha\widetilde{t}}f^2\chi''\\
&\quad - \frac{\alpha}{2\left(1-\alpha\widetilde{t}\right)}\left(f\chi' + \zeta f'\chi'\right) - \frac{\alpha}{1-\alpha\widetilde{t}}\left(\zeta f\chi'' + f\chi'\right)\Bigg) = \frac{1}{\widetilde{S}_c}\chi''\\
&\quad - \tau\left(\theta''\chi + \theta'\chi'\right).
\end{aligned}$$

$$\begin{aligned}
\Rightarrow\ &\gamma\frac{\zeta}{2}\chi' - f\chi' + \beta_c\Bigg(\frac{\gamma^2}{4}\left(3\zeta\chi' + \zeta^2\chi''\right) + ff'\chi' + f^2\chi'' - \frac{\gamma}{2}\left(f\chi' + \zeta f'\chi'\right)\\
&\quad - \gamma\left(\zeta f\chi'' + f\chi'\right)\Bigg) = \frac{1}{\widetilde{S}_c}\chi'' - \tau\left(\theta''\chi + \theta'\chi'\right).
\end{aligned}$$

$$\begin{aligned}
\Rightarrow\ &\gamma\frac{\zeta}{2}\chi' - f\chi' + \beta_c\Bigg(\frac{\gamma^2}{4}\left(3\zeta\chi' + \zeta^2\chi''\right) + \left(ff'\chi' + f^2\chi'' - \gamma\zeta f\chi''\right)\\
&\quad - \frac{\gamma}{2}\left(\zeta f'\chi' + 3f\chi'\right)\Bigg) = \frac{1}{\widetilde{S}_c}\chi'' - \tau\left(\theta''\chi + \theta'\chi'\right).
\end{aligned}$$

$$\begin{aligned}
\Rightarrow\ &\frac{1}{\widetilde{S}_c}\chi'' - \tau\left(\theta''\chi + \theta'\chi'\right) - \gamma\frac{\zeta}{2}\chi' + f\chi' - \beta_c\Bigg(\frac{\gamma^2}{4}\left(3\zeta\chi' + \zeta^2\chi''\right)\\
&\quad + \left(ff'\chi' + f^2\chi'' - \gamma\zeta f\chi''\right) - \frac{\gamma}{2}\left(\zeta f'\chi' + 3f\chi'\right)\Bigg) = 0.
\end{aligned}$$

$$\Rightarrow \left[\frac{1}{\widetilde{S}_c} - \beta_c\left(\zeta^2\frac{\gamma^2}{4} + f^2 - \gamma\zeta f\right)\right]\chi'' = -f\chi' + \gamma\frac{\zeta}{2}\chi' + \beta_c\frac{3\zeta\gamma^2\chi'}{4} + \beta_c f f'\chi' - \beta_c\frac{\gamma}{2}\left(\zeta f'\chi' + 3f\chi'\right) + \tau\left(\theta''\chi + \theta'\chi'\right). \tag{4.33}$$

4.4 Solution Framework

To solve the ODE (4.7), the following notations have been introduced as an initial step:

$$f(\zeta) = \widetilde{Y}_1, \qquad f'(\zeta) = \widetilde{Y}_1' = \widetilde{Y}_2, \qquad f''(\zeta) = \widetilde{Y}_2' = \widetilde{Y}_3.$$

The following system of ODEs has been derived to replace the momentum equation:

$$\begin{aligned}
&\widetilde{Y}_1' = \widetilde{Y}_2, && \widetilde{Y}_1(0) = \widetilde{f}_0,\\
&\widetilde{Y}_2' = \widetilde{Y}_3, && \widetilde{Y}_2(0) = 1,\\
&\widetilde{Y}_3' = -\frac{2\beta\widetilde{Y}_1\widetilde{Y}_2\widetilde{Y}_3 - \gamma\left(\widetilde{Y}_2 + \frac{\zeta}{2}\widetilde{Y}_3\right) - \widetilde{Y}_2^2 + \widetilde{Y}_1\widetilde{Y}_3 - \frac{\widetilde{P}_6}{\widetilde{P}_1}M\widetilde{Y}_2 - \widetilde{P}_3\widetilde{K}_p\widetilde{Y}_2}{\widetilde{P}_3 - \beta\widetilde{Y}_1^2}, && \widetilde{Y}_3(0) = s_1.
\end{aligned}$$

To apply the RK4 method for the numerical solution of the specified IVP described above, the parameter s_1 within the system of equations must be carefully selected. The value of s_1 should be chosen such that:

$$\widetilde{Y}_2\big(\zeta_\infty, s_1\big) = 0.$$

Newton's method will be employed to further refine the selection of s_1. This method has the following iterative scheme :

$${s_1}^{(m+1)} = s_1^{(m)} - \frac{\widetilde{Y}_2\big(\zeta_\infty, s_1^{(m)}\big)}{\left(\frac{\partial}{\partial s_1}\widetilde{Y}_2\big(\zeta_\infty, s_1\big)\right)^{(m)}}.$$

We further introduce the following notations:

$$\frac{\partial\widetilde{Y}_1}{\partial s_1} = \widetilde{Y}_4, \qquad \frac{\partial\widetilde{Y}_2}{\partial s_1} = \widetilde{Y}_5, \qquad \frac{\partial\widetilde{Y}_3}{\partial s_1} = \widetilde{Y}_6.$$

As a result of the introduction of these new notations, Newton's iterative scheme assumes the following form:

$$s_1{}^{(m+1)} = s_1^{(m)} - \frac{\widetilde{Y}_2\big(\zeta_\infty, s_1^{(m)}\big)}{\widetilde{Y}_5\big(\zeta_\infty, s_1\big)}.$$

Differentiating the aforementioned system of three first-order ODEs with respect to s_1 results in an additional system of ODEs, which can be expressed as follows:

$$\begin{aligned}
&\widetilde{Y}_4' = \widetilde{Y}_5, && \widetilde{Y}_4(0) = 0,\\
&\widetilde{Y}_5' = \widetilde{Y}_6, && \widetilde{Y}_5(0) = 0,\\
&\widetilde{Y}_6' = -\Bigg[\left(\frac{1}{\widetilde{P}_3 - \beta\widetilde{Y_1}^2}\right)^2\left(\widetilde{P}_3 - \beta\widetilde{Y_1}^2\right)\left(2\beta\left(\widetilde{Y}_1\widetilde{Y}_2\widetilde{Y}_6 + \widetilde{Y}_1\widetilde{Y}_5\widetilde{Y}_3 + \widetilde{Y}_4\widetilde{Y}_2\widetilde{Y}_3\right)\right)\\
&\quad - \gamma\left(\widetilde{Y}_5 + \frac{\zeta}{2}\widetilde{Y}_6\right) - 2\widetilde{Y}_2\widetilde{Y}_5 + \widetilde{Y}_1\widetilde{Y}_6 + \widetilde{Y}_4\widetilde{Y}_3 - 2\beta\widetilde{Y}_1\widetilde{Y}_2\widetilde{Y}_3 - \gamma\left(\widetilde{Y}_2 + \frac{\zeta}{2}\widetilde{Y}_3\right)\\
&\quad - \widetilde{Y}_2^2 + \widetilde{Y}_1\widetilde{Y}_3 - \frac{\widetilde{P}_6}{\widetilde{P}_1}M\widetilde{Y}_2 - \widetilde{P}_3\widetilde{K}_p\widetilde{Y}_2\left(-2\beta\widetilde{Y}_1\widetilde{Y}_4\right)\Bigg], && \widetilde{Y}_6(0) = 1.
\end{aligned}$$

The stopping criteria for Newton's method are established as follows:

$$\left|\widetilde{Y}_2\left(\zeta_\infty, s_1\right)\right| < \epsilon.$$

To numerically solve the energy equation using the shooting method, we will treat f and f''as known functions. The following notations will be used to implement the shooting method:

$$\theta = \widetilde{Z}_1, \qquad \theta' = \widetilde{Z}_1' = \widetilde{Z}_2'.$$

The energy equation can be expressed as the following system of coupled first-order ODEs:

$$\begin{aligned}
&\widetilde{Z}_1' = \widetilde{Z}_2, && \widetilde{Z}_1(0) = 1,\\
&\widetilde{Z}_2' = \frac{1}{\frac{\widetilde{P}_5}{\widetilde{P}_4} - \beta_e P_r\left(\frac{\gamma^2}{4}\zeta^2 + d_1^2 - \gamma\zeta d_1\right)}\Bigg(P_r\gamma\frac{\zeta}{2}\widetilde{Z}_2 - P_r d_1\widetilde{Z}_2\\
&\quad + \beta_e P_r\left(\frac{\gamma^2}{4}3\zeta\widetilde{Z}_2 + d_1 d_2\widetilde{Z}_2 - \frac{\gamma}{2}\left(\zeta d_2\widetilde{Z}_2 + 3d_1\widetilde{Z}_2\right)\right)\\
&\quad - \frac{A^* d_2 + B^*\widetilde{Z}_1}{\widetilde{P}_4} - P_r\left(\frac{\widetilde{P}_6}{\widetilde{P}_4}\right)ME_c d_2^2\Bigg), && \widetilde{Z}_2(0) = m.
\end{aligned}$$

To apply the RK4 method for the numerical solution of the initial value problem described above, it is crucial to carefully select the condition m within the system of equations. This condition m must be chosen to ensure that:

$$\widetilde{Z}_1(\zeta_\infty, m) = 0.$$

Newton's method will be employed to determine m using the following iterative scheme:

$$m^{(n+1)} = m^{(n)} - \frac{\widetilde{Z}_1\left(\zeta_\infty, m^{(n)}\right)}{\left(\frac{\partial}{\partial \widetilde{m}} \widetilde{Z}_1(\zeta_\infty, m)\right)^{(n)}}.$$

We further introduce the following notations:

$$\frac{\partial \widetilde{Z}_1}{\partial m} = \widetilde{Z}_3, \qquad \frac{\partial \widetilde{Z}_2}{\partial m} = \widetilde{Z}_4.$$

As a result of introducing these new notations, Newton's iterative scheme adopts the following form:

$$m^{(n+1)} = m^{(n)} - \frac{\widetilde{Z}_1\left(\zeta_\infty, m^{(n)}\right)}{\widetilde{Z}_3\left(\zeta_\infty, m^{(n)}\right)}.$$

Differentiating the aforementioned system of three first-order ordinary differential equations (ODEs) with respect to m yields an additional system of ODEs, which is expressed as follows:

$$\widetilde{Z}_3' = \widetilde{Z}_4, \qquad \widetilde{Z}_3(0) = 1,$$
$$\widetilde{Z}_4' = \frac{1}{\frac{\widetilde{P}_5}{\widetilde{P}_4} - \beta_e P_r \left(\frac{\gamma^2}{4}\zeta^2\right)} \left(P_r \gamma \frac{\zeta}{2} \widetilde{Z}_4 + \beta_e P_r \left(\frac{\gamma^2}{4} 3\zeta \widetilde{Z}_4 + \right) - \frac{B^* \widetilde{Z}_3}{\widetilde{P}_4} \right), \qquad \widetilde{Z}_2(0) = m.$$

The stopping criteria for Newton's method are defined as follows:

$$\left|\widetilde{Z}_1(\zeta_\infty, m)\right| < \epsilon.$$

To numerically solve the concentration equation using the shooting method, we will treat f and f''as a known function. The following notations will be used for implementing

the shooting method:

$$\chi = \widetilde{Q}_1, \qquad \chi' = \widetilde{Q}_1' = \widetilde{Q}_2'.$$

The energy equation can be formulated as the following system of first-order coupled ODEs:

$$\begin{aligned}
&\widetilde{Q}_1' = \widetilde{Q}_2, && \widetilde{Q}_1(0) = 0,\\
&\widetilde{Q}_2' = \frac{1}{-\frac{1}{\widetilde{S}_c} + \beta_c\left(\frac{\gamma^2}{4}\zeta^2 + d_1^2 - \gamma\zeta d_1\right)}\Bigg(d_1\widetilde{Q}_1 - \frac{\gamma}{2}\zeta - \frac{\beta_c 3\gamma^2\zeta\widetilde{Q}_1}{4} - \beta_c d_1 d_2\widetilde{Q}_1\\
&\quad + \beta_c\frac{\gamma}{2}\left(\zeta d_2\widetilde{Q}_1 + 3d_1\widetilde{Q}_1\right) - \tau\Bigg(\frac{1}{\frac{\widetilde{P}_5}{\widetilde{P}_4} - \beta_e\,\mathrm{pr}\left(\frac{\gamma^2}{4}\zeta^2 + d_1^2 - \gamma\zeta d_1\right)}\Bigg(P_r\gamma\frac{\zeta}{2}\widetilde{Z}_2\\
&\quad - P_r d_1\widetilde{Z}_2 + \beta_e P_r\left(\frac{\gamma^2}{4}3\zeta\widetilde{Z}_2 + d_1 d_2\widetilde{Z}_2 - \frac{\gamma}{2}\left(\zeta d_2\widetilde{Z}_2 + 3d_1\widetilde{Z}_2\right)\right) - \frac{A^* d_2 + B^*\widetilde{Z}_1}{\widetilde{P}_4}\\
&\quad - P_r\frac{\widetilde{P}_6}{\widetilde{P}_4}ME_c d_2^2\Bigg)\widetilde{Q}_1 + \widetilde{Z}_2\widetilde{Q}_2\Bigg)\Bigg), && \widetilde{Q}_2(0) = r.
\end{aligned}$$

To apply the RK4 method for the numerical solution of the initial value problem outlined above, it is essential to carefully select the condition r within the system of equations. This condition r should be chosen to ensure that:

$$\widetilde{Q}_1\big(\zeta_\infty, r\big) = 0.$$

Newton's method will be used to find r with the following iterative scheme:

$$r^{(n+1)} = r^{(n)} - \frac{\widetilde{Q}_1\big(\zeta_\infty, r^{(n)}\big)}{\left(\frac{\partial}{\partial s}\widetilde{Q}_1\big(\zeta_\infty, r\big)\right)^{(n)}}.$$

We further introduce the following notations:

$$\frac{\partial\widetilde{Q}_1}{\partial r} = \widetilde{Q}_3, \qquad \frac{\partial\widetilde{Q}_2}{\partial r} = \widetilde{Q}_4.$$

As a result of these new notations, the Newton's iterative scheme gets the form:

$$r^{(n+1)} = r^{(n)} - \frac{\widetilde{Q}_1\big(\zeta_\infty, r^{(n)}\big)}{\widetilde{Q}_3\big(\zeta_\infty, r^{(n)}\big)}.$$

Now, differentiating the system of two first order ODEs with respect to r, we get another system of ODEs, as follows:

$$\begin{aligned}
&\widetilde{Q}_3' = \widetilde{Q}_4, && \widetilde{Q}_3(0) = 0,\\
&\widetilde{Q}_4' = \frac{1}{-\frac{1}{\widetilde{S}_c} + \beta_c\left(\frac{\gamma^2}{4}\zeta^2\right)}\Bigg(-\frac{\gamma}{2}\zeta - \frac{\beta_c 3\gamma^2\zeta\widetilde{Q}_3}{4}\\
&\quad - \tau\Bigg(\frac{1}{\frac{\widetilde{P}_5}{\widetilde{P}_4} - \beta_e P_r\left(\frac{\gamma^2}{4}\zeta^2 + d_1^2 - \gamma\zeta d_1\right)}\Bigg(P_r\gamma\frac{\zeta}{2}\widetilde{Z}_2 - P_r d_1\widetilde{Z}_2\\
&\quad + \beta_e P_r\left(\frac{\gamma^2}{4}3\zeta\widetilde{Z}_2 + d_1 d_2\widetilde{Z}_2 - \frac{\gamma}{2}\left(\zeta d_2\widetilde{Z}_2 + 3d_1\widetilde{Z}_2\right)\right) - \frac{A^* d_2 + B^*\widetilde{Z}_1}{\widetilde{P}_4}\\
&\quad - P_r\frac{\widetilde{P}_6}{\widetilde{P}_4}ME_c d_2^2\Bigg)\widetilde{Q}_3 + \widetilde{Z}_2\widetilde{Q}_4\Bigg)\Bigg), && \widetilde{Q}_4(0) = 1.
\end{aligned}$$

The stopping criteria for Newton's method are defined as follows:

$$\left|\widetilde{Q}_1(\zeta_\infty, r)\right| < \epsilon.$$

4.5 Results Interpretation

Upon converting the governing PDEs that describe the fluid flow into an ODE system, a number of important factors become apparent. Through the use of graphical representations, the effects of these physical factors on the nanoparticle $\phi(\zeta)$ distributions' velocity $f'(\zeta)$, temperature $\theta(\zeta)$ and concentration are thoroughly examined. The study's findings are provided in a thorough manner, along with a detailed discussion of the significance and interpretations of each parameter's impact.

4.5.1 Analysis of Computational Results

This study looks closely at how different physical characteristics affect the Sherwood number, the Nusselt number, and the coefficient of skin friction. The coefficient of skin friction increases with increases in β, γ, f_0, M, and K_p, as Table 4.2 demonstrates. On the other hand, a rise in ϕ causes the skin friction coefficient to decrease. Nusselt number values drop as $A^*, B^* < 0$, $A^*, B^* > 0$, M, and E_c increase, as Tables 4.3 – 4.4 demonstrate. In the same way, Tables 4.3 and 4.4 show that the Sherwood number decreases as S_c and τ rise.

TABLE 4.2: The skin friction coefficient

β	γ	f_0	ϕ	M	K_p	$-f''(0)$
0.1	0.1	0	0.01	0.1	0.1	1.143796
0.2						1.166145
0.3						1.188218
0.4						1.210015
0.5						1.231535
	0.2					1.174240
	0.3					1.204360
	0.4					1.234111
	0.5					1.263453
		-0.3				0.983605
		-0.2				1.033357
		-0.1				1.086653
		0.1				1.205123
		0.2				1.271011
		0.3				1.341886
			0			1.150195
			0.05			1.116268
			0.1			1.077817
			0.2			0.989354
				0		1.099494
				0.2		1.186443
				0.3		1.227604
				0.4		1.267422
					0	1.099133
					0.3	1.228250
					0.5	1.307235
					0.7	1.381689

TABLE 4.3: The Sherwood number and Nusselt number for $A^*, B^* < 0$

β	γ	f_0	ϕ	M	K_p	A^*	B^*	β_e	E_c	β_c	S_c	τ	Nu	Sh
0.1	0.1	0	0.01	0.1	0.1	-0.5	-0.5	0.1	0.4	0.1	1	0.1	2.822722	-0.525243
0.2													2.815182	-0.517570
0.3													2.807733	-0.510141
0.4													2.800369	-0.502955
0.5													2.793095	-0.496010
	0.2												2.738675	-0.471247
	0.3												2.652305	-0.407442
	0.4												2.575000	-0.332405
	0.5												2.494946	-0.248088
		-0.3											0.811467	-0.349459
		-0.2											1.332927	-0.403540
		-0.1											2.001454	-0.462124
		0.1											3.824225	-0.592947
		0.2											5.067246	-0.665321
		0.3											6.633929	-0.721111
			0										2.785673	-0.523808
			0.05										2.974481	-0.532803
			0.1										3.173517	-0.540290
			0.2										3.612374	-0.561197
				0									2.974792	-0.535203
				0.2									2.677258	-0.515848
				0.3									2.537637	-0.506975
				0.4									2.403000	-0.498581
					0								2.834112	-0.535368
					0.3								2.801099	-0.506712
					0.5								2.780826	-0.490170
					0.7								2.761700	-0.475306
						-0.4							2.781380	-0.525267
						-0.3							2.740039	-0.525292
						-0.2							2.698697	-0.525316
						-0.1							2.657355	-0.525341
							-0.4						2.806436	-0.525248
							-0.3						2.790089	-0.525254
							-0.2						2.773683	-0.525260
							-0.1						2.757217	-0.525265
								0.01					2.764544	-0.525259
								0.03					2.777368	-0.525256
								0.05					2.790253	-0.525253
								0.07					2.803198	-0.525250
									0.2				2.891486	-0.525205
									0.3				2.857104	-0.525224
									0.5				2.788340	-0.525261
									0.6				2.753959	-0.525280
										0.01			2.822722	-0.517537
										0.03			2.822722	-0.519219
										0.05			2.822722	-0.520919
										0.07			2.822722	-0.522635
											1.2		2.822722	-0.598972
											1.4		2.822722	-0.669690
											1.6		2.822722	-0.737236
											1.8		2.822722	-0.801753
												0.3	2.822722	-0.531700
												0.5	2.822722	-0.537638
												0.7	2.822722	-0.543101
												0.9	2.822722	-0.548131

TABLE 4.4: The Sherwood number and Nusselt number for $A^*, B^* > 0$

β	γ	f_0	ϕ	M	K_p	A^*	B^*	β_e	E_c	β_c	S_c	τ	Nu	Sh
0.1	0.1	0	0.01	0.1	0.1	0.1	0.1	0.1	0.4	0.1	1	0.1	2.458815	-0.517745
0.2													2.454473	-0.510304
0.3													2.450043	-0.503107
0.4													2.445536	-0.496153
0.5													2.364151	-0.471385
	0.2												2.254077	-0.407602
	0.3												2.230822	-0.331637
	0.4												2.112974	-0.247676
	0.5												0.497754	-0.349700
		-0.3											0.997616	-0.403763
		-0.2											1.652190	-0.462327
		-0.1											3.454170	-0.593130
		0.1											4.683474	-0.665531
		0.2											3.812359	-0.722101
		0.3											2.430305	-0.523999
			0										2.596992	-0.531640
			0.05										2.772149	-0.540456
			0.1										3.156303	-0.561345
			0.2										2.615166	-0.535406
				0									2.317513	-0.516023
				0.2									2.177765	-0.507138
				0.3									2.043168	-0.498735
				0.4									2.470369	-0.535573
					0								2.448624	-0.506872
					0.3								2.434484	-0.490310
					0.5								2.420645	-0.475430
					0.7								2.419545	-0.525456
						0.2							2.376037	-0.525481
						0.3							2.332528	-0.525507
						0.4							2.289020	-0.525532
						0.5							2.444074	-0.525437
							0.2						2.424982	-0.525444
							0.3						2.405776	-0.525451
							0.4						2.386455	-0.525459
							0.5						2.401574	-0.525424
								0.01					2.415147	-0.525424
								0.03					2.428772	-0.525425
								0.05					2.442448	-0.525426
								0.07					2.533782	-0.525392
									0.2				2.498418	-0.525411
									0.3				2.427689	-0.525449
									0.5				2.392325	-0.525468
									0.6				2.376890	-0.525472
										0.01			2.463054	-0.517733
										0.03			2.463054	-0.519414
										0.05			2.463054	-0.521112
										0.07			2.463054	-0.522826
											1.2		2.463054	-0.599199
											1.4		2.463054	-0.669962
											1.6		2.463054	-0.737555
											1.8		2.463054	-0.802121
												0.3	2.463054	-0.532270
												0.5	2.463054	-0.538599
												0.7	2.463054	-0.544459
												0.9	2.463054	-0.549888

4.5.2 Velocity Profile

The present subsection includes, detailed insights into the velocity profile, denoted as $f'(\zeta)$, with respect to various physical parameters. Specifically, Figures 4.1 - 4.6 illustrate the impact of β, γ, f_0, ϕ, M and K_p on the dimensionless velocity $f'(\zeta)$. The effect of the Deborah number on the velocity profile is seen in Figure 4.1. A higher Deborah number corresponds to a lower velocity profile. The Deborah number is a physical representation of the sum of observational and relaxation time. A larger Deborah number causes the fluid motion to be more successfully resisted, which lowers the velocity profile as the relaxation time increases.

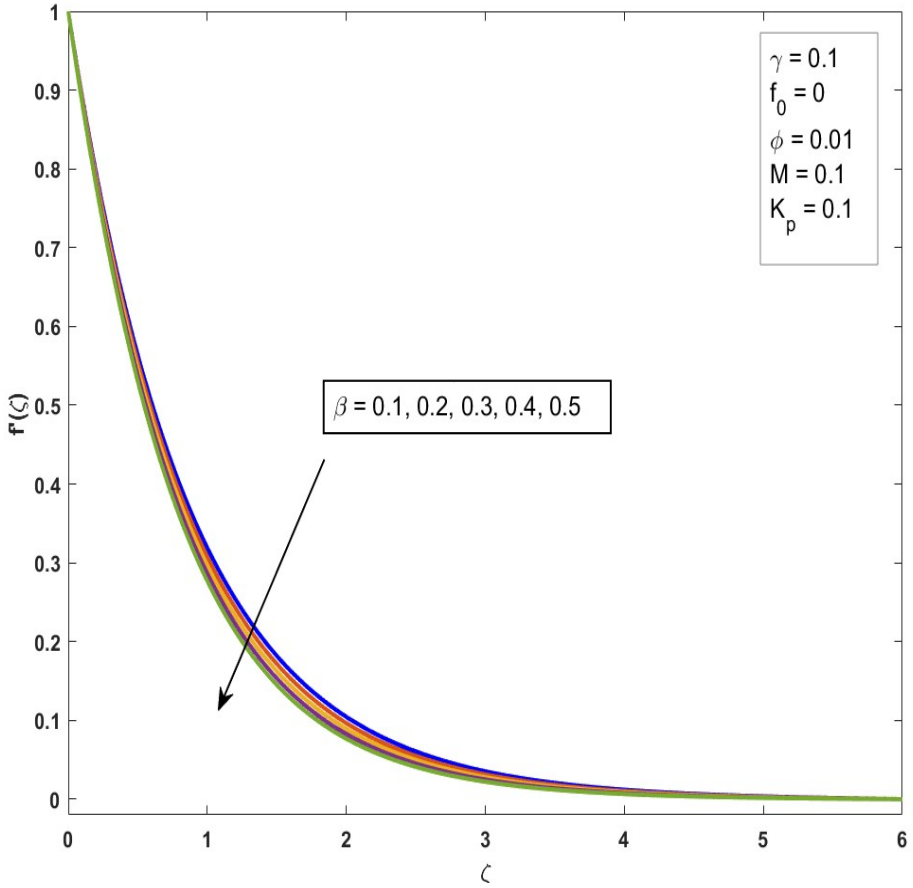

FIGURE 4.1: Impact of β on $f'(\zeta)$

Figure 4.2 illustrates the effect of the unsteadiness parameter on the velocity profile. As the value of the unsteadiness parameter increases, the velocity profile decreases. It can be observed that the velocity along the sheet initially declines with rising values

of the unsteadiness parameter, indicating a corresponding reduction in the momentum boundary layer thickness near the wall.

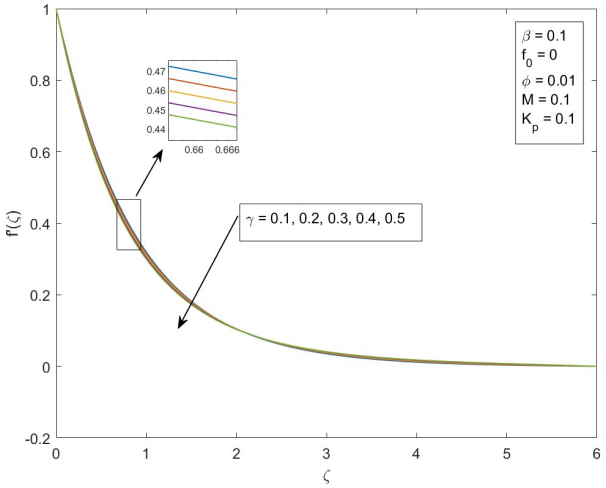

FIGURE 4.2: Impact of γ on $f'(\zeta)$

Figure 4.3 demonstrates the effect of surface injection $f_0 < 0$ and suction $f_0 > 0$ on the velocity distribution. As the injection and suction parameter increases, the velocity profile tends to exhibit a decreasing trend, and the viscous boundary layer becomes thinner due to the rise in the injection and suction parameter value. The graphical results align well with physical observations. Injection refers to the process of drawing liquid from a region of lower pressure to a region of higher pressure and suction refers to the process of drawing liquid from a region of higher pressure to a region of lower pressure, resulting in a decrease in fluid velocity.

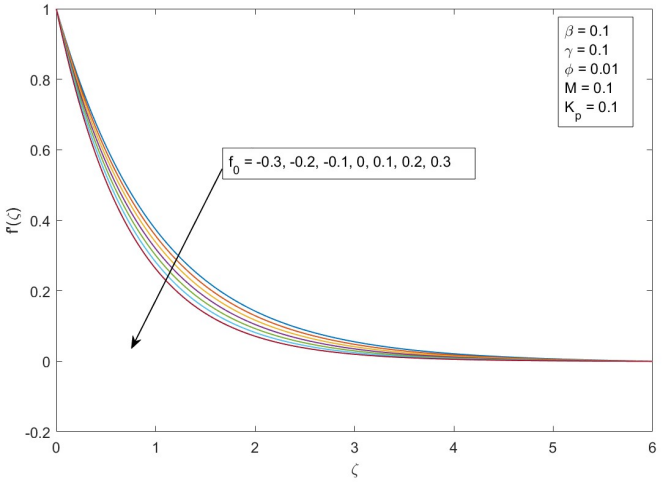

FIGURE 4.3: Impact of f_0 on $f'(\zeta)$

Figure 4.4 illustrates a key finding concerning the relationship between the volume fraction ϕ and fluid velocity. The results reveal a substantial increase in fluid velocity with an increase in the volume fraction ϕ of nanoparticles. The addition of nanoparticles to the base fluid diminishes the overall average heat absorption capacity. Consequently, this alteration in heat absorption characteristics leads to an increase in the fluid's velocity profile.

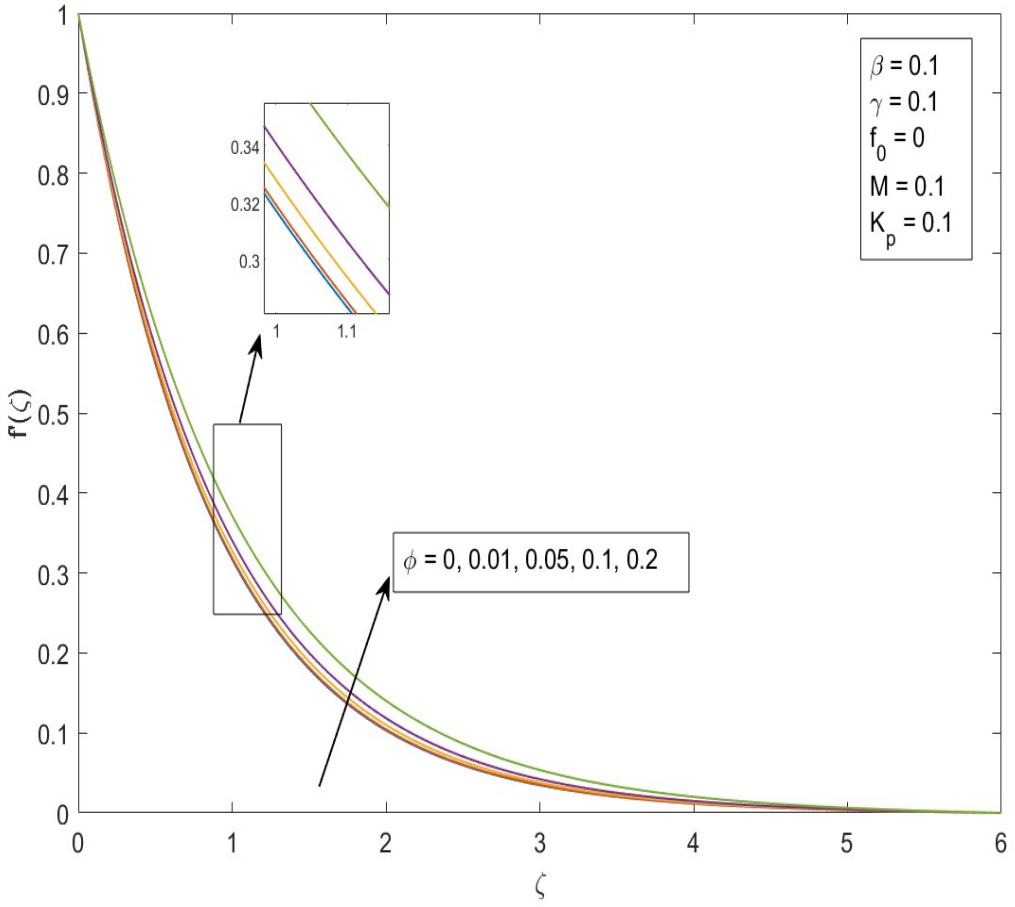

FIGURE 4.4: Impact of ϕ on $f'(\zeta)$

Figure 4.5 illustrates the effect of M on the velocity profile $f'(\zeta)$. The results indicate a negative impact on the fluid, revealing a connection where the velocity distribution and magnetic field strength are inverse. As the magnetic parameter values increase, the fluid velocity decreases. This phenomenon occurs as a result of the Lorentz force, which acts perpendicular to the vectors of the magnetic field and velocity, exerted by the magnetic

field on the moving fluid particles. By adding resistance to the fluid flow, this Lorentz force lowers the fluid's velocity.

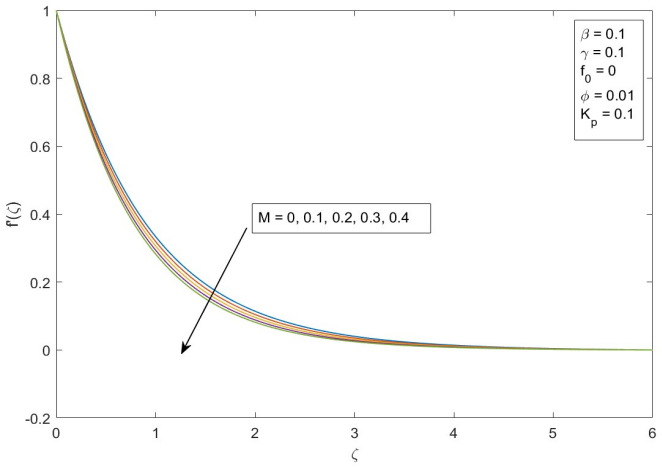

FIGURE 4.5: Impact of M on $f'(\zeta)$

Figure 4.6 is used to analyze how the porosity parameter K_p affects the velocity distribution. As the porosity parameter rises, the results shown in Figure 4.6 clearly show a decrease in the velocity distribution. This is explained by the properties of a porous media, which have a network of tiny holes or pores that prevent fluid passage. The fluid's permeability through the porous medium is directly correlated with the porosity parameter. The porous medium's resistance to fluid movement gets stronger as K_p rises. Consequently, with higher values of the porosity parameter, the fluid encounters an increased resistance from both the porous medium and its own viscosity, leading to a significant reduction in the fluid's velocity within the medium.

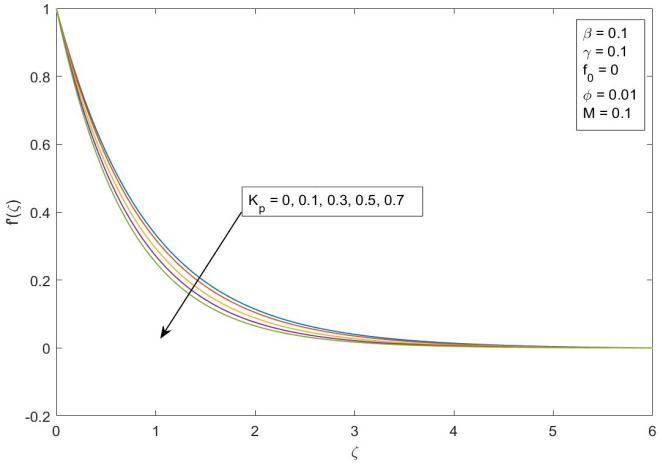

FIGURE 4.6: Impact of K_p on $f'(\zeta)$

4.5.3 Temperature Profile

Figures 4.7 and 4.8 show how non-uniform heat source and sink characteristics affect the temperature profile. Examination of these figures reveals that $A^*, B^* > 0$ adds more energy to the thermal boundary layer, thereby increasing the fluid's temperature. On the other hand, when $A^*, B^* < 0$, heat energy is extracted from the thermal boundary layer, the fluid's temperature drops.

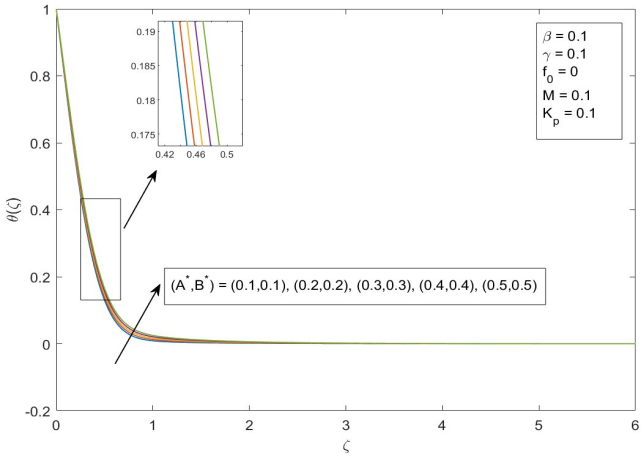

FIGURE 4.7: Impact of $A^*, B^* > 0$ on temperature profile $\theta(\zeta)$

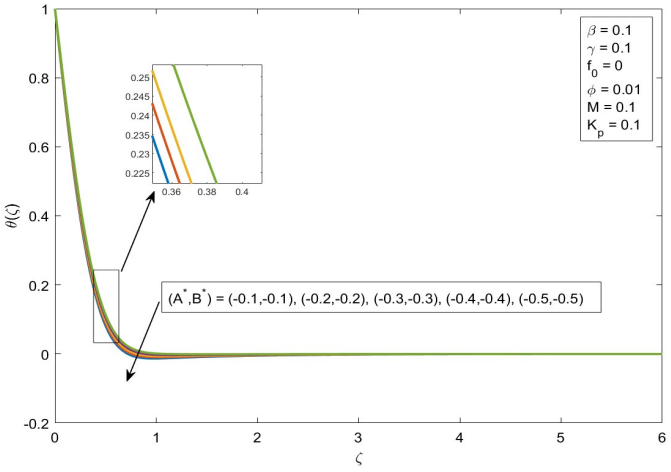

FIGURE 4.8: Impact of $A^*, B^* < 0$ on temperature profile $\theta(\zeta)$

In Figures 4.9 - 4.10, the effect of M on fluid temperature for heat sink and heat source is examined. The temperature of the fluid rises when M increases. The enhanced magnetic forces inhibit fluid movement, thereby increasing internal friction and heat generation, which in turn elevates the temperature.

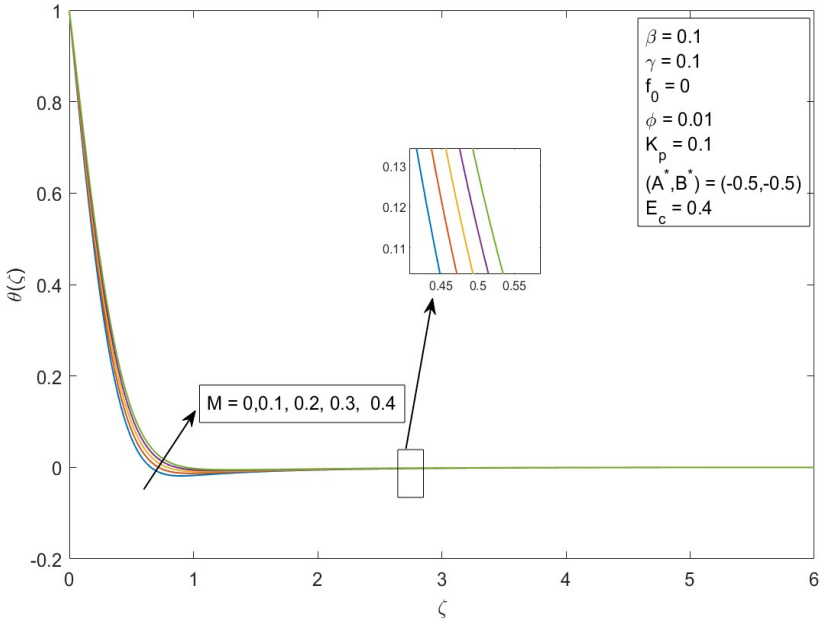

FIGURE 4.9: Impact of M for heat sink on temperature profile $\theta(\zeta)$

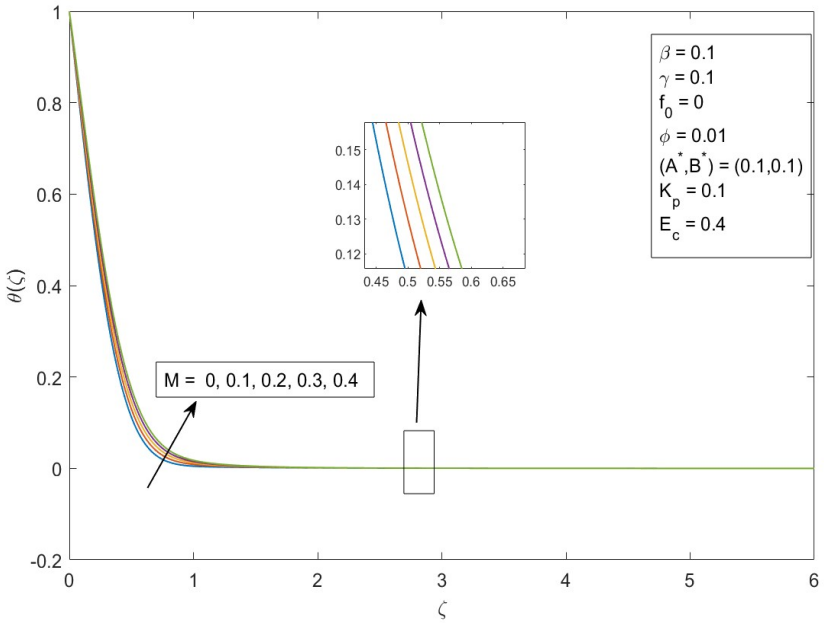

FIGURE 4.10: Impact of M for heat source on temperature profile $\theta(\zeta)$

Figures 4.11 and 4.12 illustrate that the temperature distribution increases as the E_c values rise. As E_c increases, dissipation also increases, leading to a rise in the internal energy of the fluid. Consequently, this increase in internal energy enhances the fluid's temperature distribution.

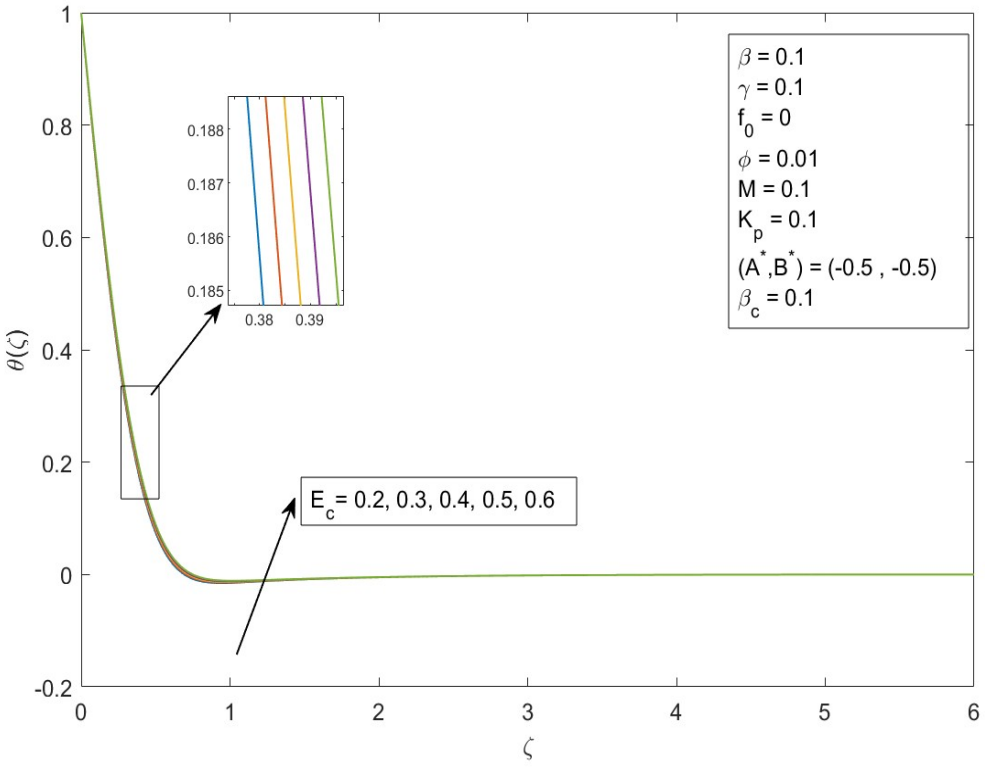

FIGURE 4.11: Impact of E_c for heat sink on temperature profile $\theta(\zeta)$

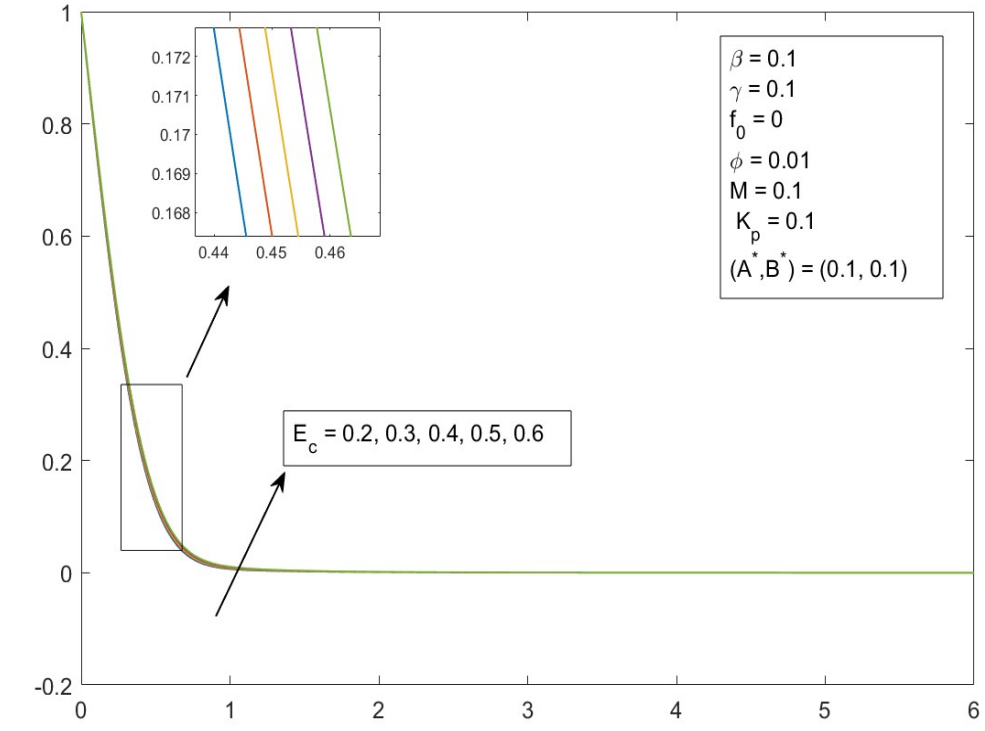

FIGURE 4.12: Impact of E_c for heat source on temperature profile $\theta(\zeta)$

4.5.4 Concentration Profile

Figures 4.13 and 4.14 illustrate the effect of the Schmidt number on the concentration profile in relation to the heat source and heat sink. It is found that the concentration gradient gets more noticeable as the Schmidt number rises. Higher Schmidt number corresponds to the stronger viscous diffusion and enhances the molecular movement. The link between mass and momentum diffusivities in a liquid flow is formally characterized by the dimensionless Schmidt number. Interestingly, the lowest Schmidt number corresponds to the maximum concentration of nanoparticles. Additionally, the figures show the thickness of the boundary layer for both the species of nanoparticles and the hydrodynamic flow, which indicates a steepening concentration gradient.

Additionally, Figures 4.15 - 4.16 demonstrate the effect of the thermophoretic parameter with respect to heat source and heat sink on the concentration profile. A decrease in the thermophoretic parameter results in a higher concentration profile. This is due to the thermophoretic effect, which creates a suction-like behavior among the particles, leading to a cooler surface and a consequent reduction in mass transfer.

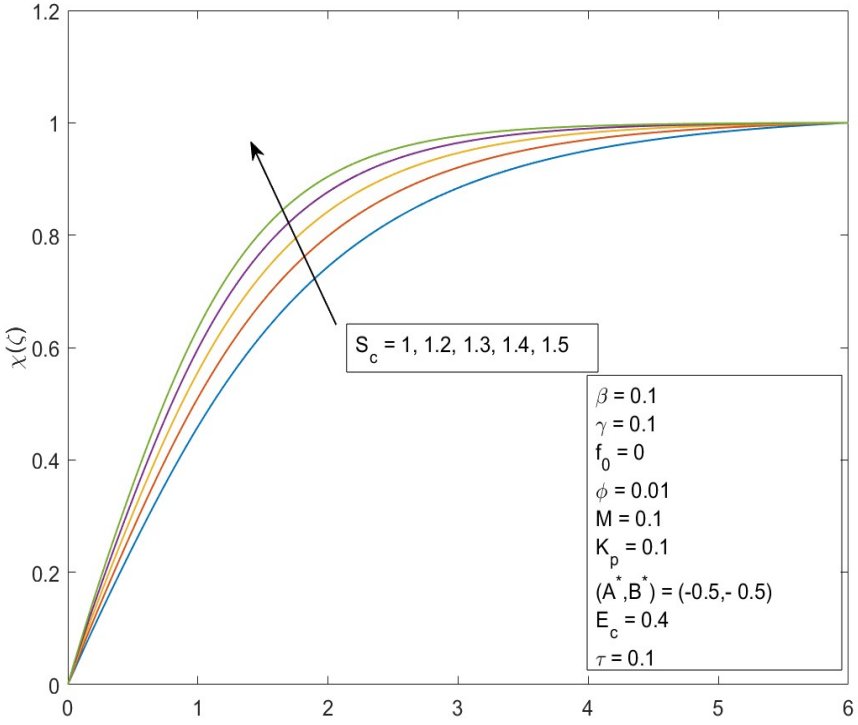

FIGURE 4.13: Impact of S_c on concentration profile $\theta(\zeta)$

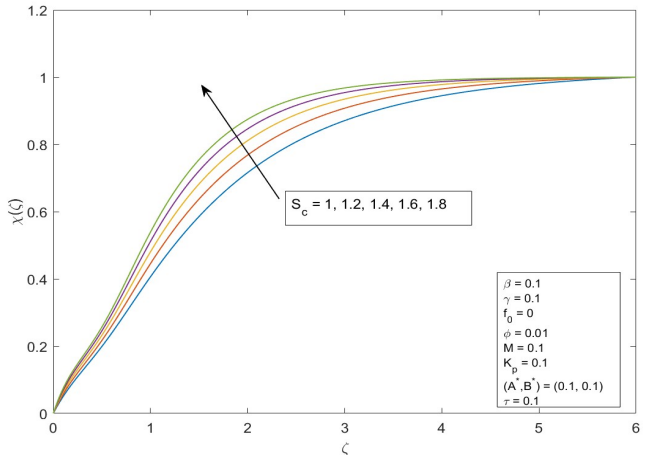

FIGURE 4.14: Impact of S_c on concentration profile $\theta(\zeta)$

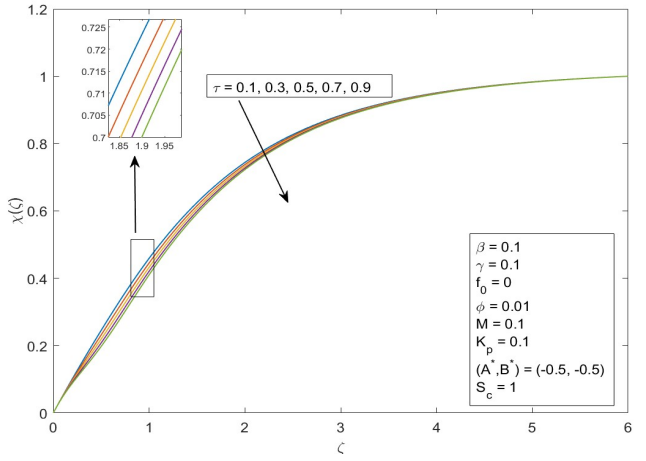

FIGURE 4.15: Impact of τ on concentration profile $\theta(\zeta)$

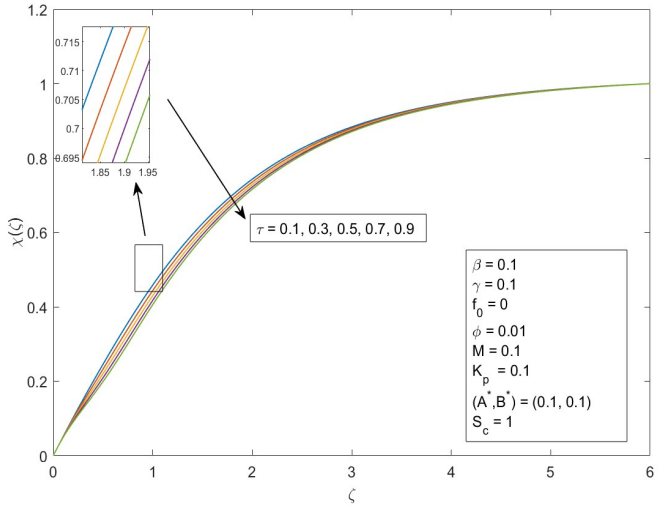

FIGURE 4.16: Influence of τ on $\theta(\zeta)$ concentration profile

4.5.5 Graphically Behavior of Physical Quantities

Figures 4.17 and 4.18 illustrate the variation in the skin friction coefficient with respect to the magnetic field and porosity parameter. Evidently, the coefficient of skin friction increases with higher values of K_p and M. Figures 4.19 - 4.20 show the variation in the Nusselt number concerning (A^*, B^*) and Eckert number E_c. We can see that if values of (A^*, B^*) and E_c increase, the Nusselt number decreases. Figures 4.21 - 4.22 show the variation in the Sherwood number concerning S_c and τ. We can see that if values of S_c and τ increase, the Sherwood number decreases.

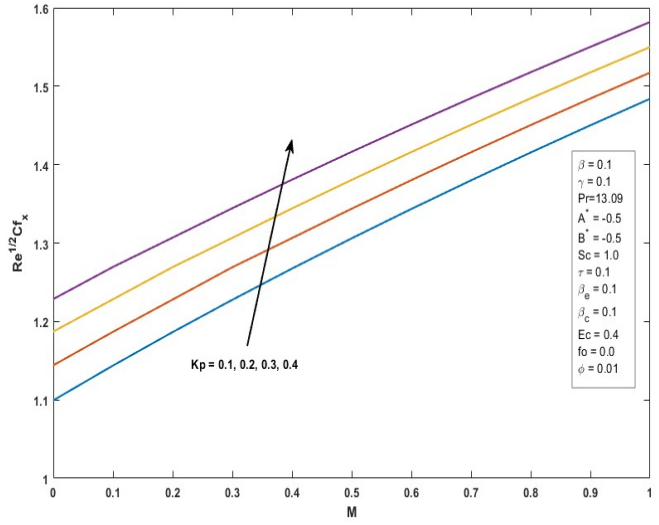

FIGURE 4.17: Skin fraction Cf versus M for different K_p values

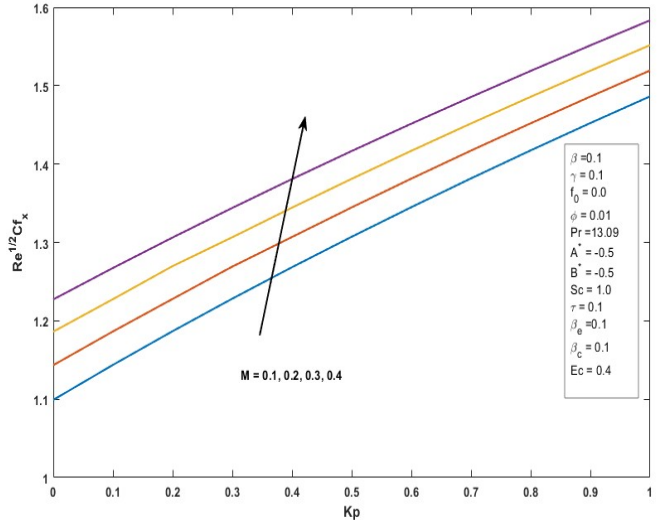

FIGURE 4.18: Skin fraction Cf vs Kp for various values of M

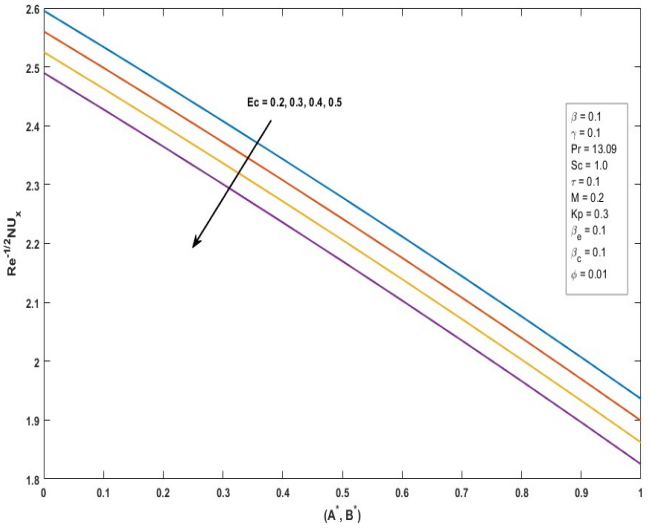

FIGURE 4.19: Nusselt number Nu vs (A^*B^*) for various values of E_c

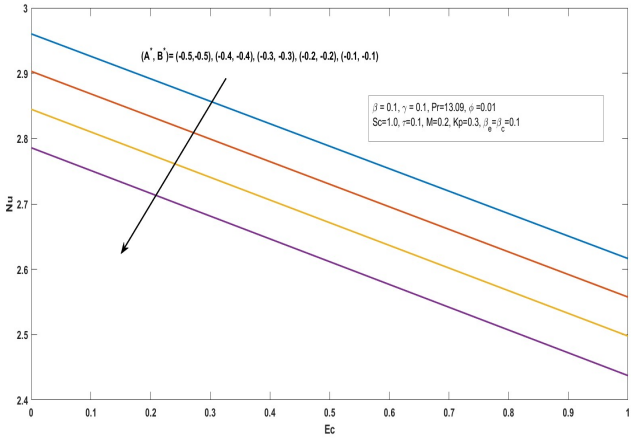

FIGURE 4.20: Nusselt number Nu vs E_c for various values of (A^*B^*)

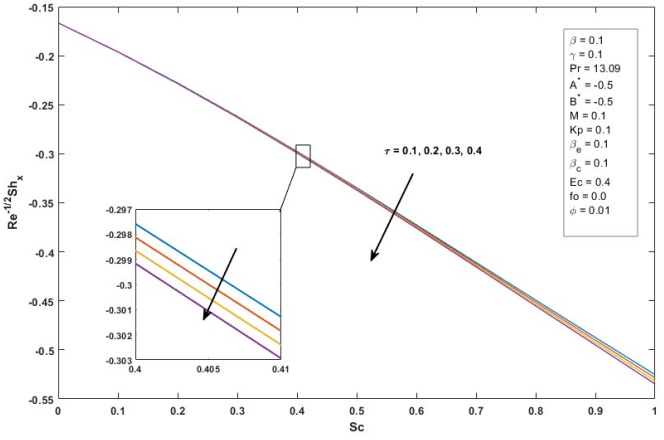

FIGURE 4.21: Sherwood number Sh versus S_c for different τ values

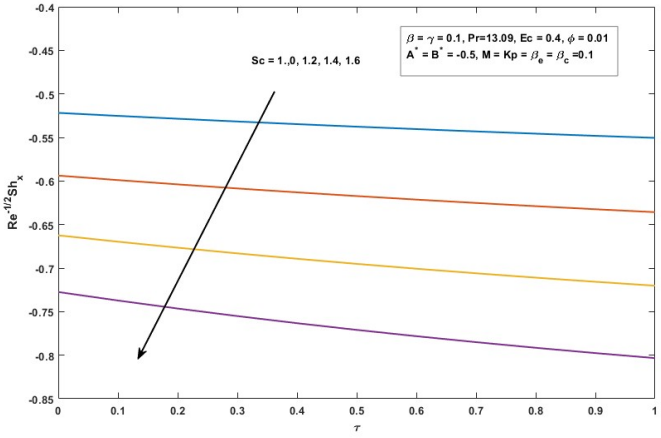

FIGURE 4.22: Sherwood number S_h against τ for different S_c values

Chapter 5

Conclusions

The present thesis incorporates the Cattaneo-Christov non-Fourier double-diffusion model, porosity parameter and the effects of a magnetic field thereby expanding and improving the work of Srilatha et al. [44]. The following are the main conclusions of the current study:

- The velocity profile decreases with an increase in the Deborah number.
- As the unsteadiness parameter increases, the velocity profile decreases.
- The velocity profile decreases as surface injection and surface suction rise.
- The velocity profile increases when the volume percentage of nanoparticles rise.
- The velocity profile decreases with an increase in the magnetic field.
- The velocity profile diminishes as the value of the porosity parameter increases.
- The fluid's temperature drops as a result of the heat sink absorbing more energy from the thermal boundary layer. The fluid's temperature rises as a result of the heat source adding more energy from the thermal boundary layer.
- The fluid's temperature rises with an increase in the Eckert number.
- The temperature of the fluid rises with an increase in M.
- A rise in the value of S_c results in an increase in the concentration profile.
- The concentration profile becomes lower as τ increases.

- The coefficient of the skin-friction increases with higher value of K_p.
- An increase in the value of M increases the skin-friction coefficient.
- An increase in the values of A^*, B^* and E_c decreases the Nusslet number.
- An increase in the values of S_c and τ leads to a reduction in the Sherwood number.

Bibliography

[1] J. B. J. Fourier, *Théorie analytique de la chaleur*, vol. 1. Gauthier-Villars, 1888.

[2] C. Cattaneo, "Sulla conduzione del calore," *Atti Sem. Mat. Fis. Univ. Modena*, vol. 3, pp. 83–101, 1948.

[3] C. Christov, "On frame indifferent formulation of the Maxwell-Cattaneo model of finite-speed heat conduction," *Mechanics Research Communications*, vol. 36, no. 4, pp. 481–486, 2009.

[4] M. Ciarletta and B. Straughan, "Uniqueness and structural stability for the Cattaneo-Christov equations," *Mechanics Research Communications*, vol. 37, no. 5, pp. 445–447, 2010.

[5] S. Han, L. Zheng, C. Li, and X. Zhang, "Coupled flow and heat transfer in viscoelastic fluid with Cattaneo-Christov heat flux model," *Applied Mathematics Letters*, vol. 38, pp. 87–93, 2014.

[6] T. Hayat, M. Imtiaz, A. Alsaedi, and S. Almezal, "On Cattaneo-Christov heat flux in mhd flow of Oldroyd-b fluid with homogeneous–heterogeneous reactions," *Journal of Magnetism and Magnetic Materials*, vol. 401, pp. 296–303, 2016.

[7] M. Waqas, T. Hayat, M. Farooq, S. Shehzad, and A. Alsaedi, "Cattaneo-Christov heat flux model for flow of variable thermal conductivity generalized Burgers fluid," *Journal of Molecular Liquids*, vol. 220, pp. 642–648, 2016.

[8] M. Khan and W. A. Khan, "Three-dimensional flow and heat transfer to Burgers fluid using Cattaneo-Christov heat flux model," *Journal of Molecular Liquids*, vol. 221, pp. 651–657, 2016.

[9] W. A. Khan, M. Khan, A. S. Alshomrani, and L. Ahmad, "Numerical investigation of generalized Fourier's and Fick's laws for Sisko fluid flow," *Journal of Molecular Liquids*, vol. 224, pp. 1016–1021, 2016.

[10] W. A. Khan, M. Khan, and A. S. Alshomrani, "Impact of chemical processes on 3d Burgers fluid utilizing Cattaneo-Christov double-diffusion: applications of non-Fourier's heat and non-Fick's mass flux models," *Journal of Molecular Liquids*, vol. 223, pp. 1039–1047, 2016.

[11] J. R. Reddy, V. Sugunamma, and N. Sandeep, "Cross diffusion effects on mhd flow over three different geometries with Cattaneo-Christov heat flux," *Journal of Molecular Liquids*, vol. 223, pp. 1234–1241, 2016.

[12] T. Hayat, M. I. Khan, M. Farooq, A. Alsaedi, M. Waqas, and T. Yasmeen, "Impact of Cattaneo-Christov heat flux model in flow of variable thermal conductivity fluid over a variable thicked surface," *International journal of heat and mass transfer*, vol. 99, pp. 702–710, 2016.

[13] M. Ali and N. Sandeep, "Cattaneo-Christov model for radiative heat transfer of magnetohydrodynamic Casson-ferrofluid: A numerical study," *Results in physics*, vol. 7, pp. 21–30, 2017.

[14] M. Waqas, M. I. Khan, T. Hayat, A. Alsaedi, and M. I. Khan, "On Cattaneo-Christov double diffusion impact for temperature-dependent conductivity of Powell–Eyring liquid," *Chinese Journal of Physics*, vol. 55, no. 3, pp. 729–737, 2017.

[15] T. Hayat, M. I. Khan, M. Waqas, and A. Alsaedi, "On Cattaneo-Christov heat flux in the flow of variable thermal conductivity Eyring–Powell fluid," *Results in Physics*, vol. 7, pp. 446–450, 2017.

[16] M. Zubair, M. Jawad, E. Bonyah, and R. Jan, "Mhd analysis of couple stress hybrid nanofluid free stream over a spinning Darcy-Forchheimer porous disc under the effect of thermal radiation," *Journal of Applied Mathematics*, vol. 2021, no. 1, p. 2522155, 2021.

[17] T. Sultan, *MHD Nanofluid Flow With Cattaneo-Christov Double Diffussion Model and Chemical Reaction*. PhD thesis, Cust Isb, 2022.

[18] Y.-M. Chu, M. Al-Buriahi, A. Khan, K. M. Katub, M. Saqlain, S. Abbas, and W. Khan, "Significance of generalized Fourier and Fick's law and stagnation point flow for magnetized viscoelastic liquids," *Materials Science and Engineering: B*, vol. 296, p. 116602, 2023.

[19] A. M. N Khan, A. A Khan, Z. Wang, H. F. Alrihieli, S. M. Eldin, F. Aldosari, and I. E. Elseesy, "Flow investigation of the stagnation point flow of micropolar viscoelastic fluid with modified Fourier and Fick's law," *Scientific Reports*, vol. 13, no. 1, p. 9491, 2023.

[20] F. Ali, A. Zaib, K. Loganathan, A. Saeed, T. Seangwattana, P. Kumam, and A. M. Galal, "Scrutinization of second law analysis and viscous dissipation on Reiner-Rivlin nanofluid with the effect of bioconvection over a rotating disk," *Heliyon*, vol. 9, no. 2, 2023.

[21] H. U. Rasheed, Q. Shah, J. Khan, T. Abbas, W. Khan, and M. I. Mohmand, "Physical insight into thermal analysis of magnetohydrodynamic stagnation point flow of micropolar nanofluid across a flexible surface equipped with porous medium and Fourier and Fick's law," *Heat Transfer*, vol. 53, no. 2, pp. 512–532, 2024.

[22] R. P. Gowda, R. N. Kumar, A. Aldalbahi, A. Issakhov, B. Prasannakumara, M. Rahimi-Gorji, and M. Rahaman, "Thermophoretic particle deposition in time-dependent flow of hybrid nanofluid over rotating and vertically upward/downward moving disk," *Surfaces and Interfaces*, vol. 22, p. 100864, 2021.

[23] S. Shehzad, F. Mabood, A. Rauf, and I. Tlili, "Forced convective maxwell fluid flow through rotating disk under the thermophoretic particles motion," *International Communications in Heat and Mass Transfer*, vol. 116, p. 104693, 2020.

[24] R. N. Kumar, A. Jyothi, H. Alhumade, R. P. Gowda, M. M. Alam, I. Ahmad, M. Gorji, and B. Prasannakumara, "Impact of magnetic dipole on thermophoretic particle deposition in the flow of Maxwell fluid over a stretching sheet," *Journal of Molecular Liquids*, vol. 334, p. 116494, 2021.

[25] S. Bashir, M. Ramzan, H. A. S. Ghazwani, K. S. Nisar, C. A. Saleel, and A. Abdelrahman, "Magnetic dipole and thermophoretic particle deposition impact on bioconvective Oldroyd-B fluid flow over a stretching surface with Cattaneo–Christov heat flux," *Nanomaterials*, vol. 12, no. 13, p. 2181, 2022.

[26] R. N. Kumar, R. P. Gowda, J. Madhukesh, B. Prasannakumara, and G. Ramesh, "Impact of thermophoretic particle deposition on heat and mass transfer across the dynamics of Casson fluid flow over a moving thin needle," *Physica Scripta*, vol. 96, no. 7, p. 075210, 2021.

[27] F. Ahmad, S. Abdal, H. Ayed, S. Hussain, S. Salim, and A. O. Almatroud, "The improved thermal efficiency of Maxwell hybrid nanofluid comprising of graphene oxide plus silver/kerosene oil over stretching sheet," *Case Studies in Thermal Engineering*, vol. 27, p. 101257, 2021.

[28] S. Chandrasekaran, M. S. Gupta, S. Jangid, K. Loganathan, B. Deepa, and D. K. Chaudhary, "Unsteady radiative Maxwell fluid flow over an expanding sheet with sodium alginate water-based copper-graphene oxide hybrid nanomaterial: An application to solar aircraft," *Advances in Materials Science and Engineering*, vol. 2022, no. 1, p. 8622510, 2022.

[29] A. Bhattacharyya, R. Sharma, S. Hussain, A. Chamkha, and E. Mamatha, "A numerical and statistical approach to capture the flow characteristics of Maxwell hybrid nanofluid containing copper and graphene nanoparticles," *Chinese Journal of Physics*, vol. 77, pp. 1278–1290, 2022.

[30] S. M. Hussain, R. Sharma, M. R. Mishra, and S. S. Alrashidy, "Hydromagnetic dissipative and radiative graphene Maxwell nanofluid flow past a stretched sheet-numerical and statistical analysis," *Mathematics*, vol. 8, no. 11, p. 1929, 2020.

[31] E. A. Algehyne, S. Rehman, R. Ayub, A. Saeed, S. M. Eldin, and A. M. Galal, "Brownian and thermal diffusivity impact due to the Maxwell nanofluid (graphene/engine oil) flow with motile microorganisms and Joule heating," *Nanotechnology Reviews*, vol. 12, no. 1, p. 20220540, 2023.

[32] W. Jamshed, R. Safdar, Z. Rehman, M. M. Lashin, M. Ehab, M. Moussa, and A. Rehman, "Computational technique of thermal comparative examination of Cu and Au nanoparticles suspended in sodium alginate as Sutterby nanofluid via extending ptsc surface," *Journal of Applied Biomaterials & Functional Materials*, vol. 20, p. 22808000221104004, 2022.

[33] A. Tassaddiq, I. Khan, and K. Nisar, "Heat transfer analysis in sodium alginate based nanofluid using MoS2 nanoparticles: Atangana–Baleanu fractional model," *Chaos, Solitons & Fractals*, vol. 130, p. 109445, 2020.

[34] A. Shaukat, M. Mushtaq, S. Farid, K. Jabeen, and R. M. Akram Muntazir, "A study of magnetic/nonmagnetic nanoparticles fluid flow under the influence of non-linear thermal radiation," *Mathematical Problems in Engineering*, vol. 2021, no. 1, p. 2210414, 2021.

[35] A. Raza, M. Y. Almusawa, Q. Ali, A. U. Haq, K. Al-Khaled, and I. E. Sarris, "Solution of water and sodium alginate-based Casson type hybrid nanofluid with slip and sinusoidal heat conditions: A prabhakar fractional derivative approach," *Symmetry*, vol. 14, no. 12, p. 2658, 2022.

[36] A. Dawar, S. Islam, Z. Shah, and S. Mahmuod, "A passive control of Casson hybrid nanofluid flow over a curved surface with alumina and copper nanomaterials: A study on sodium alginate-based fluid," *Journal of Molecular Liquids*, vol. 382, p. 122018, 2023.

[37] M. Turkyilmazoglu, "Dual and triple solutions for mhd slip flow of non-newtonian fluid over a shrinking surface," *Computers & Fluids*, vol. 70, pp. 53–58, 2012.

[38] E. J. Shaughnessy, *Introduction to Fluid Mechanics*. 2005.

[39] R. Bansal, *A Textbook of Fluid Mechanics and Hydraulic Machines*. Laxmi Publications, 2010.

[40] S. Som, *Introduction to Heat Transfer*. PHI Learning Pvt. Ltd., 2008.

[41] R. E. Collins, "Flow of Fluids through Porous Materials," 1976.

[42] J. N. Reddy and D. K. Gartling, *The Finite Element Methods in Heat Transfer and Fluid Dynamics*. CRC press, 2010.

[43] J. Kuneš, "Thermomechanics," *Dimensionless Physical Quantities in Science and Engineering. Elsevier, Oxford*, pp. 173–283, 2012.

[44] P. Srilatha, H. Abu-Zinadah, R. S. V. Kumar, M. Alsulami, R. N. Kumar, A. Abdulrahman, and R. J. Punith Gowda, "Effect of nanoparticle diameter in Maxwell nanofluid flow with thermophoretic particle deposition," *Mathematics*, vol. 11, no. 16, p. 3501, 2023.

[45] I. Waini, U. Khan, A. Zaib, A. Ishak, and I. Pop, "Thermophoresis particle deposition of cofe2o4-tio2 hybrid nanoparticles on micropolar flow through a moving flat plate with viscous dissipation effects," *International Journal of Numerical Methods for Heat & Fluid Flow*, vol. 32, no. 10, pp. 3259–3282, 2022.

[46] F. A. Alwawi, H. T. Alkasasbeh, A. Rashad, and R. Idris, "Mhd natural convection of sodium alginate Casson nanofluid over a solid sphere," *Results in Physics*, vol. 16, p. 102818, 2020.